# Final report

## Promoting effluent pasteurization in faecal sludge treatment to contribute to the prevention of Cholera outbreaks in Bangladesh´s Rohingyas refugee camps


**Authors:**

[1] Santiago SEPTIEN STRINGEL (saseptien@iom.int)

[1] Baudoin LUCE (lbaudoin@iom.int)

[2] Romain VERCHÈRE (romain.verchere@veolia.com)

[3] Nuhu AMIN (nuhu.amin@icddrb.org)

**Affiliation:**

[1] International Organization for Migration (IOM)

[2] Veolia Foundation

[3]International Centre for Diarrhoeal Disease Research, Bangladesh (ICDDR'B)



**Date:**

December 2024

# Executive summary

The solar pasteurizer project was developed to address sanitation and public health challenges in the Rohingya refugee camps in Cox's Bazar, Bangladesh, where inadequate waste management increases the risk of waterborne diseases, including cholera. Additionally, the camps face significant climate risks, including flooding, cyclones, and fire hazards, which are further exacerbated by structural vulnerabilities such as high population density, lack of space for proper wastewater treatment systems, and limited capacity to operate complex Faecal sludge treatment infrastructure. There is a critical need for innovative, space-efficient, climate-resilient, and easy-to-operate solutions to mitigate these risks.

In this context, pasteurization emerged as a promising mechanism for pathogen inactivation, offering a sustainable and scalable solution for wastewater treatment in densely populated humanitarian settings. The project aims to enhance wastewater treatment efficiency by piloting a solar thermal pasteurization system within the IOM decentralized wastewater treatment system (DEWATS) in Camp 12, treating 3,000 L/day of faecal sludge.

The project employed a robust research framework comprising site assessments, field and laboratory testing, and model development. Field tests were conducted to evaluate thermal performance and effluent quality across varying weather conditions. Laboratory experiments replicated these tests, while solar assessments and techno-economic analyses projected year-round performance and cost implications. The system's applicability was studied in other humanitarian contexts, such as Bentiu (South Sudan), Maiduguri (Nigeria), and Pemba (Mozambique), to assess replicability.

Testing revealed that the pasteuriser could function within a temperature range of 55°C to 65°C—sufficient to deactivate key pathogens like E. coli and Vibrio cholerae at 55°C, and Salmonella, Ascaris, Taenia and Shigella at 65°C, but insufficient for enteric viruses. Effluent analysis showed significant microbial reduction but little improvement in physicochemical parameters, necessitating further downstream treatment to meet discharge standards. Despite its effectiveness, the system currently falls short of treating 3,000 L/day solely through solar energy, requiring supplemental heating from a diesel generator.

Solar assessments confirmed that the target capacity cannot be achieved year-round with solar energy alone. The techno-economic analysis indicated high initial costs, although local material sourcing could lower expenses. Operational costs remained low except when diesel generators were used. Proposed improvements include expanding solar collector surface areas, integrating vacuum tube collectors, using LPG boilers to replace diesel generators and include heat recovery —strategies expected to lower operational costs and achieve a return on investment within one year. These measures could allow to achieve the treatment target and lead to temperatures around 65°C to ensure pasteurisation of most of the pathogens. To achieve full reliance on solar energy, heat recovery is a critical step.

Replicability tests in other humanitarian settings highlighted the system adaptability to diverse environmental conditions, with a stronger solar energy source leading to a higher performance, as it is the case of Bentiu, Pemba and Maiduguri compared to the Rohingya

camp. The study underscores the importance of tailoring the technology to specific contexts to enhance scalability and effectiveness.

In conclusion, the solar pasteuriser project successfully demonstrated the potential of solar energy to improve sanitation, prevent cholera outbreaks, and reduce pathogen transmission in densely populated humanitarian settings. The pasteuriser, driven by solar energy, presents a sustainable and cost-effective solution for pathogen reduction, aligning with broader humanitarian sanitation goals. Future efforts will focus on optimizing the system, incorporating energy-efficient solutions, and expanding deployment to other vulnerable regions.

## Acknowledgments

The authors would like to express their sincere gratitude to ELRHA for its financial support and funding, as well as for their flexibility and understanding in accommodating unforeseen circumstances that delayed the project's progress.

We extend our appreciation to the IOM technical, support, and drivers staff for their invaluable assistance in ensuring the smooth progression of the project and for their dedication in addressing and resolving any challenges encountered along the way.

A special thanks goes to the volunteers from the Veolia Foundation, whose active contributions and unwavering dedication played a significant role in the commissioning and continuous improvement of the technology.

We are grateful to ICDDR'B for their laboratory support, field assistance, and sampling efforts, and for always providing a welcoming and collaborative environment.

Our appreciation also goes to IHE-Delft for organizing an internship related to this project and for lending essential laboratory materials, fostering a spirit of knowledge-sharing and collaboration.

Additionally, we thank RVO for funding the travel of the IHE-Delft intern to Bangladesh, facilitating crucial hands-on involvement.

We acknowledge the DPHE laboratory for hosting the experimental work carried out by the IHE-Delft intern and for their support with materials and sampling.

The authors are thankful to the staff at Solargis for their generosity in sharing data from their software, which greatly benefited the project.

We extend our gratitude to the Bangladesh National Weather Service for providing critical weather data measurements, which contributed significantly to the project's analysis.

Our heartfelt thanks go to the Rohingya volunteers, whose kindness, cooperation, and helpful attitude were essential to the project's success.

We would also like to recognize the Cox’s Bazar WASH Cluster for their role in disseminating the project and promoting awareness.

Finally, our sincere thanks to the Global WASH cluster, Climate Change working group and Sanihub for inviting us as guest speakers at their seminar, providing a valuable platform to share our insights and findings.

# Contents

# List of Figures

# List of Tables

# List of Abbreviations

| | |
|---|---|
| BOD | Biological oxygen demand |
| COD | Chemical oxygen demand |
| DEWATS | Decentralised wastewater treatment plant system |
| E. | Escherichia |
| FS | Faecal sludge |
| GHI | Global horizontal irradience |
| GTI | Global tilted irradiance |
| ICDDR | International Centre for Diarrhoeal Disease Research, Bangladesh |
| IHE | International Institute for Hydraulic and Environmental Engineering |
| IOM | International organization for Migration |
| LPG | Liquefied petroleum gas |
| PPMoV | Pepper mild mottle virus |
| PV | Photovoltaic |
| ROI | Return of investment |
| RVA | Rotavius A |
| RVO | Netherlands Enterprise Agency |
| SEC | Specific energy consumption |
| TC | Total coliforms |
| TMY | Typical meteorological data |
| TN | Total nitrogen |
| TP | Total phosphorous |
| TS | Total solids |
| TSS | Total suspended solids |
| WASH | Water, Sanitation and Hygiene |

## Chemical nomenclature

| | |
|---|---|
| $NO_3^-$ | Nitrates |
| pH | Potential of hydrogen |
| $PO_3^{-4}$ | Phosphates |

# 1. Introduction

This section provides a comprehensive overview of the project, laying the groundwork for the subsequent discussions in the report. It begins with the background of the project, establishing the context and relevance of the study. Following this, the problem statement identifies the key challenges or gaps that the project aims to address, highlighting the significance of the work undertaken.

The aim and objectives of the project are then clearly defined, outlining the specific goals and intended outcomes. Additionally, the scope of the report is detailed, describing the boundaries of the study and the focus areas covered. Finally, the section concludes with the outline of the final report, offering readers a roadmap of the content and structure to expect in the chapters that follow.

## 1.1. Background

### *1.1.1. Rohingya refugee camp*

The Rohingya population originates from Arakan, a region that was officially renamed Rakhine State in 1974 under Myanmar's administrative restructuring. During Burma's parliamentary government (1948–1962), the Rohingya were recognized as an ethnic group and held citizenship rights, including voting and political representation. However, after the 1962 military coup, successive governments pursued policies of delegitimization and institutionalized oppression. From then, the Rohingya have been increasingly stripped of their fundamental rights, facing systematic discrimination, restricted movement, and violent military crackdowns.

As a result of attacks enacted by the Myanmar military and Buddhist extremists in August 2017, nearly one million Rohingya have sought refuge in Bangladesh (UNHCR, 2020). In this context, the Bangladeshi government has settled these individuals primarily in the hilly regions of Cox's Bazar District, in the Ukhia and Teknaf sub-districts, as it can be observed in Figure 1. As of June 2023, the estimated total population within the camps, including the officially recognized camps at Kutupalong and Nayapara, had exceeded 1.1 million, with the majority relying heavily on humanitarian support for basic needs (JRB, 2020).

### *1.1.2. WASH situation in the Rohingya camp*

Overcrowding has severely restricted the availability of adequate water, sanitation, and hygiene (WASH) facilities.

National and international humanitarian agencies and non-governmental organisations have undertaken hard work to ensure adequate sanitation in the Rohingya camps and manage faecal sludge waste but the situation remains challenging. Hygienic conditions must be significantly improved to prevent water-related outbreaks. Pathogens of concern in Bangladesh that can affect the Rohingya community have been identified, with diarrheal diseases posing the greatest threat, especially to vulnerable populations such as children and

the elderly. The primary causes of diarrhea in Bangladesh are the bacteria Vibrio cholerae (Huq et al., 2005; Longini Jr et al., 2002; Lopez et al., 2012)and Escherichia coli (Alam et al., 2006). Other concerning pathogens include Shigella, Salmonella, Norovirus GII, Giardia, and Ascaris lumbricoides (Dey et al., 2016; Foster et al., 2021).

Cholera is endemic in Bangladesh, with peaks occurring before and after the monsoon season. It has posed a significant health risk in the Rohingya camps since 2017, with epidemic outbreaks reported in 2019, 2021, 2023, and 2024 according to the World Health Organization.

The high population density in the Rohingya camps presents significant challenges for water, sanitation, and hygiene (WASH) infrastructure, particularly in ensuring effective faecal sludge management. National and international humanitarian agencies, along with non-governmental organizations, have made extensive efforts to improve sanitation conditions in the camps. However, structural vulnerabilities, limited space, and exposure to environmental hazards continue to pose challenges to sustainable sanitation solutions.

Ensuring improved hygienic conditions is essential in reducing the risk of waterborne diseases and safeguarding public health. Pathogens of concern in Bangladesh that can affect the Rohingya community have been identified, with diarrheal diseases posing a major public health concern, particularly for vulnerable groups such as children and the elderly. The primary causes of diarrhea in Bangladesh include Vibrio cholerae (Huq et al., 2005; Longini Jr et al., 2002; Lopez et al., 2012) and Escherichia coli (Alam et al., 2006), while other significant pathogens include Shigella, Salmonella, Norovirus GII, Giardia, and Ascaris lumbricoides (Dey et al., 2016; Foster et al., 2021).

Cholera is endemic in Bangladesh, with seasonal peaks occurring before and after the monsoon period. It has remained a consistent health risk in the Rohingya camps since 2017, with epidemic outbreaks reported in 2019, 2021, 2023, and 2024 (WHO, 2024).

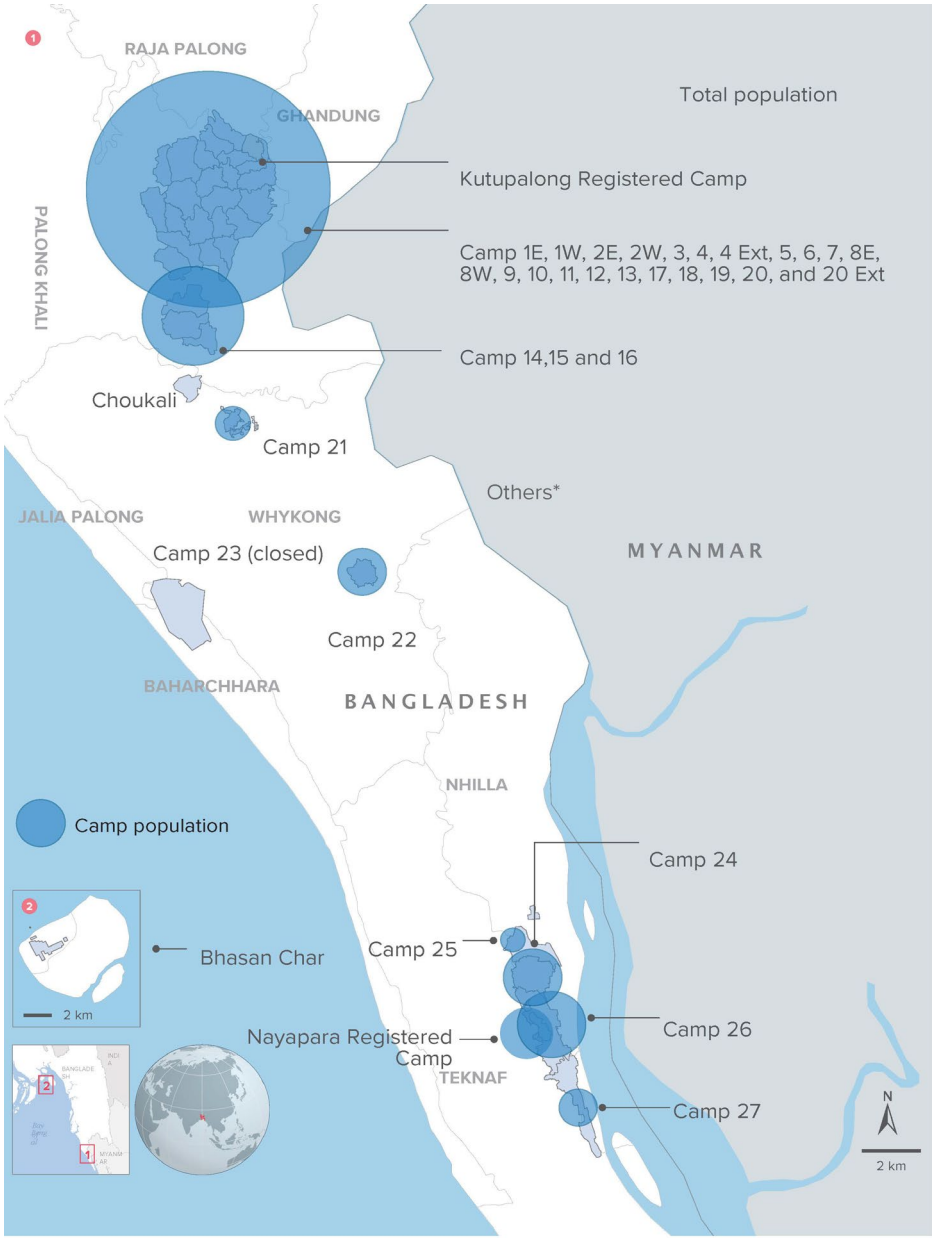


*Figure 1. Map of the Rohingya camps in Bangladesh* (UNHCR, 2022)

### *1.1.3. Solar pasteurisation*

Pasteurisation is identified as a process that can eliminate pathogens by heating the medium in which they are found. Several pasteurisation applications can be found in literature for sludge treatment with good treatment performance, potentially allowing to remove pathogens such as E. Coli, Salmonella, Helminth ova, Enterococcus faecalis, Shigella and Pseudomonas (Atenodoro-Alonso et al., 2015; Bohnert, 2017; Koottatep et al., 2014; Lang & Smith, 2008; Spinks et al., 2006; Ziemba & Peccia, 2011). Pasteurisation usually requires heat input, which can be supplied by electricity, burning fuel, or solar energy. Given the rising costs of electricity and fossil fuels, coupled with supply difficulties due to political tensions and long-term depletion, as well as the current panorama to fight climate change, solar energy presents

an attractive alternative for pasteurisation, offering lower running costs and a more sustainable approach.

According to its geographical location in the globe and the irradiance received yearly, Bangladesh is a suitable country to implement solar-based technologies (Wazed et al., 2010). Hence, a solar pasteuriser is a viable technology to implement at the Rohingya refugee camp as an emergency sanitation response to prevent soil the contamination of soil and water from pathogens.

## 1.2. Problem statement

The Rohingya crisis of 2017 has led to the establishment of the largest refugee camp with more than one million of inhabitants, located near Cox's Bazar, Bangladesh, which poses significant sanitation challenges to the humanitarian response. In Camp 12, the IOM operates one decentralized wastewater treatment system (DEWATS) to treat approximately 3 $m^3$/day of faecal sludge from lined pit latrines, serving around 5,000 people, as depicted in Figure 2. The system separates solids and liquids through settlement and filtration, with digestion of solids under anaerobic conditions. The first two tanks act as traditional septic tanks, while subsequent tanks use coconut husks for upflow filtration. The treated effluent is then discharged into the ground through infiltration trenches. Nonetheless, while anaerobic processes are fundamentally designed to remove organic load in a DEWATS, removal of pathogens is also achieved, although not to the degree to comply with national and international standards. Therefore, the effluent can still present pathogens at levels representing a hazard for the local community, thereby the need of further treatment.

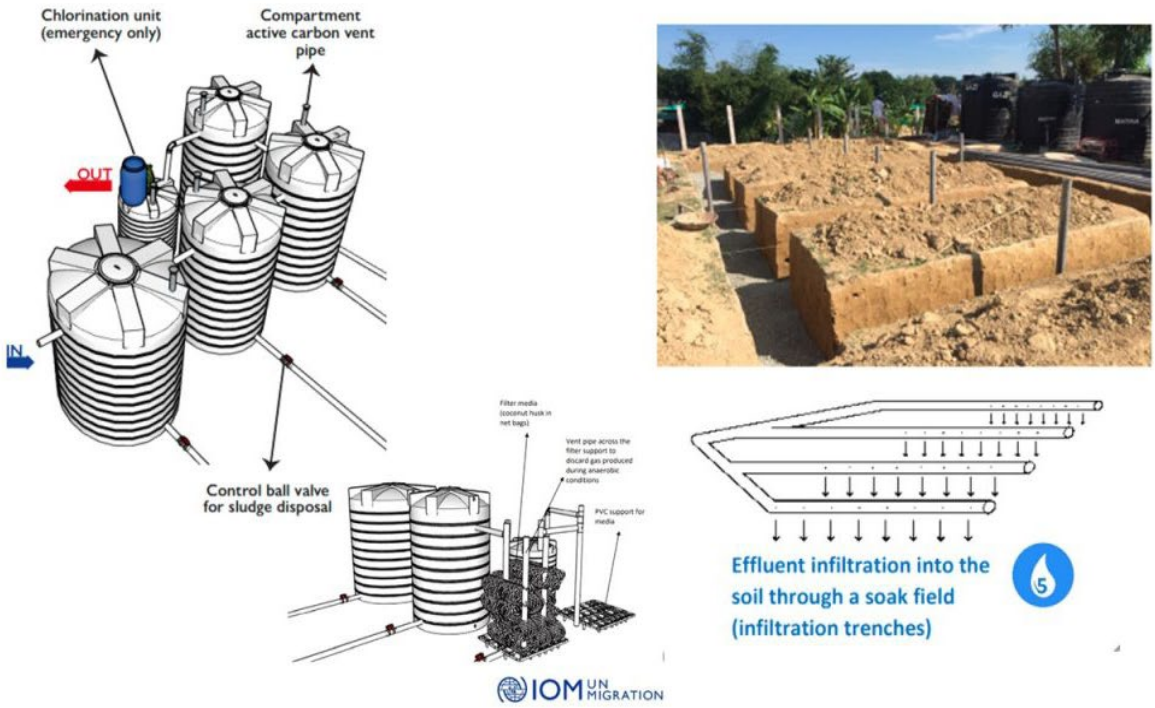


*Figure 2. Drawing of the IOM DEWATS system and photograph of the infiltration trenches* (SaniHUB, 2024)

A solar pasteuriser has been then installed in Camp 12 of the Rohingya refugee camp for the post-treatment of the effluent from the DEWATS (treated faecal sludge) before discharging it into the ground, with funding from the ELRHA. The solar pasteuriser has been developed by Veolia Foundation based on their Saniforce technology, which produces biogas through anaerobic digestion and burns it to generate the heat for pasteurisation. Due to space constraints, the system was modified to use solar thermal energy for the pasteurization process, rather than burning the biogas produced by the anaerobic digester. As the DEWATS in Camp 12 treats 3,000 L/day of faecal sludge, the solar pasteuriser needs to handle this amount daily.

Given the novelty of this technology, it is essential to assess its operation, performance, and techno-economic viability within the context of faecal sludge management at the Rohingya camp, as well as other contexts.

## 1.3. Research framework

### *1.3.1. Aim*

The aim of this project is to evaluate the feasibility of utilizing the solar pasteurizer to treat the effluent from a DEWATS that treats faecal sludge (FS) within Camp 12 of the Rohingya refugee camp, in particular for the prevention of cholera outbreaks. Additionally, the project seeks to assess the potential for replicating this approach in other humanitarian settings.

### 1.3.2. Specific objectives

The specific objectives of this work are as follow:

- To identify the maximum temperature achievable by the solar pasteurizer and its correlation with varying weather conditions.
- To characterize the thermal behaviour of the system.
- To determine the temperature-time conditions required for effective pathogen inactivation.
- To assess whether the solar pasteurizer can meet the target of treating 3,000 L/day of FS.
- To determine the optimal operating conditions that maximize pasteurization efficiency and the volume of treated FS.
- To identify areas for improvement and optimization of the system.
- To evaluate the techno-economic feasibility of the solar pasteurizer.
- To assess the replicability of the technology in other humanitarian settings.

### 1.3.3. Research questions

The research questions to be addressed in this project is as follows:

- What is the maximum temperature that can be achieved in the solar pasteurizer under varying weather conditions?
- What are the temperatures and holding times required to achieve effective pasteurization?
- What is the optimal temperature and holding time specific to meet our objectives?
- How does heating the sludge affect its organic (biodegradable and non-biodegradable) and nutrient content?
- What is the realistic amount of sludge that the technology can treat per day under our conditions, and what are the associated costs?
- In what ways can the technology be improved and optimized?
- How can this technology be replicated in other humanitarian settings?

### 1.3.4. Scope

This investigation will be conducted through field testing of the solar pasteurizer in Camp 12 of the Rohingya refugee camp in Bangladesh. Due to time constraints, tests will be carried out only from June to October. This period coincides with the monsoon and post-monsoon seasons, characterized by high rainfall and, consequently, lower solar irradiance. Therefore, the results will be obtained in the most pessimist case.

The feedstock of the solar pasteuriser was FS from pit latrines that was treated by a DEWATS. The scope includes characterizing the thermal behaviour and pasteurization performance of the system. This involves measuring temperature dynamics within the system and analysing

treated FS at different time intervals and temperatures to determine pathogen content and assess pasteurization effectiveness. Physiochemical parameters in the sludge will be also measured to evaluate the impact of the process on its properties. In addition, laboratory pasteurization tests will be conducted to compare field results and determine the pathogens deactivation kinetics. A model coupling the thermal dynamics and the microbial deactivation kinetics will be developed from the experimental data, and it will be used to predict the evaluate the overall performance of the system.

Using data from the thermal analysis, predictions of system performance throughout the year will be made through a solar assessment. Following this, a techno-economic analysis will be performed to estimate capital costs, including initial investment and running costs derived from the tests. Finally, the data obtained will extrapolated to refugee camps in other geographical contexts, along with solar assessments, to evaluate the replicability of the technology in different humanitarian settings.

## 1.4. Outline of the report

This report is structured to provide a detailed examination of the proposed solar pasteurization system for treating the effluent from a DEWATS (treated faecal sludge) in the Rohingya refugee camp. The following sections outline the content and objectives of each chapter:

- Introduction: This section introduces the context of the project, providing background information on the Rohingya camp and the public health hazards related to sanitation. It also discusses the implementation of DEWATS technology in Camp 12, managed by IOM, and explores solar pasteurization as a viable treatment option for the FS effluent produced by the system. The aim and objectives of the project are outlined, followed by a description of the report's scope and a brief overview of the structure.
- Methodology: This section presents the research approach and key methods used throughout the study. It includes a literature review, followed by detailed descriptions of the solar pasteurizer testing process, pasteurization laboratory tests, solar assessment, and techno-economic analysis. Additionally, replicability tests in various contexts and the development of a model to characterise the performance of the system are explained.
- Pasteurization Performance Analysis: This chapter focuses on the evaluation of the solar pasteurization system's effectiveness. It includes the characterization of DEWATS effluent after pasteurization, thermal behavior analysis of the solar pasteurizer, and an assessment of the expected treatment capacity, including pathogen removal, the volume of faecal sludge treated, and energy consumption.
- Solar Assessment: This section examines the environmental conditions critical for the system's performance, including weather patterns and sunshine conditions throughout the year. It also discusses the expected treatment capacity over the

course of the year and explores possible improvements to the system to optimize its performance.

- Techno-Economic Analysis: This section describes the techno-economic analysis based on
  different cases, including solar-only energy use for the pasteurization process, use of electric resistance and/or gas boiler as supplementary energy sources and the application of the improvements to the system.
- Replicability Tests: This section evaluates the potential for replicating the solar pasteurization system in other regions with similar needs. Case studies are presented for other refugee camp in Bentiu (South Sudan), Maiduguri (Nigeria), and Pemba (Mozambique), analysing the feasibility and potential challenges in each context.
- Conclusions and way forward: The final section summarizes the key findings and provides recommendations for future steps. It discusses the impact of the project and suggests avenues for further research or scaling up the system in other locations.

Each chapter of the report builds upon the previous one, providing a comprehensive understanding of the solar pasteurization system, its effectiveness, and its potential for broader application.

# 2. Methodology

This section outlines the methodology used in the project. It begins with a general description, followed by the literature review approach, details of field and laboratory tests, and subsequent data analysis. The methodology also covers the development of a model, solar assessment, techno-economic analysis, and replicability studies.

## 2.1. Literature review

The first step was conducting a literature review to understand the project's context and the technology involved. The review focused on Bangladesh and the Rohingya refugee camps but is applicable to similar settings globally. Key areas of investigation included:

- Rohingya Crisis and Health Challenges: Understanding the health problems caused by inadequate sanitation and hygiene in the camps, including identifying potential pathogens.
- Pasteurization Process: Examining the relationship between temperature and time in pathogen inactivation, with examples of pathogen inactivation in sludge matrices from existing literature.
- Solar Pasteurization: Assessing Bangladesh's suitability for solar energy, identifying solar pasteurization technologies used in water and sanitation applications, and determining key parameters for the process.
- Applicability Evaluation: Compiling information from the literature to predict process behaviour and identify optimal parameters to meet the project objectives.

A detailed literature review is available in Supporting Document A.

## 2.2. Research framework development

The research framework began with a detailed characterization of the study location. This initial step provided crucial context for understanding the environmental and operational conditions under which the solar pasteurizer would be deployed. A thorough description of the solar pasteurizer setup followed, offering insights into the design and components critical to the system's function. The framework also outlined the specific tests conducted during the project. Field tests focused on evaluating the treated effluent through physicochemical and microbial analyses, and the thermal behaviour of the system under different temperature and holding time conditions. These tests spanned various weather patterns to ensure comprehensive performance evaluation. Laboratory tests complemented the field experiments by replicating conditions on a smaller scale, enabling controlled pasteurization trials and microbial assessments to compare with the field data.

Data analysis formed a key component of the framework, leveraging results from both field and laboratory tests. This stage involved modelling and predicting the system's performance, estimating daily treatment volumes, and calculating energy consumption. Thermal data from field tests and microbial data from laboratory tests were combined to develop a model predicting the pasteurizer's performance under real-world operating conditions. A solar

assessment was then undertaken to identify weather patterns and predict system performance over a year based on the thermal data from the field tests. This included analysing potential modifications to improve the system.

A holistic approach was adopted to assess the techno-economic feasibility of the project in the current context and its potential applicability in other humanitarian settings. The capital and operational costs of the solar pasteurization installation were analyzed. Metrics such as specific energy consumption, costs, and surface area footprint were calculated for the current system and proposed improvements. The research framework included applying the solar assessment and techno-economic analysis to three additional geographical contexts: Bentiu (South Sudan), Maiduguri (Nigeria), and Pemba (Mozambique). This involved assessing system performance, energy consumption, and costs based on local conditions.

In overall, the research framework encompasses the characterisation of the study location, followed by an overview of the solar pasteurizer setup, the tests to conduct, and the data analysis to perform. Finally, it outlines the methodology used to assess the project's feasibility in our context and its potential applicability in other humanitarian settings. The research framework is summarized in Figure 3, with further details available in the research framework report.

The Research Framework is detailed in Supporting Document B.

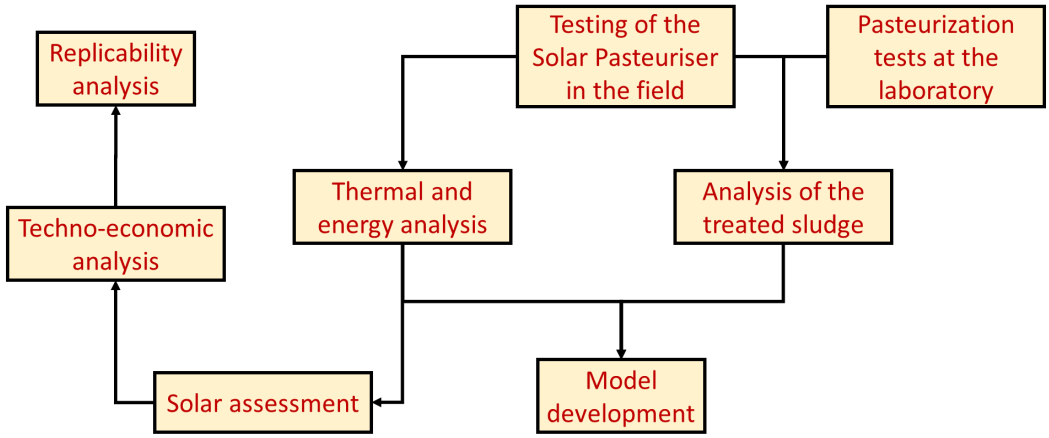


*Figure 3. Summary of the research framework*

## 2.3. Pasteurization tests

The following section describes the solar pasteurizer installation and outlines the pasteurization tests conducted at the field and laboratory as part of the project.

### *2.3.1. Description of solar pasteurizer installation*

A solar pasteurizer was installed at Camp 12, adjacent to the decentralised wastewater treatment plant system (DEWATS), which processes faecal sludge (FS) from local pit latrines.

The DEWATS facility treats liquid slurry FS with less than 3% total solids, processing approximately 3,000 L per day.

Veolia Foundation developed the solar pasteurizer, which was commissioned between late May and early June 2024. System modifications and installations have been ongoing since that time. A list of these modifications can be found in Appendix A.

The system comprises several key components, detailed in Table 1. Photographs of the system are displayed in Figure 4. Figure 5 presents the final installation layout. Additional photographs can be found in Appendix B. The process flow diagram can be found in Supporting Document C.

*Figure 4. Photographs of the installation*

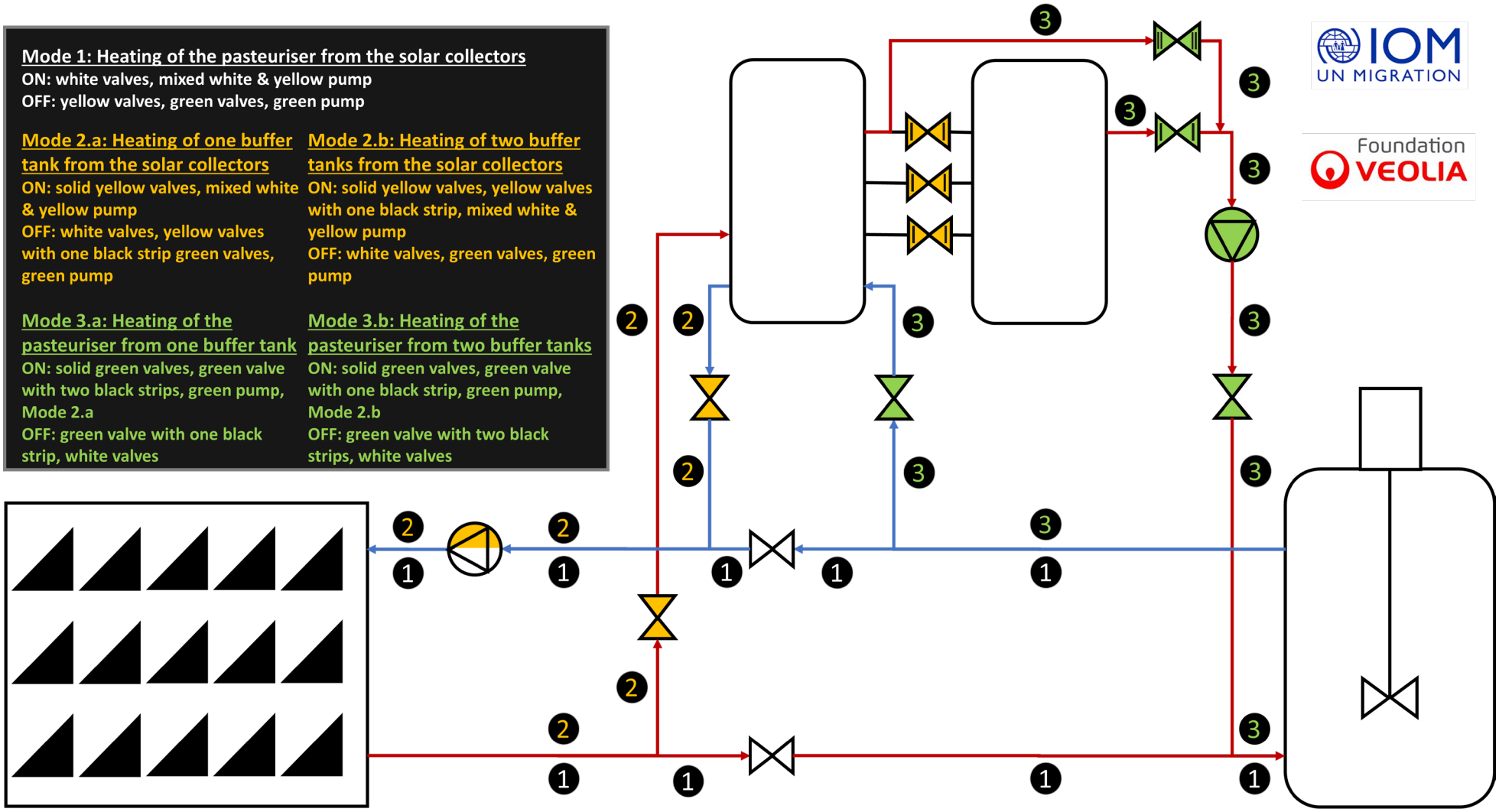


*Figure 5. Solar pasteurisation installation scheme with operating modes*

*Table 1. List of the key components from the solar pasteuriser installation*

| Component of the installation | Function | Quantity | Specifications |
|---|---|---|---|
| Flat plate solar collectors | Harness solar thermal energy | 15 | Absorber surface area: 2.28 $m^2$/unit |
| Buffer tank | Storage the heat from the solar energy | 2 | Volume: 800 L/unit |
| Pasteuriser tank | Pasteurisation | 1 | Volume: 500 L |
| Blade stirrer | Stirring the pasteuriser for enhanced and homogenous heating | 1 | Power: 500 W |
| Electric resistance | Heating of the buffer tanks | 2 | Power: 3000 W |
| Circulation pumps | Circulation of the water heat carrier through the system | 3 | Power: 33 – 60 W<br>Head: up to 1.4 bar<br>Flowrate: up to 25 L/min |
| Temperature sensors (electronic sensors and mechanical gauges) | Measurement of temperature at different locations of the installation | 11 | - |
| Float flowmeter | Measurement of the heat carrier flowrate | 2 | - |
| Pressure gauge | Measurement of pressure in the system | 2 | - |
| Pressure booster | Automatic pressurization of the system after a pressure decrease below 2 bar | 1 | Power: 180 – 2200 W<br>Head: up to 3.34 bar |
| Photovoltaic (PV) panels | Generation of electricity from the solar energy for the system | 3 | Capacity: 330 Wp/unit |
| Inverter | Transformation of the direct current from the PV panels to alternative current | 1 | Capacity: 2400 W |
| Battery | Store the surplus of electricity generated by the PV panels | 2 | Capacity: 130 AH |
| Diesel generator | Generation of electricity for the electric resistance and pressure booster | 1 | Capacity: 3 kW |

The pasteurizer operates in three distinct modes:

- Mode 1: Heated water from the solar collectors directly heats the pasteurizer tank through a heating jacket.
- Mode 2: Heated water from the solar collectors is used to heat the buffer tanks via a heating coil. Mode 2a utilizes one buffer tank, while Mode 2b uses two tanks.

- Mode 3: Hot water stored in the buffer tanks is used to heat the pasteurizer through the heated jacked. Mode 3a involves one buffer tank, while Mode 3b uses two tanks.

Modes 1 and 2 operate within the primary hydraulic circuit, whereas Mode 3 functions within a secondary hydraulic circuit. Both circuits maintain a pressure of approximately 2 to 2.5 bar, with a heat carrier water flow rate of up to 27 L/min. In Mode 2, heat carrier water flow rate is regulated with respect to the temperature differential between the collector outlet and the buffer tank heating zone. If this difference decreases, the flow rate is reduced. Circulation halts if the buffer tank temperature exceeds that of the collectors.

The standard operating procedure of the solar pasteurizer can be consulted in the Supporting Document D.

### *2.3.2. Tests in the solar pasteurizer*

Testing was conducted during two experimental campaigns from June to October 2024. Tests typically began between 8 and 10 AM and concluded between 1 and 4 PM depending on the conducted test.

The first experimental campaign, from June 5 to July 10, focused exclusively on Modes 2b and 3b, as hydraulic connections to integrate the solar collector to the pasteurizer and bypass one of the tanks were not yet established. Only one pasteurization batch per day was conducted under Mode 3b. The second campaign, from September 9 to October 30, tested all operating modes, with multiple pasteurization batches conducted daily.

*Table 2. Analyses conducted in the raw and treated samples at different temperature and holding time*

| Type of analysis | Parameter measured | Reason to conduct analysis |
|---|---|---|
| Microbial analysis | Escherichia coli | To characterize pathogen content |
| | Vibrio cholerae | |
| | Ascaris eggs | |
| | Rotavirus | |
| | Norovirus (GI and GII) | |
| | Pepper mild mottle virus | |
| Physiochemical analysis | Total solids | To characterise the pollution content |
| | Total suspended solids | |
| | Chemical oxygen demand | |
| | Biological oxygen demand | |
| | Total nitrogen | To characterise the nutrient content |
| | Ammonium | |
| | Nitrates | |
| | Total phosphorous | |
| | Phosphates | |
| | pH | To characterise the acido-basic behavior |

Most tests were performed using water as feedstock to assess the system's thermal performance. The effluent from DEWATS (i.e. treated faecal sludge) was used as feedstock selectively for laboratory analysis. Pasteurization tests were conducted at five target temperatures (50°C, 55°C, 60°C, 65°C, and 70°C) and five holding times (0, 15, 30, 60, and 120 minutes). The tests conducted in the solar pasteuriser are summarised in Appendix C.

Sample analysis was performed at the FS laboratory from the International Centre for Diarrhoeal Disease Research, Bangladesh (ICDDR'B) in Dhaka, Bangladesh. Samples include raw FS and pasteurized effluent at the various temperatures and holding times. The analysis included the determination of the microbiological and physicochemical properties displayed in Table 2. The protocols including for the effluent analysis can be seen in Supporting Document E.

## 2.4. Pasteurisation tests at the laboratory

Additional pasteurization tests were conducted in the laboratory by heating faecal sludge on a magnetic stirrer to predetermined temperatures. After specified holding times, small samples was collected for microbial and physicochemical analysis.

Microbial analysis focused on Escherichia coli and faecal coliforms (TC), while physicochemical tests measured total solids, suspended solids, volatile solids, pH, electrical conductivity, total phosphorus, total nitrogen, and ammonia. Testing explored temperatures ranging from 50°C to 80°C and holding times between 5 minutes and 3 hours. Figure 6 provides visual representation of the laboratory pasteurisation tests setup.


*Figure 6. Laboratory pasteurisation tests setup*

The first stage of testing took place in Delft, Netherlands, using local wastewater. The second stage occurred at Cox's Bazar, Bangladesh, using the same DEWATS effluent than the one from the pilot tests. This work was conducted by an intern from the International Institute for Hydraulic and Environmental Engineering in Delft (IHE-Delft), with funding from the Netherlands Enterprise Agency (RVO) and a collaboration with the faecal sludge management laboratory from the Department of Public Health Engineering. More information is available in the internship report in Supporting Document F.

The data from the laboratory tests at ICDDR'B and IHE Delft is compiled in Supporting Document G.

### *2.4.1. Data analysis*

The data analysis from the tests in the field encompassed:

- Weather conditions (irradiance, air temperature, sky conditions);
- Heating rates, power, heat transfer, and efficiency of solar collectors, tanks, and the pasteurizer;
- Heat losses in buffer tanks and pasteurizer;
- Overall thermal efficiency and energy consumption;
- Usable fraction of solar energy.

Analysis relied on the technical specifications of the different components of the system, temperature and flowrate measurement for heat balance calculations, electricity consumption readings from the inverter of the PV system, and daily weather data provided by the Bangladesh Weather Service. Global Horizontal Irradiance (GHI) was converted to Global Tilted Irradiance (GTI) at a 20° tilt (matching the collectors inclination) using Solargis software results showing the difference between two metrics at a given month.

The equations for the determination of the different parameters are shown in Appendix D. The results from the first and second experimental campaign are shown in Supporting Document H and I respectively, while the compilation of the results can be found in Supporting Document J.

### *2.4.2. Pasteurisation model*

A model was developed by combining thermal data from the pilot tests and microbial data from laboratory experiments. This model predicts system performance under varying operational modes and weather conditions, enabling the estimation of daily batch capacity and electrical energy consumption. The model development is described in Appendix C.

The deactivation model for E. coli was derived using the Chick-Watson approach, based on data from the wastewater tests conducted in Delft. Due to measurement issues with E. coli in the DEWATS effluent, the model could not be calibrated with data from our geographical context. Therefore, results from this model should be interpreted with caution.

Tank and pasteurizer heating were modeled using experimentally determined heat transfer coefficients. The collector temperatures was calculated using an empirical correlations as a function of the total irradiance observed during experiments. Heat losses in the pasteurizer and storage tanks were factored into the model using empirical expressions obtained through testing.

The pasteurization model is available in Supporting Document K.

## 2.5. Analytical methods for the assessment of the process techno-economic viability

### *2.5.1. Solar assessment*

The solar assessment aimed to evaluate the system's year-round performance. The process began by determining the typical meteorological year (TMY) data, including monthly average irradiance data considering different tilting plane angles, daylight hours, and other relevant weather parameters such as air temperature and rainfall. This data was obtained using Solargis software at the coordinates from the DEWATS installation at Camp 12, i.e. 21.178665, 92.153898 (21°10'43", 092°09'14").

Once acquired, the irradiance data was combined with performance metrics from pilot field tests to calculate the treatment capacity of the pasteurizer. For this, the total energy available for the system in a day was calculated through the irradiance values at a selected titling angle, the total surface offered by the collectors and the overall system efficiency. From this calculation, the volume that can be heated to the target pasteurization temperature was ascertained.

The first phase of this study assessed the system in its current state. In the second phase, potential improvements were proposed and tested by adjusting specific parameters within the solar assessment model to predict enhanced performance outcomes.

### *2.5.2. Techno-economic analysis*

A techno-economic analysis was conducted for the existing system, followed by evaluations under various scenarios reflecting the potential system improvements outlined. The analysis encompassed capital and operating costs required for system operation and maintenance. Capital costs considered only material expenses for each scenario, while operating costs included fuel consumption and consumables, excluding salaries. The analysis also accounted for the system's surface area footprint.

Key performance indicators summarizing the techno-economic analysis included:

- Specific operating and capital costs – expressed in € per $m^3$ of treated effluent;
- Specific energy consumption – measured as electricity use in kWh per $m^3$ of treated effluent;
- Specific surface area – measured in $m^2$ per $m^3$ of treated effluent.

### *2.5.3. Replicability analysis*

The solar assessment and techno-economic analysis were extended to evaluate the system's replicability across three three densely populated humanitarian settings  located in different geographical regions:

- Bentiu, South Sudan – Coordinates: 9.26, 29.8 (09°15'36", 029°48'00").
- Maiduguri, Nigeria – Coordinates: 11.839538, 13.153621 (11°50'22", 013°09'13").
- Pemba, Mozambique – Coordinates: -12.9645, 40.517 (-12°57'52", 040°31'01").

Figure 7 illustrates their global locations. The objective was to assess the feasibility of deploying the system in these areas. Solargis software provided the TMY data for each site. Performance metrics from the pilot system were applied to predict treatment capacity, costs, energy consumption and surface area footprint from the techno-economic analysis model.

Two scenarios were covered: one representing the pasteurizer configuration currently used in Camp 12, and the other reflecting the most optimal conditions identified from the techno-economic analysis.

*Figure 7. Localisation in the globe of the displacement sites in Pemba, Mozambique (yellow pin), Bentiu South Soudan (red pin) and Maiduguri, Nigeria (blue pin)*

The methodology followed for the solar assessment coupled to the techno-economic and replicability analysis is described in Appendix F. The solar assessment and techno-economic analysis is available in Supporting Document L, M, N and O for the Rohingya Camp, Bentiu, Maidugauri and Pemba, respectively.

# 3. Pasteurization performance analysis

This chapter provides a comprehensive analysis of the performance of the solar pasteurization system used for the treatment of the effluent of a decentralized wastewater treatment system (DEWATS), corresponding to faecal sludge from pit latrines, at the Rohingya refugee camp. The focus is primarily on the system's capacity to destroy microbial contaminants during pasteurization tests, as well as the thermal behavior of the system under varying operational conditions.

In addition to microbial destruction, the chapter explores the physicochemical properties of the effluent post-pasteurization. These parameters are critical in assessing the overall quality of the treated effluent and determining compliance with relevant national and international water discharge regulations.

The analysis includes:

- Microbial Destruction Efficiency – Evaluating the extent to which the pasteurization process reduces pathogens such as Escherichia coli, Ascaris eggs, and rotavirus A (RVA).
- Thermal Behavior – Assessing how the solar pasteurizer's components (including collectors, buffer tanks, and the pasteurizer itself) respond to different irradiance levels, heating rates, and heat retention.
- Physicochemical Properties – Examining parameters such as chemical oxygen demand (COD), biological oxygen demand (BOD), total nitrogen (TN), total phosphorus (TP), total solids (TS), and total suspended solids (TSS) to determine how pasteurization affects the effluent's organic and nutrient content.
- Regulatory Comparison – Comparing the treated effluent's quality to existing environmental discharge standards to evaluate compliance and identify areas requiring further treatment or downstream processes.

By the end of this chapter, the performance of the solar pasteurizer will be assessed in detail, providing insights into its strengths, limitations, and areas for potential optimization.

## 3.1. Characterization of the DEWATS effluent after pasteurization

The characterization of DEWATS effluent following pasteurization involved a comprehensive analysis of both microbial content and physicochemical properties. Microbial analysis focused on identifying the presence and reduction of pathogens, including coliforms and E. coli, to assess the effectiveness of the pasteurization process. Physicochemical parameters, such as pH, turbidity, COD and nutrient concentrations, were measured to evaluate the overall quality of the effluent and its suitability for potential reuse or discharge.

This dual approach provides insights into the effluent's compliance with regulatory standards and its potential impact on the environment or downstream applications.

The summary of the results from the microbial and physio-chemical properties can be observed in Supporting Document E.

### 3.1.1. Microbial analysis

Microbial analysis of the DEWATS effluent was conducted by ICDDR'B to evaluate the effectiveness of the pasteurization process in reducing pathogen concentrations. The results, presented in Table 3, reveal important insights into the behavior of different microorganisms under varying pasteurization conditions.

*Table 3. Concentration of E. coli, Ascaris and RVA during testing of the solar pasteuriser pilot*

| Pasteurisation | | E.Coli (cfu / 100 ml) | | | Ascaris (eggs/L) | | | RVA (gc/L) | | |
|---|---|---|---|---|---|---|---|---|---|---|
| T (°C) | t (min) | Test 1 | Test 2 | Test 3 | Test 1 | Test 2 | Test 3 | Test 1 | Test 2 | Test 3 |
| 50 | 0 | 5600 | 5700 | - | 0 | 0 | - | 339707 | - | - |
| | 15 | 300 | 280 | - | 0 | 0 | - | 327277 | - | - |
| | 30 | 1700 | 1800 | - | 80 | 80 | - | 331611 | - | - |
| | 60 | 1000 | 1000 | - | 0 | 0 | - | 313922 | - | - |
| | 120 | 3000 | 2900 | - | 0 | 0 | - | 599446 | - | - |
| 55 | 0 | 0 | 1300 | 1200 | 0 | 240 | 240 | 10562 | 7129 | 818908 |
| | 15 | - | 0 | 0 | - | 0 | 0 | - | 11180 | 410682 |
| | 30 | 0 | 0 | 0 | 1360 | 0 | 0 | 82629 | 12249 | 480238 |
| | 60 | 0 | 0 | 0 | 360 | 1200 | 1200 | 40650 | 1910 | 512132 |
| | 120 | 100 | 0 | 0 | 180 | 0 | 0 | 51009 | 429 | 371326 |
| 60 | 0 | 450 | 6900 | 7000 | 0 | 0 | 0 | 14430 | 279824 | - |
| | 15 | 0 | 0 | 0 | 1200 | 7000 | 7000 | 26372 | 305527 | - |
| | 30 | 0 | 0 | 0 | 600 | 2800 | 3200 | 21621 | 282839 | - |
| | 60 | 0 | 0 | 0 | 1000 | 2000 | 1800 | 16630 | 475119 | - |
| | 120 | 0 | 0 | 0 | 1400 | 2800 | 2800 | 14741 | 290831 | - |
| 65 | 0 | 800 | 47000 | 52000 | 0 | 320 | 320 | 19717 | 110146 | - |
| | 15 | 0 | 0 | 0 | 0 | 0 | 0 | 8009 | 228274 | - |
| | 30 | 0 | 0 | 0 | 0 | 0 | 0 | 3940 | 192717 | - |
| | 60 | 0 | 0 | 0 | 40 | 60 | 60 | 6852 | 288967 | - |
| | 120 | 0 | 0 | 0 | 7 | 0 | 0 | 5196 | 255735 | - |
| 70 | 0 | 2800 | 2700 | - | 20 | 20 | - | 298482 | - | - |
| | 15 | 0 | 0 | - | 0 | 0 | - | 12230 | - | - |
| | 30 | 0 | 0 | - | 0 | 0 | - | 50753 | - | - |
| | 60 | 0 | 0 | - | 0 | 0 | - | 50753 | - | - |
| | 120 | 0 | 0 | - | 0 | 0 | - | 32878 | - | - |

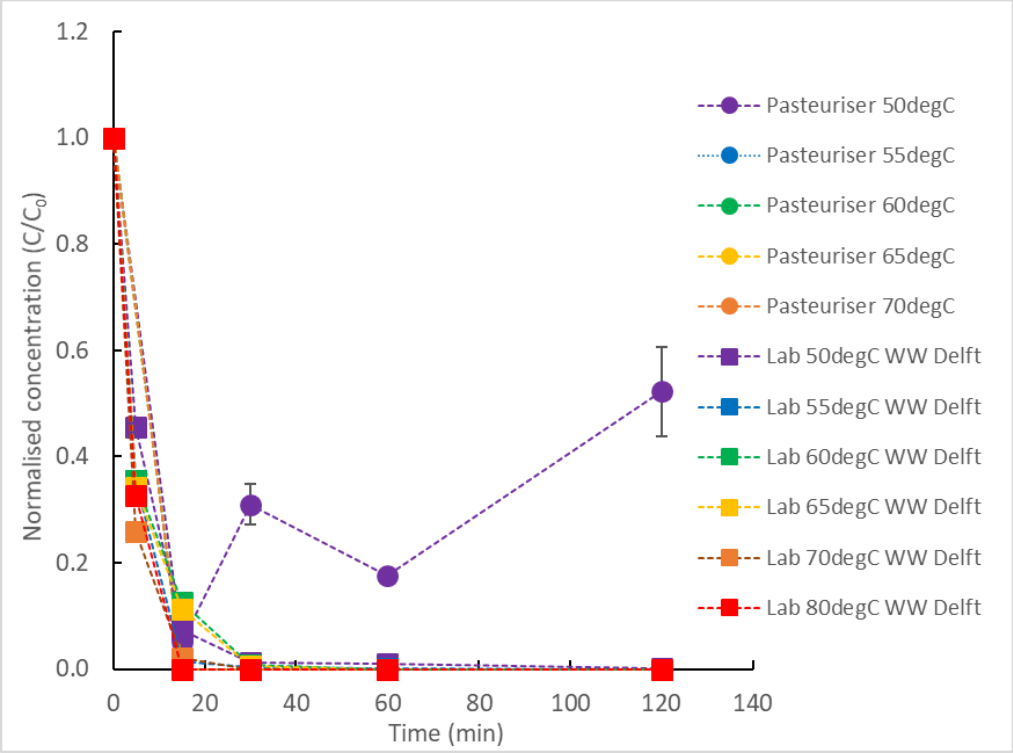


*Figure 8. Normalised concentration of E. coli after the pasteurisation tests at the solar pasteuriser pilot and at the laboratory using wastewater from Delft, Netherlands*

At 50°C, E. coli was detected, indicating partial elimination but not complete inactivation. However, at temperatures exceeding 55°C, no E. coli was observed, confirming that higher temperatures are essential for effective pathogen removal. A comparison between effluent from the Rohingya camp and wastewater from Delft showed that E. coli in the DEWATS effluent appeared more resistant at 50°C (Figure 8). This discrepancy could be attributed to environmental adaptation, as E. coli strains in Bangladesh may have developed greater tolerance to high temperatures compared to those in the Netherlands. Despite this, at temperatures above 55°C, the inactivation trend for E. coli was consistent across both effluent sources, suggesting that the resistance observed at lower temperatures is overcome with sufficient heat.

Ascaris eggs were not detected at 70°C, suggesting complete inactivation at this temperature. At lower temperatures, however, Ascaris eggs were sometimes present, though the results appeared inconsistent. This inconsistency likely stems from variability in the measurement process rather than the pasteurization conditions themselves, raising concerns about the reliability of the detection methods used. While the data suggests higher temperatures are necessary for full inactivation, the irregular results at lower temperatures highlight the need for improved measurement techniques to accurately assess parasitic inactivation.

The pasteurization process had limited impact on RVA, with only slight reductions observed at 70°C and negligible effects at lower temperatures. This finding underscores the challenge of inactivating viral pathogens, which appear to be more heat-resistant than bacterial or parasitic contaminants.

Neither Salmonella nor Vibrio cholerae were detected in the DEWATS effluent samples, and as a result, these pathogens were not assessed during pasteurization tests. Other viruses, including Pepper Mild Mottle Virus (PPMoV) and norovirus, were present in the effluent but were not affected by the pasteurization process at any of the temperatures tested.

These results demonstrate that while pasteurization at temperatures above 55°C is effective in eliminating bacterial contaminants such as E. coli, higher temperatures or additional disinfection methods may be necessary to achieve comprehensive inactivation of parasitic and viral pathogens.

### *3.1.2. Physiochemical properties*

The analysis of pasteurization laboratory tests, as detailed in Table 4, indicates no significant change in COD and BOD. This suggests that pasteurization does not substantially affect the organic matter content of the effluent. Despite the application of heat, the levels of COD and BOD remain relatively stable, indicating that the pasteurization process does not break down or remove organic pollutants to any measurable extent.

*Table 4. Physiochemical properties of the DEWATS effluent after the pasteurisation laboratory tests*

| Pasteurisation | | BOD (mg/L) | COD (mg/L) | TN (mg/L) | TP (mg/L) | TS (g/L) | TSS (g/L) |
|---|---|---|---|---|---|---|---|
| T (°C) | t (min) | | | | | | |
| 50 | 0 | 372 ± - | 1260 ± 10 | 645 ± 1 | 94 ± 0 | 1.00 ± - | 0.17 ± 0.03 |
| | 30 | 349 ± - | - ± - | - ± - | - ± - | - ± - | - ± - |
| | 60 | - ± - | 1375 ± 21 | 632 ± 6 | 46 ± 1 | 0.95 ± 0.21 | 0.10 ± 0.00 |
| | 120 | - ± - | 1250 ± 0 | 617 ± 1 | 86 ± 0 | 0.90 ± 0.14 | 0.18 ± 0.07 |
| 65 | 0 | 372 ± - | 1260 ± 10 | 645 ± 1 | 94 ± 0 | 1.00 ± - | 0.17 ± 0.03 |
| | 30 | 268 ± - | - ± - | - ± - | - ± - | - ± - | - ± - |
| | 60 | - ± - | 1385 ± 7 | 627 ± 1 | 64 ± 0 | 0.90 ± 0.14 | 0.13 ± 0.05 |
| | 120 | - ± - | 1250 ± 0 | 617 ± 1 | 34 ± 0 | 0.85 ± 0.07 | 0.15 ± 0.07 |
| 80 | 0 | 372 ± - | 1260 ± 10 | 645 ± 1 | 94 ± 0 | 1.00 ± - | 0.17 ± 0.03 |
| | 30 | 241 ± | - ± - | - ± - | - ± - | - ± - | - ± - |
| | 60 | - ± - | 1325 ± 21 | 599 ± 1 | 55 ± 1 | 0.95 ± 0.07 | 0.12 ± 0.02 |
| | 120 | - ± - | 1290 ± 14 | 607 ± 6 | 44 ± 2 | 0.85 ± 0.21 | 0.17 ± 0.00 |

However, reductions in TN and TP were observed, suggesting that pasteurization may have a slight impact on nutrient concentrations. The decrease in TN is likely due to the volatilization of ammonia, a common outcome when nitrogenous compounds are exposed to high temperatures. This is a plausible explanation for the observed nitrogen loss, as ammonia is prone to evaporate under thermal conditions.

The reduction in TP, however, is less easily explained. Phosphorus compounds are generally non-volatile, and the formation of precipitates at elevated temperatures is unlikely, given that no decrease in TSS was recorded. The absence of TSS reduction suggests that no significant

precipitation occurred during pasteurization. As a result, the mechanism behind the observed decline in TP remains uncertain and warrants further investigation.

*Table 5. Comparison of the physiochemical properties of the DEWATS effluent after tests in the pilot solar pasteuriser compared to the regulations (black filling: non measured; red filling: non-compliant to any of the regulations; yellow filling: compliant with both regulations)*

| Pasteurisation | | pH | BOD (mg/L) | COD (mg/L) | $NO_3^-$ (mg/L) | $PO_4^{-3}$ (mg/L) | TSS (g/L) | TC (CFU/100 ml) |
|---|---|---|---|---|---|---|---|---|
| T (°C) | t (min) | | | | | | | |
| 50 | 0 | 8.16 | 149 | 507 | 86.04 | 100.32 | 0.223 | 5650 |
| | 15 | 7.87 | | | | | - | 290 |
| | 30 | 7.87 | | | | | - | 1750 |
| | 60 | 7.88 | 165 | 654 | 88.98 | 115.48 | 0.323 | 1000 |
| | 120 | 7.89 | | | | | - | 2950 |
| 55 | 0 | 9.19 | 129.5 | 503 | 97.645 | 41.395 | 0.0945 | 833 |
| | 15 | 7.81 | 126 | 487 | 72.08 | 51.41 | 0.067 | 0 |
| | 30 | 8.505 | 172.5 | 1037.5 | 94.95 | 40.02 | 0.4865 | 0 |
| | 60 | 8.56 | 171 | 1001.5 | 93.89 | 38.005 | 0.473 | 0 |
| | 120 | 8.625 | 181.5 | 990.5 | 89.67 | 38.195 | 0.4825 | 33 |
| 60 | 0 | 8.82 | 142 | 531 | 118.59 | 42.93 | 0.093 | 4783 |
| | 15 | 8.155 | 261 | 1534 | 103.84 | 40.6 | 0.771 | 0 |
| | 30 | 8.365 | 261 | 1462 | 108.85 | 38.73 | 0.8 | 0 |
| | 60 | 8.34 | 262 | 1501 | 101.96 | 39.59 | 0.616 | 0 |
| | 120 | 8.34 | 244 | 1553 | 101.68 | 35.53 | 0.683 | 0 |
| 65 | 0 | 7.95 | 133 | 498 | 70.06 | 46.05 | 0.113 | 33267 |
| | 15 | 7.545 | 151 | 573 | 71.9 | 47.83 | 0.156 | 0 |
| | 30 | 7.555 | 147 | 581 | 70.83 | 48.02 | 0.145 | 0 |
| | 60 | 7.575 | 142 | 587 | 70.93 | 47.36 | 0.206 | 0 |
| | 120 | 7.65 | 141 | 581 | 69.67 | 42.78 | 0.15 | 0 |
| 70 | 0 | 7.88 | 162 | 492 | 88.08 | 111.62 | 0.115 | 2750 |
| | 15 | 7.61 | | | | | - | 0 |
| | 30 | 7.66 | | | | | - | 0 |
| | 60 | 7.65 | 180 | 464 | 88.08 | 97.76 | 0.176 | 0 |
| | 120 | 7.72 | | | | | - | 0 |
| **The Environment Conservation Rules 1997, Ministry of Environment and Forest. Schedule 9 - Standards for Sewage Discharge** | | - | 40 | - | 250 | 35 | 0.1 | 1000 |
| **Department of Environment Guidelines update 5 March 2023, Schedule 3 - Standards for Sewage Discharge** | | 6<br>9 | 30 | 125 | 50 | 15 | 0.1 | 1000 |

A slight decrease in TS was also noted, which may be attributed to the volatilization of certain organic compounds during the heating process. Although the reduction is modest, it reflects the potential for minor losses of volatile substances during pasteurization. This effect, while not pronounced, indicates that thermal treatment can influence the physical and chemical composition of the effluent, albeit to a limited extent.

The results from field pasteurization tests, as outlined in Table 5, were compared to existing regulatory standards for effluent discharge. The pH of the effluent was found to be slightly basic, yet it remained within the acceptable limits specified by regulations. This aligns with the findings from laboratory pasteurization, suggesting that the pasteurization process does not significantly alter the pH of the treated effluent.

Despite this compliance in pH, no consistent trend was observed in BOD or COD. The absence of a clear reduction in these parameters indicates that pasteurization alone does not effectively reduce the organic load of the effluent. As a result, the pasteurized effluent did not meet regulatory thresholds for BOD and COD, underscoring the need for additional treatment steps to achieve full compliance.

Regarding nutrient levels, nitrate concentrations complied with at least one of the regulatory standards. However, phosphate levels consistently exceeded permissible limits, indicating that pasteurization has little to no effect on phosphorus removal. Similarly, TSS did not show significant reductions, suggesting that the physical separation of particulate matter is not enhanced by the pasteurization process.

Although Total Coliforms (TC) were not directly measured in this study, the absence of E. coli in pasteurized effluent suggests that TC levels are likely minimal or non-existent. This inference aligns with the understanding that E. coli serves as a reliable indicator of faecal contamination, and its complete inactivation implies effective microbial reduction across the effluent.

In summary, the solar pasteurizer demonstrates strong efficacy in pathogen removal, particularly for E. coli. However, its influence on physicochemical properties such as organic load and nutrient concentrations is minimal. Consequently, while the pasteurizer contributes positively to microbial safety, achieving full regulatory compliance for effluent discharge depends on the integration of downstream processes. Pasteurization serves as an important step in pathogen control but is insufficient as a standalone treatment method for complete effluent quality management.

## 3.2. Thermal and energy characterisation of the solar pasteurizer

This section characterizes the thermal performance of the solar pasteurizer and its sub-components. Weather data is presented to provide context for the conditions under which the data was collected. The thermal analysis encompasses heating rates, energy transfer, and efficiency at both the component and system levels.

It also allows to understand performance differences between operational modes, highlighting variations in thermal behavior and energy utilization. Additionally, patterns in the

use of solar thermal energy and overall energy consumption are identified, contributing to a comprehensive assessment of the system's operational dynamics and efficiency.

The energy and thermal analysis of each test can be found in Supporting Document F and G for the first and second experimental campaign, respectively. Supporting Document H compiles the overall of this data.

### *3.2.1. Weather conditions during the tests*

Testing of the solar pasteurizer was conducted between June and October, during which significant variations in irradiance were observed. Average irradiance during this period ranged from 100 to 700 W/m², with peak values reaching up to 900 W/m², as illustrated in Figure 9. These fluctuations in solar energy availability highlight the dynamic nature of weather conditions in the region and the impact of daily and seasonal changes on pasteurizer performance.

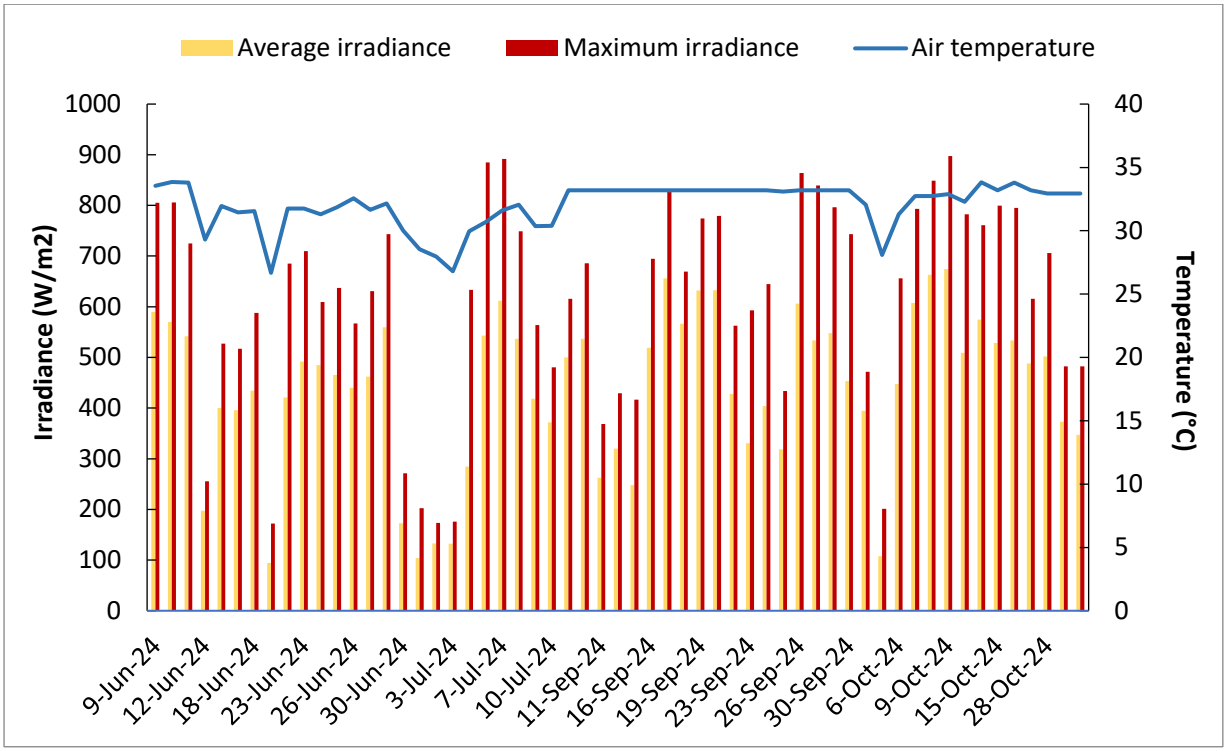


*Figure 9. Daily average and peak irradiance, and average air temperature, during the tests in the solar pasteuriser*

The first experimental campaign, carried out from June to July, experienced lower irradiance levels compared to the second campaign conducted between September and October. This discrepancy is likely attributable to the monsoon season, which typically spans June and July and is characterized by heavy cloud cover and frequent rainfall, limiting the availability of direct sunlight. In contrast, irradiance levels were generally higher and more stable during the

September to October period, reflecting the transition to post-monsoon conditions with clearer skies and increased solar exposure.

Throughout the testing period, air temperatures remained relatively stable, fluctuating between 27°C and 34°C. This consistency in ambient temperature provided a stable thermal environment for the pasteurizer, minimizing the influence of external temperature variations on system performance.

The observed differences in irradiance between the two testing periods underscore the seasonal dependence of solar pasteurization systems. These findings highlight the importance of accounting for local climatic conditions when designing and optimizing solar-based treatment processes, particularly in regions subject to monsoon seasons or other weather patterns that may reduce solar availability.

### *3.2.2. Thermal characterization of the individual components*

The thermal performance of the solar pasteurizer's key components, including the collectors, pasteurizer, and buffer tanks, is summarized in Table 6. The analysis considers scenarios involving one or two buffer tanks and examines the differences between operational Modes 2 and 3.

*Table 6. Summary of the thermal characterization of each of the main components of the solar pasteuriser pilot*

| | Heating rate (°C/h) | Power (kW) | Heat (kWh) | Efficiency | Heat loss rate (°C/h) |
|---|---|---|---|---|---|
| **Collectors** | - | 6.7 ± 6.3 | 17.2 ± 3.7 | 37% ± 27% | - |
| **Pasteurizer** | 9.7 ± 4.7 | 5.4 ± 2.7 | 11.3 ± 5.3 | 97% ± 53% | 0.3 ±0.5 |
| **Buffer tanks in Mode 2a** | 4.7 ± 1.7 | 3.7 ± 2.0 | 16.4 ± 13.3 | - | 0.2 ± 0.1 |
| **Buffer tanks in Mode 2b** | 2.2 ± 1.5 | 3.7 ± 2.2 | 13.3 ± 11.7 | 74% ± 30% | 0.2 ± 0.2 |
| **Buffer tanks in Mode 2a** | 0.5 ± 4.6 | 0.8 ± 3.6 | -1.4 ± 14.1 | - | 0.2 ± 0.1 |
| **Buffer tanks in Mode 2b** | -2.2 ± 3.3 | -4.0 ± 5.6 | -5.3 ± 9.6 | - | 0.2 ± 0.2 |

The collectors demonstrated an average efficiency of approximately 37%, with significant variation depending on irradiance and environmental conditions. When compared to values reported in the literature (Figure 10), this efficiency falls within the expected range, indicating that the collectors perform well under typical operational conditions.

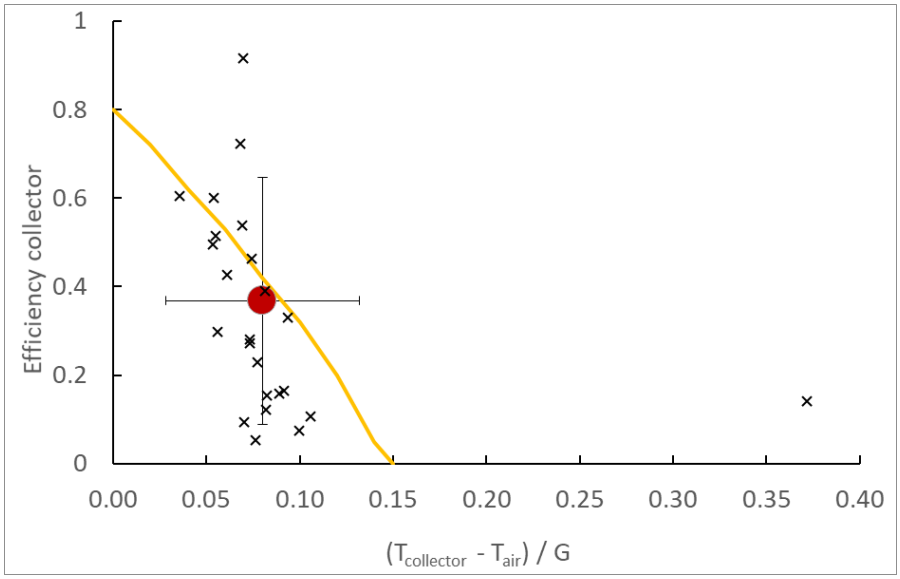


*Figure 10. Efficiency of the collectors measured during the pasteurisation tests (cross: individual experimental points; red dot: the average) compared to the results from literature showed by a yellow line*

The pasteurizer exhibited near-total efficiency, with performance approaching 100%. The pasteurizer heats faster than the buffer tanks, primarily due to its lower volume and higher surface area, which enhance heat transfer. Since the heat transfer coefficient is similar for both the pasteurizer and the buffer tanks (approximately 150 W/m²/°C), the difference in heating rate can be attributed to the pasteurizer's design, which facilitates more efficient thermal exchange. As expected, the heating rate of the pasteurizer increased with larger temperature gradients, reinforcing the relationship between thermal efficiency and temperature differentials.

Heat loss during pasteurization was minimal, resulting in a temperature decrease of roughly 0.3°C per hour. This low heat loss rate suggests that the pasteurizer retains heat effectively, contributing to its high overall efficiency.

The buffer tanks demonstrated an efficiency of around 75%. Due to their larger volume compared to the pasteurizer, the tanks heated at a slower rate. When only one buffer tank was used, the heating rate doubled, reflecting the reduced thermal mass and increased responsiveness to solar input. Similar to the pasteurizer, the heating rate of the buffer tanks increased as the temperature difference between the incoming heat source and the tank contents widened.

Heat loss from the buffer tanks was measured at approximately 0.2°C per hour. Although this value appears small, cumulative heat loss over extended periods, such as overnight or during non-operational hours, can lead to significant reductions in stored thermal energy. This highlights the need for thermal insulation or supplementary heating strategies to maintain temperatures during periods of inactivity.

During Mode 3 operation, the buffer tanks exhibited negative power, indicating that thermal energy was being transferred from the tanks to the pasteurizer. This energy transfer reflects the higher heating rate of the pasteurizer compared to the tanks. Consequently, even when

solar heating was active, the buffer tanks experienced temperature drops, except in cases where solar input was sufficiently high to offset the energy demands of the pasteurizer.

These findings underscore the importance of balancing the thermal performance of the pasteurizer and buffer tanks to optimize system efficiency and ensure consistent pasteurization outcomes.

### *3.2.3. Thermal characterization of the whole system*

The overall efficiency of the solar pasteurization system was assessed under various operational modes and environmental conditions. As shown in Figure 11, Mode 1 demonstrated slightly higher efficiency compared to other modes. This suggests that directly heating the pasteurizer using energy from the solar collectors, without relying on buffer tanks, is the most effective approach when solar radiation is high. Under such conditions, the system can efficiently transfer heat directly to the pasteurizer, maximizing energy use without the need for intermediate storage.

The overall efficiency of the solar pasteurizer was around 22%.

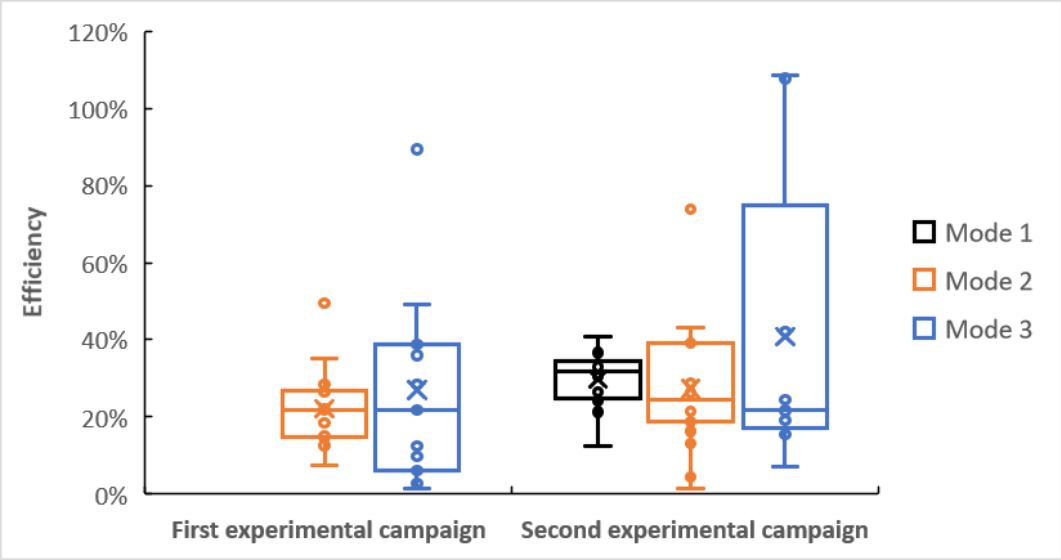


*Figure 11. Efficiency of the system for each of the experimental campaign and operational mode*

However, during periods of reduced solar radiation, Mode 3 may offer better performance. In Mode 3, the buffer tanks serve as thermal storage, gradually releasing heat to the pasteurizer as needed. This allows the system to continue operating even when solar input is insufficient, preventing interruptions in the pasteurization process. The flexibility of switching between direct heating (Mode 1) and buffered heating (Mode 3) ensures the system can adapt to varying weather conditions and irradiance levels.

The analysis of solar energy usage, presented in Figure 12, reveals that approximately 80% of the available solar energy was effectively utilized during the day. The remaining 20% was not

harnessed due to system downtime, such as during batch changes in the pasteurizer or instances when the buffer tanks ceased heating because their temperature exceeded that of the collectors. These operational pauses highlight opportunities for improving energy capture and storage to further optimize system performance.

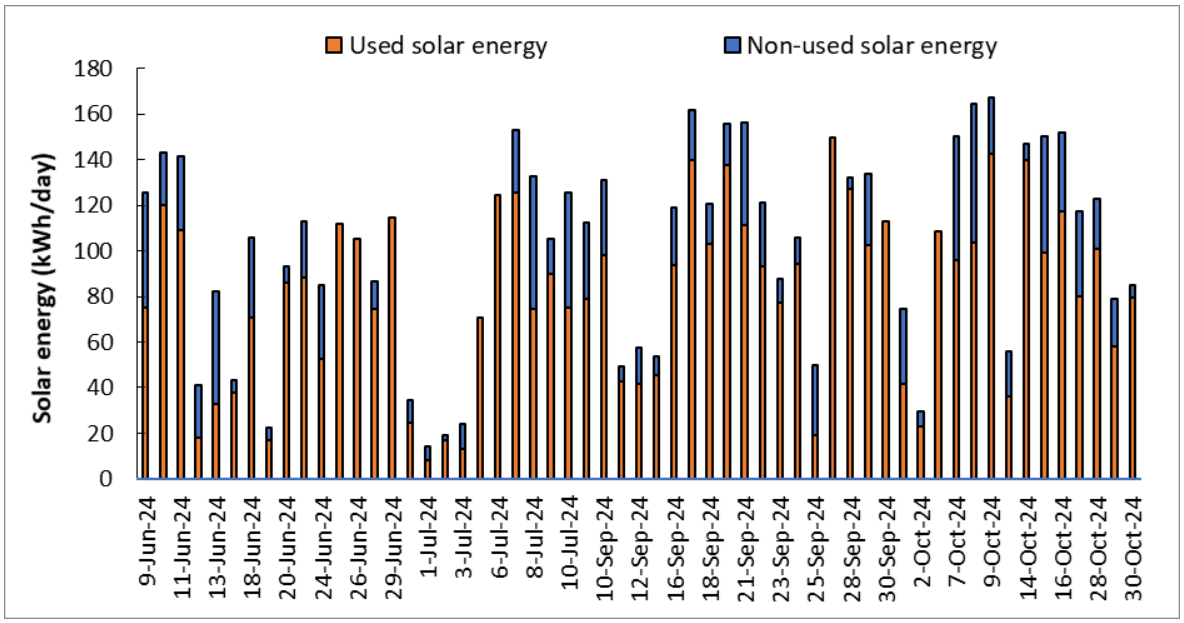


*Figure 12. Amount of the solar thermal energy that is used and not-used by the system*

Energy consumption by the system, depicted in Figure 13, indicates that the majority of energy use is attributed to electric heating. On days without electric heating, energy consumption was minimal, often falling below 1 kWh/day. The electric resistance heater was primarily engaged during overcast or rainy days, when solar irradiance was insufficient to meet thermal demands. The system's electrical components were powered by a 2.4 kW photovoltaic (PV) system, while the electric heater required the use of a 5 kW diesel generator.

As illustrated in Figure 14, a comparison between solar and electric heating during the testing period shows that the electric heater was heavily utilized in June and July, coinciding with the monsoon season and reduced solar availability. In contrast, electric heating was largely unnecessary during September and October, as improved weather conditions allowed for greater reliance on solar energy. T This seasonal variation underscores the importance of having an additional energy source as a backup during periods of low solar irradiance. While solar energy can effectively meet thermal demands during clearer months, relying solely on it may lead to operational interruptions during overcast or rainy periods. Incorporating a backup energy source, such as electric heating powered by a generator, ensures the pasteurizer can maintain consistent performance regardless of weather conditions, thereby enhancing reliability and operational continuity.

The thermal characterization of the entire system highlights the interplay between solar and electric heating and the need for operational flexibility to maintain consistent pasteurization performance throughout the year.

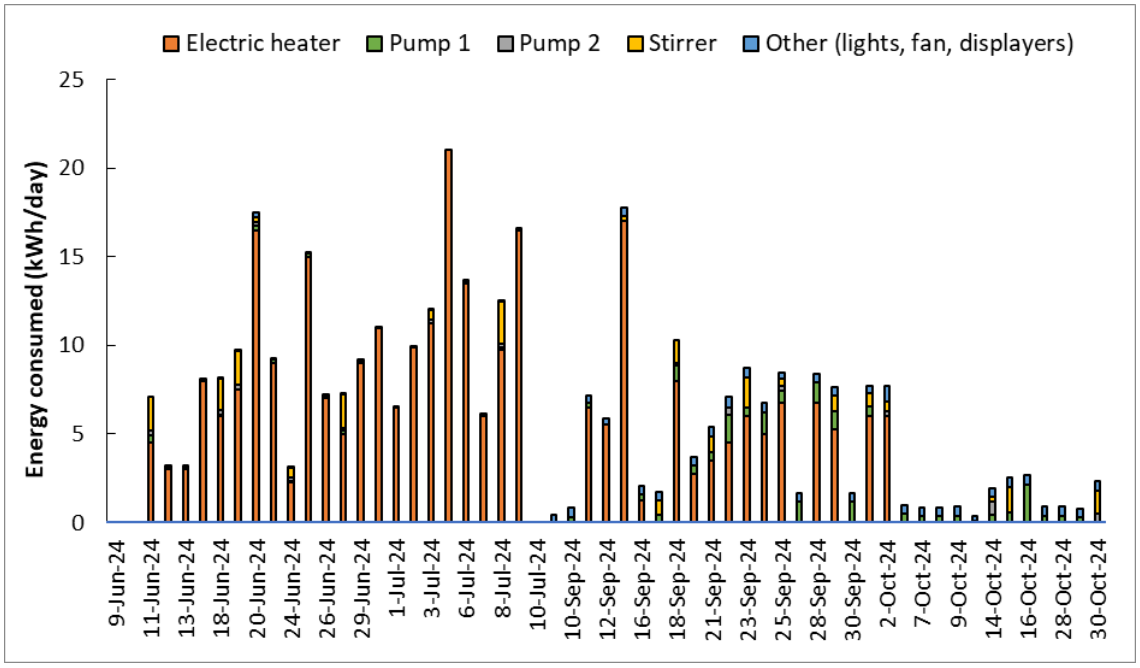


*Figure 13. Energy consumed by the different electric components during the tests in the solar pasteuriser*

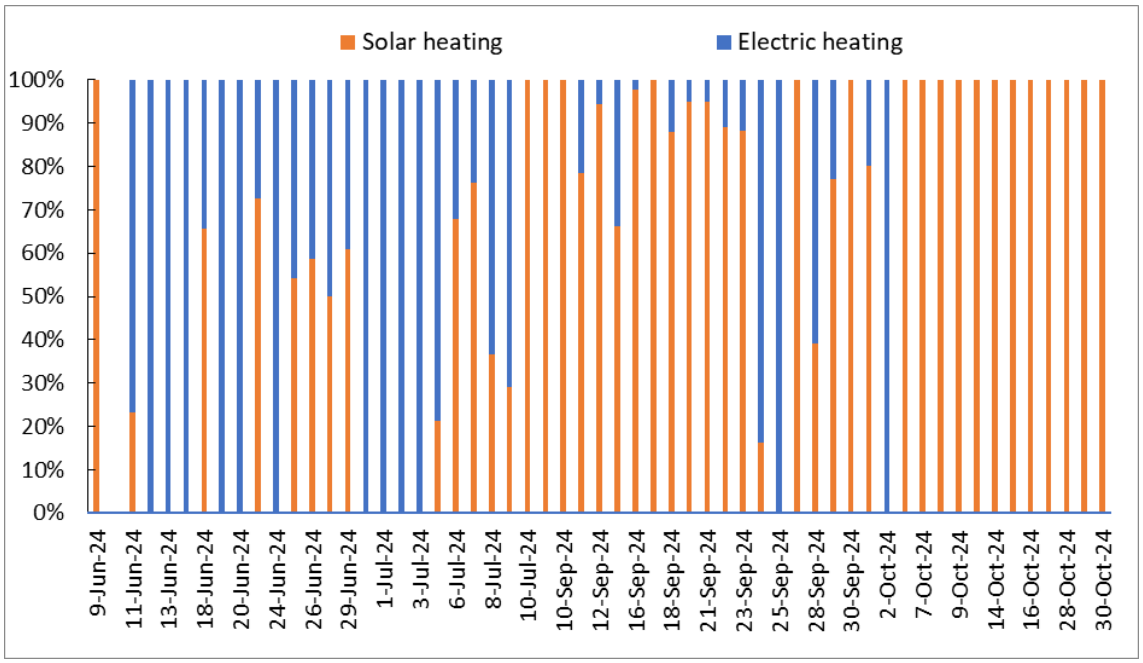


*Figure 14. Fraction of the contribution of the solar energy and electric heating during the tests in the solar pasteuriser*

## 3.3. Expected treatment capacity of the solar pasteurizer

The simulation results presented in this section are based on a model developed from experimental correlations with an $R^2$ value ranging from 0.2 to 0.7. As such, the model does not provide a perfect fit to all scenarios. Additionally, the deactivation model was constructed using pasteurization tests conducted with wastewater from the Netherlands, which may differ from the feedstock utilized in this study.

While the model offers valuable estimations and insights, it should not be interpreted as an exact representation of real-world conditions. The results reflect approximations that can be influenced by the experimental parameters and feedstock variability.

The model development is detailed in Appendix E. The model can be consulted in Supporting Document I.

### *3.3.1. Maximum achievable pasteurizer temperature*

The maximum temperature achievable in the solar pasteurizer was determined using the model developed during the project. This model couples the thermal behavior of the system with microbial deactivation dynamics, allowing for a comprehensive assessment of pasteurizer performance under varying conditions.

To estimate the maximum pasteurizer temperature, irradiance values were input into the model to compute the solar collector temperature. The corresponding pasteurizer temperature was then derived, assuming prolonged exposure to solar irradiance over a 9-hour period, representing the total duration of sunlight in Bangladesh. While this scenario assumes constant irradiance—an unrealistic condition—it provides an estimate of the maximum temperature the pasteurizer can achieve.

Figure 15 illustrates the relationship between irradiance and the temperatures of both the collector and pasteurizer. After the assumed 9-hour exposure, the collector and pasteurizer temperatures converge, approaching thermodynamic equilibrium. At an irradiance of 1600 $W/m^2$, the highest attainable temperature in the system, 120°C, is reached in the collectors, while the pasteurizer temperatures can reach up to 100°C. This level of temperature cannot be exceeded, since the boiling point of water at 2 bar – the operating pressure of both the primary and secondary circuits. Therefore, from temperatures beyond this limit water transitions to steam, preventing further temperature increases without significant system modifications to manage phase changes.

During testing, irradiance levels did not exceed 900 $W/m^2$. Therefore, the maximum achievable temperature is around 70°C under more realistic conditions, i.e. irradiance lower than 900 $W/m^2$. It is important to note that the model was calibrated using average data, which may limit its accuracy in predicting results outside this range. The maximum achievable temperature represents the typical upper limit, but it does not imply that the system cannot surpass it. In fact, during testing, the system occasionally exceeded this temperature. However, the model suggests that such instances are rare and not representative of normal operation.

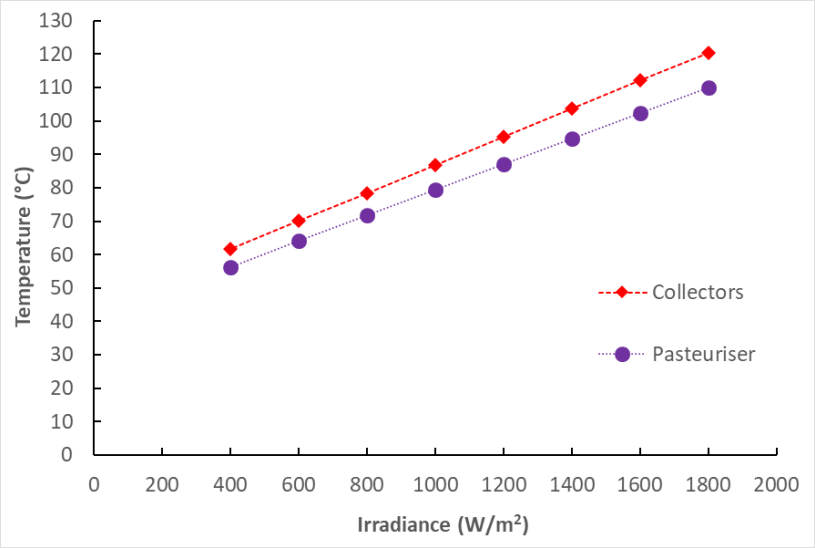


*Figure 15. Maximum temperature achieved in the pasteuriser as a function of irradiance after 9 hours of exposure*

### 3.3.2. Maximum treatment capacity

The maximum treatment capacity of the solar pasteurizer was evaluated using the thermal-microbial model developed during the project. The model simulated the maximum volume of sludge that can be heated to a given temperature in the pasteurizer over a 9-hour period, based on two solar irradiance levels—800 W/m² and 1600 W/m² (Figure 16). As with the previous section, this scenario is not intended to reflect realistic conditions but rather to define the physical limits of the system.

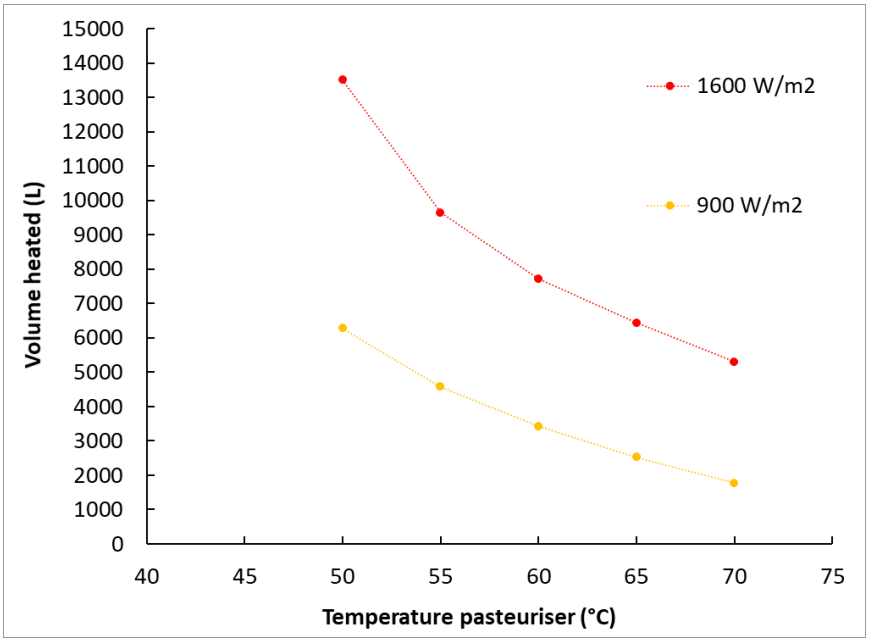


*Figure 16. Volume of sludge that can be heated as a function of the pasteuriser temperature for two different irradiances after 9 hours of exposure*

At 1600 W/m²—the maximum irradiance level before water boils in the collectors—the pasteurizer's treatment capacity exceeds the target of 3000 L/day. Under the maximum irradiance recorded during the tests, i.e. 900 W/m², this target is only achievable if pasteurization temperatures remain below 65°C. Consequently, 65°C appears to be the operational limit of the current system for treating 3000 L/day. However, reaching this capacity would require continuous exposure to peak irradiance of 900 W/m² for 9 hours, which remains an impossible scenario.

### *3.3.3. Treatment capacity in a real scenario*

The treatment capacity of the solar pasteurizer under real operating conditions was evaluated through one-day simulation across different operational configurations. These simulations assess the amount of sludge that can be treated, the energy consumption, the impact on the buffer tanks and the E. coli removal. Each batch processed by the pasteurizer corresponded to 500 L of sludge.

Irradiance data from tests conducted on September 16, with an average of approximately 520 W/m², was used for the simulations. This value closely reflects the annual average irradiance for the area, making it a realistic benchmark for the model.

#### *3.3.3.1. Simulation Results*

The initial simulations were conducted to evaluate the impact of Mode 1 versus Mode 3 operation, the number of buffer tanks (one or two), the initial temperature of the buffer tank(s), the target pasteurization temperature and the use of electric heating. For this, five operational scenarios were simulated:

- Mode 1 only – Heating of the pasteurizer from the solar collectors;
- Mode 3a only – Heating of the pasteurizer from one buffer tank;
- Mode 3b only – Heating of the pasteurizer from two buffer tanks;
- Mode 3b with electric heating – Heating of the pasteurizer from two buffer tanks and electric heating.

The simulations focus on three temperatures for the pasteurizer – 55°C, 60°C, and 65°C – as they represent the most feasible operating conditions. Lower temperatures (e.g., 50°C) were excluded, as they showed insufficient E. coli reduction in earlier tests (refer section 3.1.1). Similarly, 70°C is considered close to the upper operational limit identified in the previous section. The system simulation was conducted for three buffer tank temperatures—50°C, 60°C, and 70°C—reflecting the typical operating range observed during testing.

The assumptions for the simulations are as follows:

- Pasteurization was held during 15 minutes at the target temperature once reached, followed by an additional 15 minutes to accommodate batch changes.

- The initial temperature of the feedstock was 30°C, which was consistently observed during the pasteurizer tests.

The results of the simulations, summarized in Table 7, reveal a clear relationship between pasteurization temperature and system performance. The system's capacity to treat sludge decreases by approximately one batch (500 L) for every 5°C increase in pasteurization temperature. However, this reduction in volume is offset by a significant improvement in pathogen reduction, with the log reduction of E. coli increasing by 2 to 3 logs for each 5°C increment. At 55°C, the system can treat between 1,500 and 2,500 L/day, achieving a 1 to 2 log reduction in E. coli. At 60°C, the treatment volume decreases to 1,000 – 2,000 L/day, but the E. coli reduction improves to 3 to 5 logs. By increasing the pasteurization temperature to 65°C, the system can process between 500 and 1,500 L/day, achieving the highest pathogen reduction of 5 to 7 logs. These results indicate that while increasing the pasteurization temperature enhances pathogen inactivation, it also reduces the overall volume of sludge that can be processed.

When comparing operational modes, the results show that Mode 1 and Mode 3 deliver similar treatment capacities under most conditions. However, Mode 3b, which begins with an initial buffer tank temperature of 70°C, allows for the treatment of one additional batch of sludge. This advantage comes at the cost of significant temperature drops in the buffer tanks, which can exceed 10°C by the end of the day. Combining Mode 3b with the use of an electric heater allows for the processing of an additional batch of sludge while reducing the temperature drop in the buffer tanks. Despite this benefit, the use of electric heating results in a considerable increase in specific energy consumption (SEC). Without an electric heater, SEC remains below 5 kWh/m$^3$, but with the heater, it exceeds 10 kWh/m$^3$, increasing operational costs due to greater diesel consumption.

The simulations also highlight the influence of buffer tank configurations on system performance. In Mode 3, operating with two buffer tanks and at higher temperatures enhances sludge treatment capacity due to more stored thermal energy that is available for the process. However, this approach results in greater thermal losses, causing buffer tank temperatures to drop significantly by the end of the day. Interestingly, when buffer tanks operate at 50°C, the temperature increases slightly by the end of the day rather than decreasing. At 60°C, the temperature loss is moderate, but at 70°C, significant drops occur, which cannot be offset by electric heating. In Mode 1, buffer tank temperatures also decrease due to heat loss, although this is partially mitigated during pasteurization when the system operates in Mode 2, allowing the tanks to recover some thermal energy. Higher initial buffer tank temperatures lead to greater temperature drop (and higher heat loss), suggesting that operating at lower temperatures may be more practical for consistent performance, as the electric heater is unable to compensate for significant temperature drops.

The simulations indicate that the system fails to achieve its pasteurization targets under any of the tested conditions. Therefore, further optimization is required to determine if achieving

this target is feasible and to evaluate the associated trade-offs. This aspect will be explored in the next section.

*Table 7. Performance metrics of the solar pasteuriser in real conditions considering a pasteurisation time of 15 minutes*

| Pasteurisation temperature | Tanks temperature | Operation conditions | $V_{treated}$ (L/day) | SEC (kWh/m$^3$) | $\Delta T_{tanks}$ (°C) | log reduction E.coli |
|---|---|---|---|---|---|---|
| 55°C | 70°C | Mode 1 | 1500 | 2.5 | 2 | 1.5 - 2.5 |
| | | Mode 3b | 2000 | 1.9 | -16 | 1 - 2 |
| | | Mode 3b + electric heating | 2500 | 9.0 | -5 | 1 - 2 |
| 60°C | 50°C | Mode 3a | 1000 | 4.6 | 7 | 4 - 5 |
| | | Mode 3b | 1000 | 4.8 | 5 | 3 - 6 |
| | 60°C | Mode 3a | 1000 | 4.0 | -2 | 3.5 - 5 |
| | | Mode 3b | 1000 | 3.9 | -2 | 3.5 - 5.5 |
| | 70°C | Mode 1 | 1000 | 3.0 | -4 | 2.5 - 3.5 |
| | | Mode 3a | 1000 | 3.3 | -10 | 3 - 4.5 |
| | | Mode 3b | 1500 | 2.6 | -13 | 2.5 - 3.5 |
| | | Mode 3b + electric heating | 2000 | 15.8 | -10 | 2 - 3 |
| 65°C | 70°C | Mode 1 | 500 | 5.2 | -4 | 7 |
| | | Mode 3b | 1000 | 3.6 | -9 | 4 - 7 |
| | | Mode 3b + electric heating | 1500 | 20.8 | -7 | 4 - 5 |

#### 3.3.3.2. Operational Optimization

Simulations were conducted under conditions assumed to be the most optimal for system operation. The process commenced with Mode 3 in the morning, due to low solar irradiance. As solar irradiance increased, the system transitioned to Mode 1, maximizing direct pasteuriser heating during peak solar hours, typically from 9:30 AM to 2:30 PM. After peak hours, the system returned to Mode 3 to utilize stored heat from the buffer tanks. Electric heating was limited to the early morning (7:00 to 9:30 AM) and late afternoon (2:30 to 5:00 PM) to minimize energy consumption while maintaining adequate buffer tank temperatures. The buffer tanks were maintained at 60°C, as this temperature represented a compromise between heat storage capacity and temperature loss. Two pasteurization durations were evaluated: 15 and 45 minutes, with an additional 15 minutes allocated for batch changes. The results of these simulations are summarized in Table 8.

Under these optimal conditions, the system achieved maximum treatment volume while minimizing SEC and temperature loss in the buffer tanks compared to the previous cases. However, our treatment goal (3000 L/day) was not realized. Temperature losses in the tanks were low or slightly positive, indicating that the selected buffer tank temperature supported sustained operation. Although SEC remained elevated, it was lower than in previous simulations where the electric heater was used more extensively.

Extending the pasteurization duration to 45 minutes improved E. coli reduction by approximately 1 log but reduced daily capacity by about one batch. While longer pasteurization times facilitates buffer tank recharging, this approach limits the feasibility of conducting multiple batches per day. Consistent with earlier findings, the volume of treated sludge decreased as pasteurization temperature increased.

In summary, the system was unable to meet the treatment target while operating at the highest pasteurization temperatures. The current setup allows for either higher sludge treatment volumes at lower temperatures, resulting in lower E. coli deactivation, or lower treatment volumes at higher temperatures with enhanced deactivation. To improve performance, significant system modifications would be required, as discussed in the next chapter.

*Table 8. Performance metric of the solar pasteuriser for an optimal operation in real conditions*

| Pasteuriser temperature | Time pasteurisation | $V_{treated}$ (L/day) | SEC (kWh/m$^3$) | $\Delta T_{tanks}$ (°C) | log reduction E.coli |
|---|---|---|---|---|---|
| **55°C** | **15 minutes** | 2000 | 9.2 | -0.7 | 1 - 2 |
| | **45 minutes** | 2000 | 9.2 | -3.2 | 1.5 - 2.5 |
| **60°C** | **15 minutes** | 1500 | 12.8 | -3.5 | 2.5 - 4.5 |
| | **45 minutes** | 1000 | 18.2 | 1.5 | 5 - 6 |
| **65°C** | **15 minutes** | 1000 | 18.9 | -0.2 | 5.5 - 7 |
| | **45 minutes** | 500 | 35.7 | 2.6 | 5.5 - 7 |

In conclusion, the current system is unable to meet the established treatment targets without supplemental energy. Solar energy alone during the day is insufficient to pasteurize the desired volume of sludge and recharge the buffer tanks, even when operating under optimal conditions. As a result, the system must either process a lower quantity of sludge per day to maintain lower costs or rely on a backup energy source, which would increase operational expenses. The next chapter will discuss potential improvements in the process design to achieve the treatment goals.

### *3.3.4. Estimation of the pasteurization performance*

Diagrams from the literature were used to estimate the pasteurization potential of the process under realistic operating conditions. The previous sections demonstrated that the pasteurizer could operate between 55°C and 65°C, with pasteurization durations ranging from a few minutes to a maximum of one hour. It is important to note that there is a temperature ramp-up period before reaching the target pasteurization temperature, during which the sludge is exposed to temperatures where pasteurization can begin.

In the first diagram (Figure 17), the operating conditions are positioned in Zone C, representing combinations in inconsistent log reductions—achieving less than 1-log for some microbial groups and more than 3-log for others. Zone A identifies time-temperature settings

that ensure a minimum 3-log (99.9%) reduction for all microbial groups across all matrices. Zone B includes settings that achieve at least a 1-log (90%) reduction for all microbial groups and matrices, while Zone D represents combinations where reductions remain consistently below 1-log for all microbial groups and matrices.

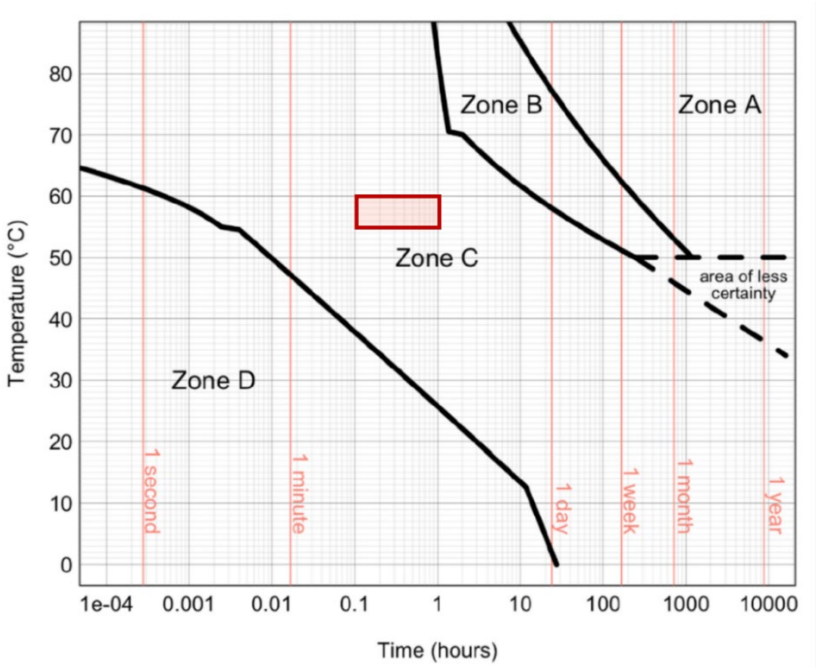


*Figure 17. Different level of pasteurisation as a function of temperature and time* (Espinosa et al., 2020), *including the zone of operation of the solar pasteuriser (red square)*

The second diagram (Figure 18) provides a more detailed analysis of specific pathogens that can be deactivated. Pathogens such as Vibrio cholerae (which is the pathogen of major concern in this project), Entamoeba histolytica, and Taenia can be effectively deactivated at 55°C. However, temperatures of at least 60°C are required to inactivate Salmonella, Ascaris, and Shigella. Enteric viruses, such as norovirus and rotavirus, pose greater challenges, as only pasteurization at temperatures higher than 65°C may effectively reduce their presence. However, these conditions are already at the operational limits of the system.

As a result, while the pasteurizer shows promise in reducing bacterial, protozoan, and helminth pathogens, its ability to inactivate viruses remains uncertain under normal operating conditions. To ensure broader pathogen reduction, modifications to the pasteurizer may be necessary, particularly for pathogens requiring higher temperatures for effective deactivation.

Operating at temperatures near 65 °C enhances the deactivation of more types of pathogens and leads to higher log reductions (e.g., 1–2 log reductions at 55 °C versus 5–7 log reductions at 65 °C). Therefore, for more effective pasteurization, it is advisable to operate at the upper end of the 55–65 °C range. However, the final decision should consider the volume of sludge requiring treatment and the desired pasteurization level.

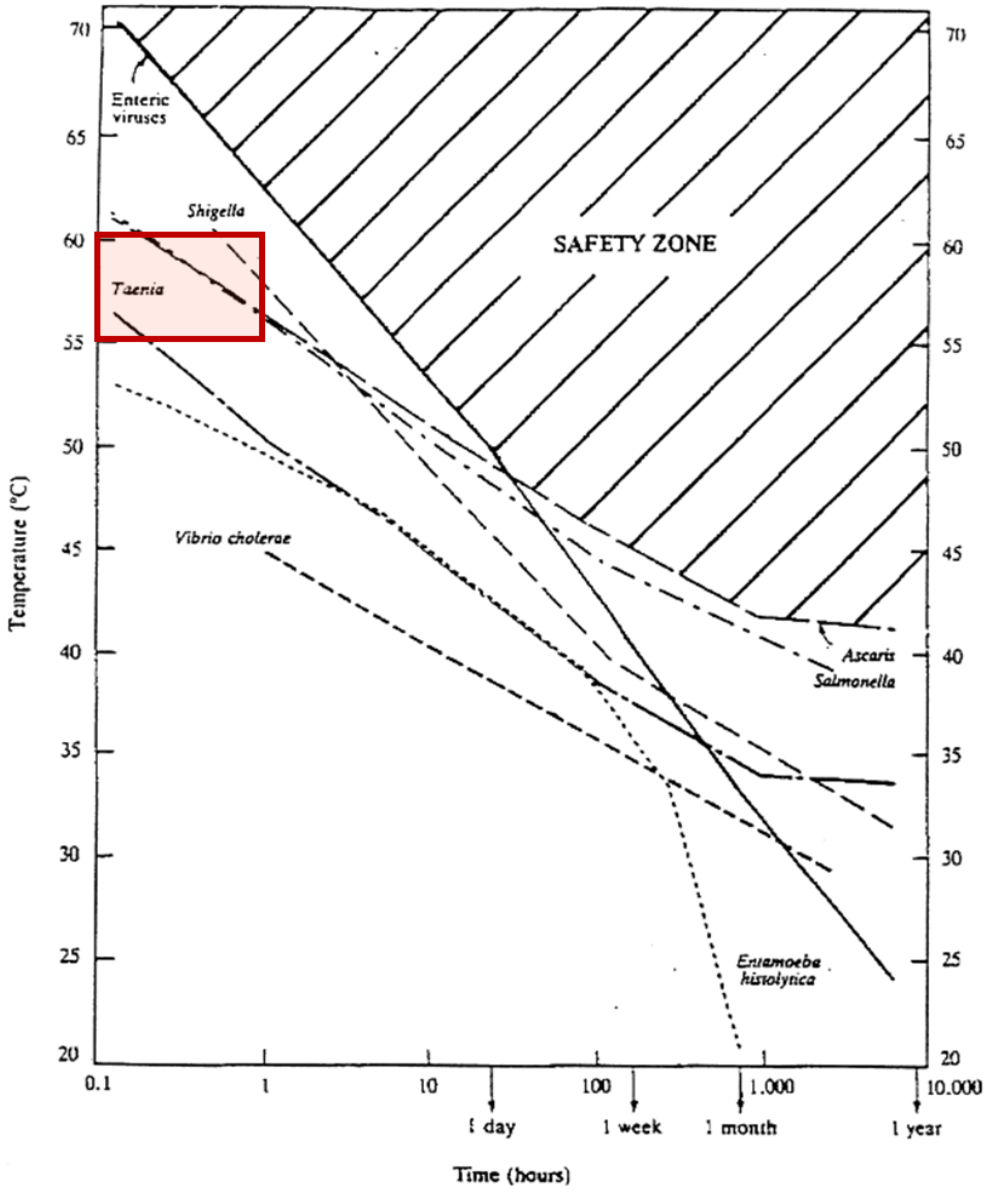


*Figure 18. Temperature–time relationships for safe water pasteurisation* (Feachem et al., 1983)*, including the zone of operation of the solar pasteuriser (red square)*

## 3.4. Summary

The optimal operating conditions for the pasteurizer involve running Mode 1 during peak solar hours (typically from 9 AM to 2 PM) and switching to Mode 3 during early mornings and late afternoons to enhance performance. Electric heating is employed to recover energy lost in the buffer tanks, maximizing treatment capacity and improving pasteurization efficiency. This approach helps retain heat in the tanks but results in higher specific energy consumption (SEC). Buffer tank temperatures are maintained around 60°C, balancing heat retention and temperature loss.

The solar pasteurizer operates effectively within a temperature range of 55 to 65°C. At these temperatures, the system achieves a minimum 1 to 2 log reduction of E. coli and successfully deactivates key pathogens such as Vibrio cholerae (main focus of this project), Taenia, and Entamoeba histolytica. Pathogens like Salmonella, Ascaris, and Shigella require temperatures above 60°C for effective deactivation. However, pasteurization at these temperatures has minimal impact on enteric viruses such as norovirus and rotavirus, as confirmed through experimental data.

Operating at 65°C limits the system's capacity to treat sludge, allowing the treatment of only one-third of the sludge total volume to treat. Although higher temperatures enhance pathogen reduction, the trade-off is a significantly reduced treatment capacity. Conversely, lowering the pasteurization temperature increases the volume of sludge processed, but some pathogens may remain active or deactivated at a lower extent, resulting in lower pathogen reduction. The decision on the operating pasteurization temperature must balance the required treatment capacity and desired level of pathogen reduction, considering the context constraints.

While the pasteurizer effectively produces effluent that meets microbial content standards (such as total coliforms), it does not significantly alter physicochemical parameters such as COD, BOD, or nutrient concentrations. Therefore, pasteurization alone does not fulfill all regulatory requirements for effluent discharge. To ensure full compliance, the pasteurizer must be integrated with additional downstream processes to address the effluent's physicochemical properties. Despite this limitation, the pasteurizer remains crucial for pathogen reduction and significantly contributes to microbial safety as part of a comprehensive treatment system.

Due to the potential presence of certain pathogens, effluent reuse should be approached cautiously and restricted to specific applications. To enhance safety and broaden reuse possibilities, operating the pasteurizer consistently at 65°C is recommended. Additionally, increasing the pasteurizer's treatment capacity is necessary, as the current system cannot meet the target treatment volume. Improving both operational temperature and capacity is essential to maximize the pasteurizer's effectiveness and expand its role in sanitation projects. Measures to address these improvements are discussed in the next chapter.

# 4. Analysis of the techno-economic viability for the implementation of the solar pasteurizer in humanitarian emergency settings

The previous section identified that while operating between 55°C and 60°C effectively reduces Escherichia coli and Vibrio cholerae, it does not consistently meet treatment capacity targets or fully address more resilient pathogens such as Ascaris and enteric viruses. Consequently, the goal is to explore solar assessment and techno-economic analysis to identify practical solutions for optimizing the pasteurization system to eliminate the pathogens in faecal sludge (FS). In our case, the FS corresponds to the effluent of a decentralized wastewater treatment system (DEWATS) that treats FS from pit latrines.

This chapter addresses the need to operate the pasteurization system at temperatures higher than 60°C to ensure effective pathogen inactivation. While 70°C is challenging to achieve consistently, targeting 65°C offers a practical compromise that enhances pathogen removal while remaining attainable under current system conditions. The focus is on exploring solar assessment and techno-economic strategies to reach this temperature while maintaining treatment capacity targets.

The solar assessment focuses on understanding weather patterns and estimating the plant's capacity based on irradiance levels. This involves conducting a year-round assessment of solar energy availability and evaluate the system's performance under different seasonal and meteorological conditions. The techno-economic analysis evaluates the financial viability and cost implications of implementing the proposed modifications. Following the solar and techno-economic assessments, the feasibility of replicating the pasteurization system in other humanitarian contexts is explored. The analysis considers other geographical locations such as Bentiu (South Sudan), Maiduguri (Nigeria), and Pemba (Mozambique).

By examining these factors, this section aims to provide a comprehensive framework for enhancing the system's performance and tehcno-economic vaiablity, and expanding its applicability to other humanitarian settings.

The methodology for this analysis, with the relevant parameters, is given in detail in Appendix F.

## 4.1. Solar assessment and techno-economic analysis of the current system

This analysis begins by assessing the solar radiation throughout the year at the Rohingya camp location (Ukhia, Cox's Bazar) to evaluate the treatment potential. Based on this assessment, solutions are explored to achieve the target temperature of 65°C and a treatment capacity of 3000 L/day. The costs associated with the current system configuration are also examined.

The solar assessment coupled with the techno-economic analysis can be found in Supporting Document J.

### 4.1.1. *Year-round weather patterns in the region from the Rohingya Camp*

Figure 19 illustrates the average hourly irradiance for each month of the year. The highest irradiance levels occur in March and April, peaking at 900 W/m², while the lowest irradiance is observed in June and July, peaking at 600 W/m². This decrease corresponds to the monsoon season, which coincided with the first experimental campaign.

Throughout the year, irradiance begins to rise significantly between 6-7 AM, reaching its peak around 11 AM to 12 PM. By 3-4 PM, solar irradiance attains low levels. This pattern results in approximately 9 hours of potential operational time from 7 AM to 4 PM, with around 5 peak solar hours.

Irradiance as a function of tilting angle is shown in Figure 20. The optimal tilting angle varies by month. On average, the optimal tilt is approximately 25° (Figure 21), closely matching the current collector inclination of 20°. The difference in irradiance between the average annual optimal tilt and the monthly optimal tilt is minimal (ranging from 0% to 10%), resulting in an overall annual difference of around 3%.

Although the panel angles could be adjusted monthly to maximize the received solar irradiance, the potential gain is minor compared to the added complexity of implementing an adjustable tilting system. Therefore, operating at a fixed inclination set to the annual optimal angle may be the most practical solution.

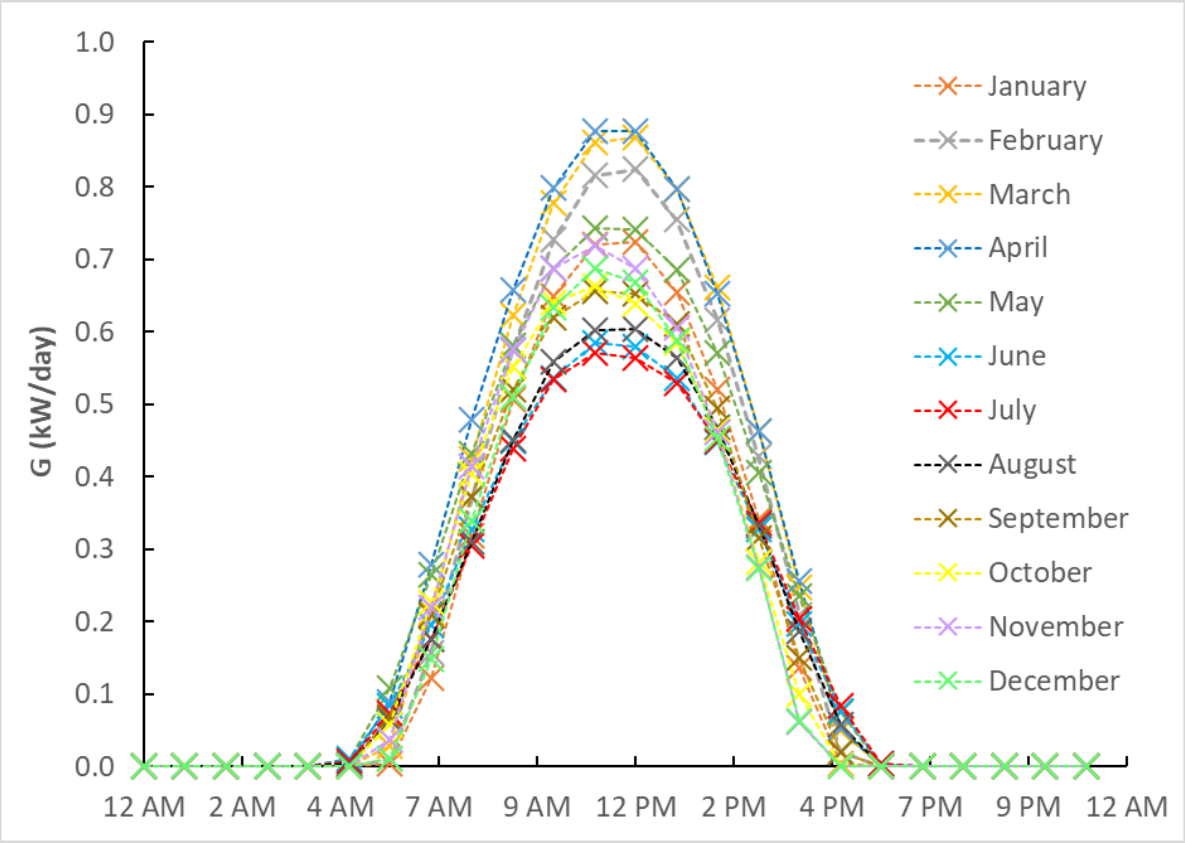


*Figure 19. Hourly average irradiance received in an horizontal plane in monthly basis*

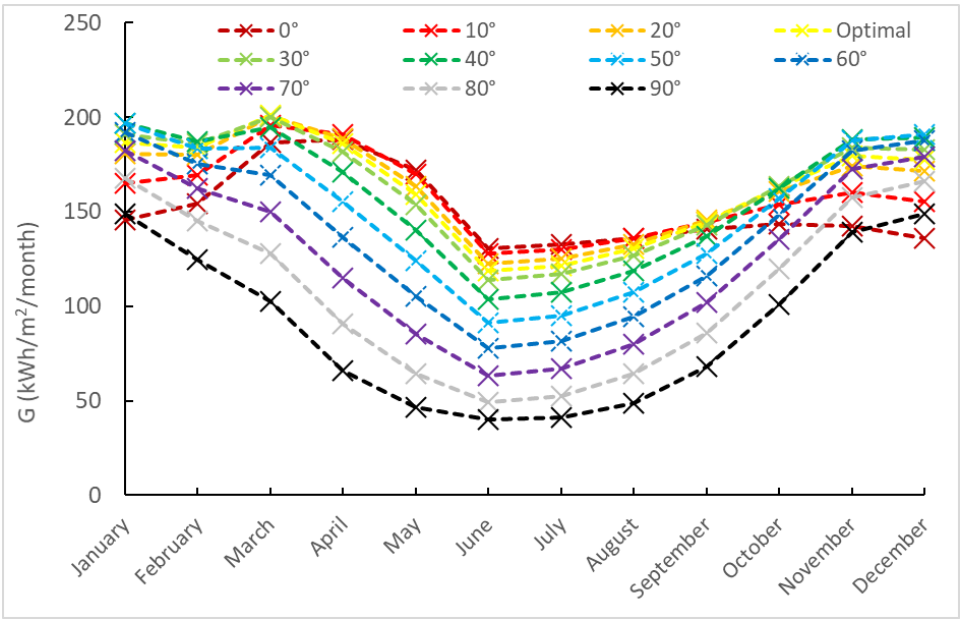


*Figure 20. Monthly irradiance as a function of the tilting angle*

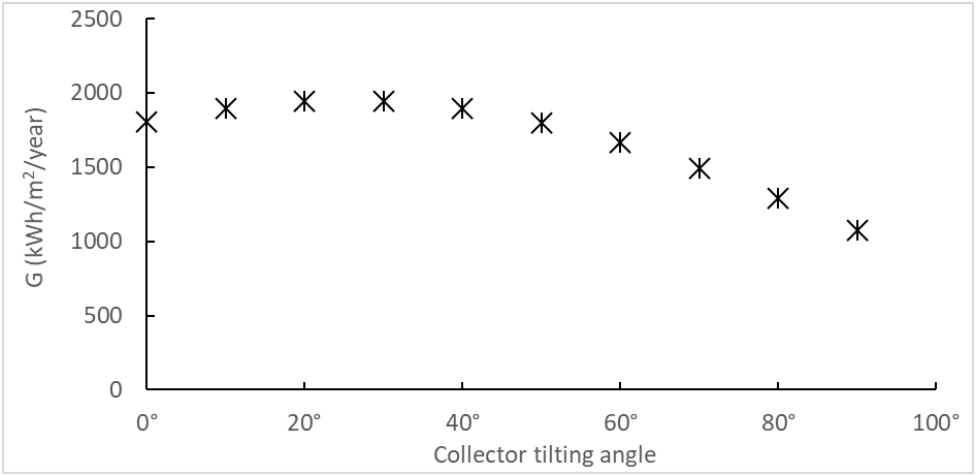


*Figure 21. Yearly irradiance as a function of the tilting angle*

### *4.1.2. Year-round average treatment capacity of the pasteurizer*

Based on solar irradiance at a 20° tilt, the total surface area of the collectors, and the whole system efficiency (determined to be approximately 22% from the experimental efficiencies of the system different components and the usable solar energy fraction), it is possible to estimate the available thermal energy for heating the pasteurizer to the desired temperature.

Figure 22 illustrates that the treatment target of 3000 L/day is never reached throughout the year for pasteurization temperatures between 50°C and 70°C. Although the capacity at 50°C comes close, this temperature is insufficient for effective pathogen inactivation. At 60°C, the system can treat between 500 and 1500 L/day, depending on the month. At 70°C, the treatment capacity does never exceed 1000 L/day.

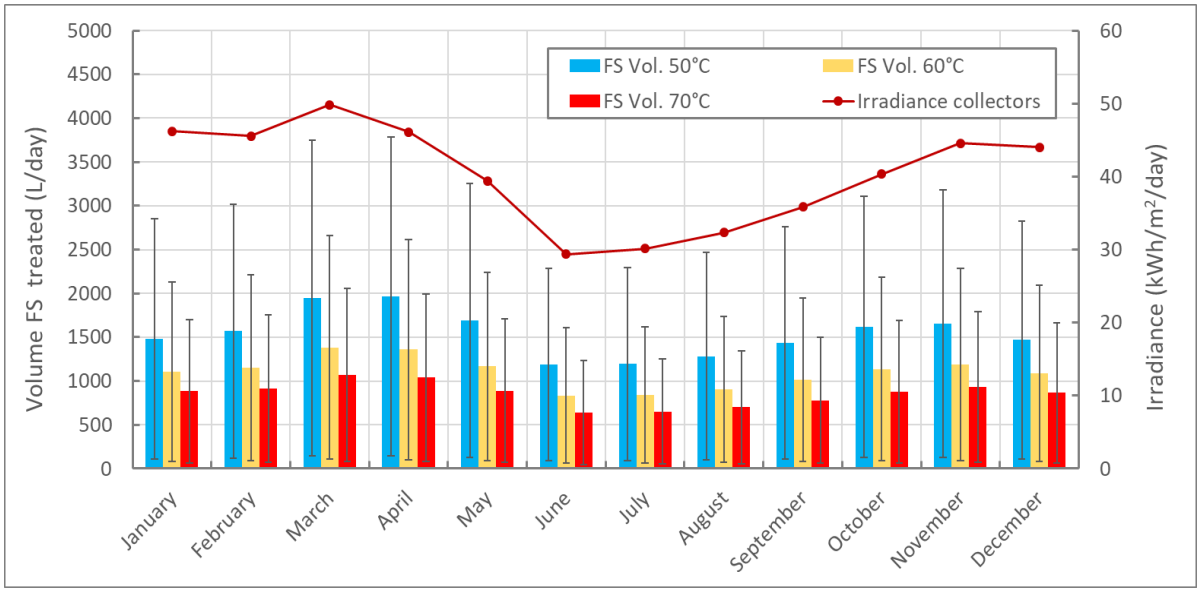


*Figure 22. Treatment capacity of the solar pasteuriser system at the current status and average solar irradiance for each month of the year*

These findings align with the analysis from the previous section, highlighting the limitations imposed by available solar energy. The primary constraint is that the solar energy alone is insufficient to meet the required treatment levels. As a result, an auxiliary energy source is necessary to achieve the target capacity. This explains the improved treatment capacity observed when electric heating was integrated as previously discussed.

### *4.1.3. Techno-economic analysis of the current installation*

In this section, the initial stage of the techno-economic analysis was performed using the current equipment. The objective is to identify opportunities for optimization and cost reduction, while assessing strategies to achieve the target treatment capacity. The techno-economic analysis was then conducted in different contexts to evaluate capital costs, operating costs, energy consumption, surface area footprint and return of investment (ROI). The capital costs cover the pasteurizer tank, solar equipment (buffer tanks, hoses, sensors, fittings, and frames), photovoltaic (PV) system (panels, battery, inverter), and minor items (pressure booster, piping, electric materials, instrumentation, and furniture). Operating costs cover fuel and consumables such as cleaning materials, personal protective equipment, and stationary items. The energy consumption is limited to electricity usage. The surface area accounts for the zone with solar collectors, as well as the exterior and interior spaces of the shed housing the equipment, including buffer tanks, the pasteurizer, and other related components.

The baseline scenario relies solely on solar energy. As the solar collectors were purchased from France, the impact of sourcing collectors from India, where costs are lower, was analyzed. Additionally, the effect of using a stirrer under different conditions was examined. In the baseline, the stirrer operates 90% of the time, being active during both heating and

pasteurization, except during batch changes. An alternative scenario assumes 70% operation, limiting the stirrer's use to the heating phase. A third scenario evaluates intermittent stirrer operation (35%) based on observations that the stirrer minimally influences heating rates but helps maintain uniform temperature distribution and probably prevents the settling of suspended solids. This could be achieved by intermittent operation so that it does not need to be operating at full time. Another scenario involves replacing the PV system with the use of the diesel generator for power generation (3 kW). Another scenario considered the use of a diesel generator to supply the additional electricity needed to treat 3000 L/day of sludge. In this case, upgrading the existing diesel generator to a higher-capacity model was necessary, resulting in increased capital costs. The current generator lacks sufficient capacity to generate the heat required to achieve the 3000 L/day treatment target.

The results of the techno-economic analysis are summarized in Table 9. Capital costs are relatively high, driven primarily by the pasteurizer tank (€17k), the solar equipment (€11k), consisting of buffer tanks, hydraulic connections, sensors, and supporting frames, and the flat plate collectors (€8k). A potential cost reduction strategy involves purchasing similar solar collectors from India (€150/unit) instead of France (€520/unit), offering savings of approximately €6k.

Reducing stirrer operation from 90% to 70% or 35% lowers the energy consumption from 1.13 to 0.61 kWh/day. This reduction could enable the use of smaller, less expensive PV systems or diesel generators, leading to slight decreases in overall costs. However, further validation is required to confirm that intermittent stirrer operation does not compromise process performance.

Using a diesel generator instead of a PV system for electricity generation lowers initial capital costs (€1.2k) but increases running costs by approximately €1/day. A cost-benefit analysis indicates that it would take over three years for the PV system to become more cost-effective than the generator. Using a diesel generator to supply electricity for heating the buffer tanks to achieve the treatment target of 3000 L/day significantly increases operational costs. In this scenario, the specific capital cost and surface area decrease by approximately one-third, driven by the higher volume of treated sludge without requiring substantial additional capital investment or land. However, this comes at the expense of a fivefold increase in specific running costs and a tenfold rise in specific energy consumption.

Overall, while capital costs are high, they could be mitigated by sourcing materials from local (Bangladesh) or regional (India, China) markets. Solar collectors are the most straightforward component to replace, whereas pasteurizer tanks and specialized solar equipment may pose greater challenges. Running costs and energy consumption remain relatively low unless a diesel generator supplements the thermal energy required to treat 3000 L/day. This presents a trade-off between lower operational costs with reduced treatment capacity and higher costs to meet the full target.

Compared to other emergency sanitation technologies as listed in the Octopus platform (https://octopus.solidarites.org/case-studies), the cost of the solar pasteuriser installation tends to involve higher specific capital cost, but lower specific operating costs. Indeed, most

of the emergency technologies found in Octopus (e.g., anaerobic reactors, waste stabilisation ponds) have a specific capital cost lower than €10k/$m^3$·day and specific operating cost higher than €10k/$m^3$·day, whereas in the solar pasteuriser system the specific capital cost exceeds €30k/$m^3$·day but the specific operating costs remains below €10k/$m^3$·day for most of the scenarios.

## 4.2. Techno-economic viability for the system improvements

In this section, the focus is on exploring potential improvements to enhance the viability of the system. The primary objective is to maximize the treated volume using only solar energy, reducing backup fuel consumption and minimizing costs, while maintaining a treatment capacity of 3000 L/day and achieving a pasteurization temperature of up to 65°C. The techno-economic analysis related to the implementation of these improvements is presented in Table 10.

For this study, the baseline system assumes collectors purchased from India. The PV system is retained to enhance sustainability and mitigate risks associated with fluctuations in diesel prices, even though diesel generators may be more cost-effective in the short term. Stirrer operation is maintained at 90%, as the cost difference compared to partial operation is low, and the effects of intermittent stirrer use are not yet fully characterized. A diesel generator remains part of the system to ensure the target treatment capacity is met, i.e. 3000 L/day.

*Table 9. Techno-economic metrics based on the current status of the solar pasteuriser system, including alternative options*

| | Baseline configuration | Panels from India | Stirrer | | Diesel generator for electricity | Diesel generator for heating |
|---|---|---|---|---|---|---|
| | | | 70% | 35% | | |
| **Treatment capacity with only solar (L/day)** | 960 | 960 | 960 | 960 | 960 | 960 |
| **Total treatment capacity (L/day)** | 960 | 960 | 960 | 960 | 960 | 3000 |
| **Capital cost (€)** | 38900 | 33350 | 38900 | 38900 | 37700 | 38500 |
| **Specific capital cost (€/$m^3$·day)** | 40521 | 34740 | 40521 | 40521 | 39271 | 12833 |
| **Operating cost (€/day)** | 3.29 | 3.29 | 3.29 | 3.29 | 4.13 | 44.81 |
| **Specific operating costs (€/$m^3$)** | 3.42 | 3.42 | 3.42 | 3.42 | 4.30 | 14.94 |
| **Energy consumption (kWh/day)** | 1.13 | 1.13 | 0.95 | 0.59 | 0.95 | 35.76 |
| **Specific energy consumption (kWh/$m^3$)** | 1.18 | 1.18 | 0.99 | 0.62 | 0.99 | 37.26 |
| **Specific surface area ($m^2$)** | 130 | 130 | 130 | 130 | 130 | 130 |
| **Specific surface area ($m^2$/$m^3$·day)** | 135 | 135 | 135 | 135 | 135 | 43 |

*Table 10. Techno-economic metrics of the proposed improvements for the installation*

| | Baseline configuration | + 10 flat plate collectors | Vacuum tube collectors | | LPG boiler | Heat recovery | | Optimal case | |
|---|---|---|---|---|---|---|---|---|---|
| | | | 15 collectors | 25 collectors | | Low-cost | Mid-range | No heat recovery | Heat recovery |
| **Treatment capacity with only solar (L/day)** | 960 | 1600 | 1047 | 1745 | 960 | 1481 | 3222 | 1745 | 2694 |
| **Total treatment capacity (L/day)** | 3000 | 3000 | 3000 | 3000 | 3000 | 3000 | 3000 | 3000 | 3000 |
| **Capital cost (€)** | 34950 | 36450 | 35700 | 37700 | 35350 | 37950 | 42950 | 38100 | 41100 |
| **Specific capital cost (€/m$^3$·day)** | 11650 | 12150 | 11900 | 12567 | 11783 | 12650 | 14317 | 12700 | 13700 |
| **Operating cost (€/day)** | 44.81 | 31.78 | 43.03 | 28.81 | 10.67 | 23.31 | 1.93 | 7.82 | 4.00 |
| **Specific operating costs (€/m$^3$)** | 14.94 | 10.59 | 14.34 | 9.60 | 3.56 | 7.77 | 0.64 | 2.61 | 1.33 |
| **Energy consumption (kWh)** | 35.76 | 24.84 | 34.27 | 22.35 | 0.95 | 17.73 | 1.57 | 0.95 | 0.95 |
| **Specific energy consumption (kWh/m$^3$·day)** | 11.92 | 8.28 | 11.42 | 7.45 | 0.32 | 5.91 | 0.52 | 0.32 | 0.32 |
| **Specific surface area (m$^2$)** | 130 | 155 | 130 | 155 | 130 | 130 | 130 | 155 | 155 |
| **Specific surface area (m$^2$/m$^3$·day)** | 43 | 52 | 43 | 52 | 43 | 43 | 43 | 52 | 52 |
| **ROI (months)** | - | 4 | 14 | 6 | 0 | 5 | 6 | 3 | 5 |

### 4.2.1. Increase of surface area for solar thermal energy collection

The first proposed improvement is to expand the solar energy collection surface by increasing the number of collectors. This enhances the amount of solar thermal energy harnessed, providing more thermal energy to meet operational targets. In the current installation, space allows for the addition of 10 more collectors of similar dimensions to the existing ones, assuming that can be sourced locally. *Figure 23* indicates how to accommodate this expansion.

As observed in Table 10, adding more panels increases capital costs by approximately 5% (€1500). Still, it reduces operating costs by 30% (€13/day) due to lower diesel requirements, resulting in a ROI within 4 months. The surface area increases with this expansion by around 10% (from 130 to 155 m²). Given the availability of space for this expansion and the rapid ROI, expanding the panel array is considered a worthwhile option.

*Figure 23. Possible aspect of the installation after adding 2 rows of 5 solar collectors (note: added collectors represented by a blue square)*

### 4.2.2. Use of vacuum tube collector

Another improvement involves using vacuum tube collectors instead of flat plate collectors, as they are known to be more efficient. For this study, the efficiency of evacuated tube collectors is estimated using efficiency curves from Figure 24. The area in the plot representing the efficiency of flat plate collectors (based on test results) is marked by a blue square. This area is then projected onto the vacuum tube collector curve (represented by a red square), revealing an efficiency of approximately 60%. The collectors are assumed to have similar dimensions in both cases.

As shown in Table 10, this improvement results in a slight increase in treatment performance, with an associated capital cost increase of 2%. This is because vacuum tube collectors are typically around 30% more expensive than flat plate collectors of the same dimensions. Running costs are reduced by approximately 4% due to increased efficiency leading to a lower diesel consumption. The ROI is estimated at 14 months, making this a viable option for system improvement.

It can be noted that the gain in treatment performance increases only slightly when using vaccum tube collectors. Despite their higher efficiency, vacuum tube collectors have a smaller aperture area—the effective surface directly exposed to and absorbing solar radiation—

compared to flat plate collectors of the same external dimensions. Indeed, flat plate collectors utilize nearly the entire surface to absorb solar energy, whereas the gaps between vacuum tubes reduce the effective area available for solar collection. The gain in efficiency from vacuum tube collectors is then partially offset by their lower aperture surface with respect to their overall external dimensions.

To match the absorber area of 15 flat plate collectors (baseline), 25 vacuum tube collectors are required. This raises capital costs by up to 8%, while reducing operating costs by around 36%, achieving a ROI in approximately 6 months. This can be then considered a cost-effective improvement, although the surface requirement will augment of around 20%.

In addition, vacuum tube collectors can operate at higher temperatures than flat plate collectors, facilitating faster heating of the pasteurizer. Indeed, vacuum tube collectors are more suitable for industrial applications. They also offer modularity and scalability, allowing surface area to be adjusted by adding or removing individual tubes.

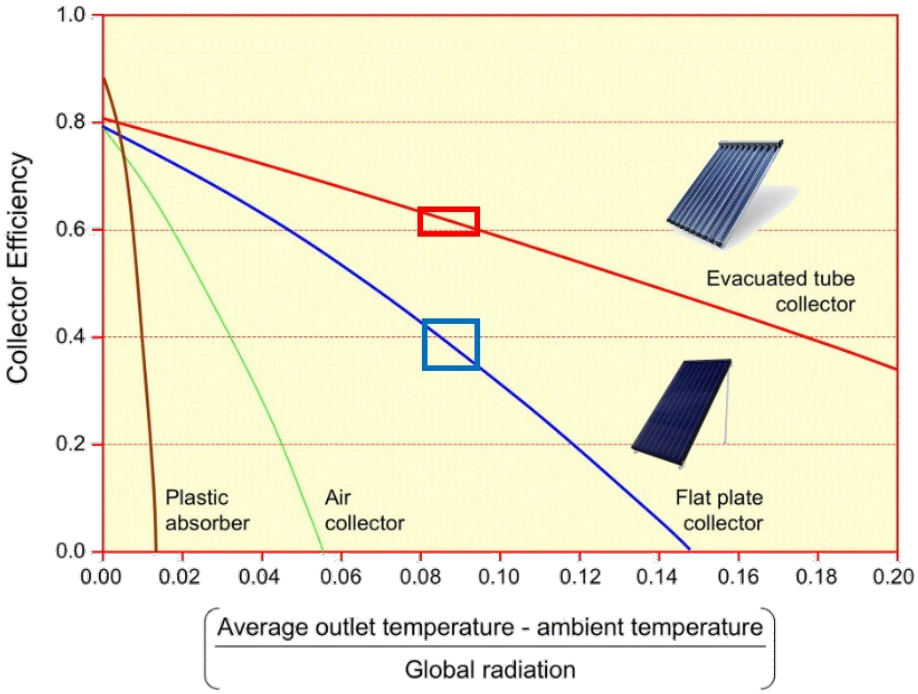


*Figure 24. Efficiency of various types of collectors as a function of the environmental conditions (blue square showing the location of the efficiency of flat plate collectors in our context; red square providing the projection of the efficiency of evacuated tube collector in our context)*

### *4.2.3. LPG boiler*

Replacing the diesel generator used to power the electric resistance with an liquefied petroleum gas (LPG) boiler to heat the buffer tanks offers a significant opportunity to reduce operating costs. According to Table 10, this modification does not increase capital costs (because of the same cost of a boiler and diesel generator) but results in a 75% reduction in operating costs and a nearly 97% decrease in specific energy consumption (SEC). This immediate cost reduction stems from the higher efficiency of boilers in converting

combustion energy directly into heat. Unlike diesel generators, which first convert combustion energy into electricity and then use electric heaters to generate heat, an LPG boiler provides a direct path to heat production. Diesel generators typically operate at an efficiency of 30-40%, while LPG boilers achieve efficiencies of around 90%.

While diesel generators can also power the electrical equipment from the installation, thereby eliminating the need for a PV system (so minus €2k in the capital cost), the ROI for LPG boilers and a PV system remains rapid in this case, with payback expected within 6 months. Implementing LPG boilers represents a crucial step toward enhancing the viability of the solar pasteurization process. Furthermore, boilers could potentially be fueled by biogas from nearby digesters, enhancing the sustainability of the process.

#### *4.2.4. Heat recovery*

The final proposed improvement involves heat recovery through pre-heating at the inlet of the pasteurizer. This would be achieved by installing a heat exchanger to transfer heat between the incoming and outgoing sludge. Two types of heat exchangers are considered:

- Low-cost heat exchanger – Estimated cost of €3,000 with a heat recovery efficiency of 35%.
- Mid-range heat exchanger – Estimated cost of €8,000 with a heat recovery rate of 70%.

These cost estimates are approximate and can vary widely, so results should be interpreted with caution.

For the low-cost option, capital costs increase by up to 10%, with a 50% reduction in operating costs, resulting in a ROI within 5 months. For the mid-range exchanger, capital costs rise by around 25%, but the treatment capacity is met using solar energy only and consequently the operating costs are at their minimum value, i.e. €1.93/day. The investment is subsequently recovered in 6 months.

Heat exchangers offer a promising method to enhance system performance, potentially allowing to rely almost exclusively in solar energy with a ROI of a few months. However, it is important to consider the impact of heat exchangers on the system's surface area requirements, though this effect cannot be precisely quantified at this stage.

A direct heat exchanger between the inlet and outlet sludge streams is one possible approach with already existing industrial cases, as demonstrated in Figure 25. However, implementing this type of heat exchanger for sludge poses challenges due to the presence of suspended solids, which can lead to fouling, and the potentially high viscosity of the sludge.

To mitigate these issues, a technological alternative involves using an external circuit to facilitate heat exchange between two tanks containing the input and output sludge, as illustrated in Figure 26.

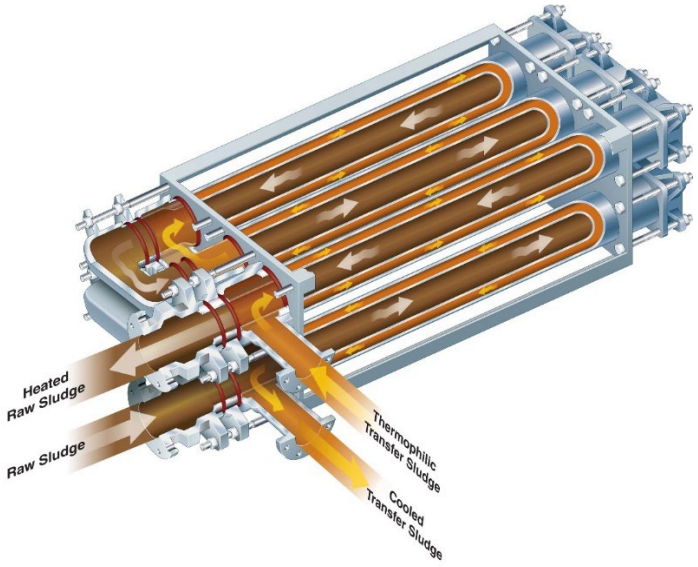


*Figure 25. Sludge heat exchanger technology, "HeatX", offered by Walker Process Equipment* ***(Walker Process Equipement, 2018)***

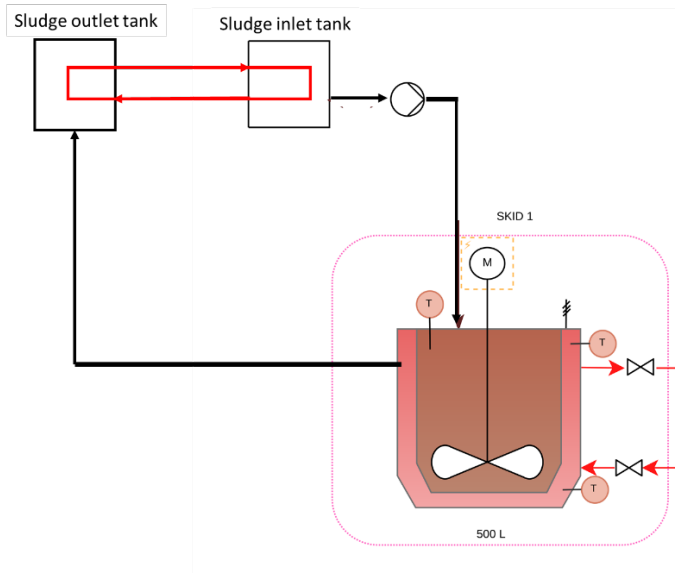


*Figure 26. Possible configuration in the current solar pasteurisation system for heat recovery through a heat exchanger between inflow and outflow sludge*

### *4.2.5. Summary*

The proposed improvements show a significant positive impact on the viability of the pasteurization process. The optimal configuration involves implementing 25 vacuum tube collectors, an LPG boiler as an energy backup, and a low-cost sludge pre-heater. This combination allows the system to approach closely the target of treating 3000 L/day using predominantly solar energy with minimized operational costs.

The combination of the enhancements leads to an estimated 20% increase in capital costs while reducing operating costs by approximately 90% compared to the baseline. This results

in a rapid ROI of around 5 months. However, the practical effectiveness of heat exchangers for sludge energy recovery remains uncertain.

In the absence of a heat exchanger, the system still performs well, albeit with a considerable reduced capacity to treat sludge using solar energy alone. In contrast, the investment is recovered faster (in approximately 3 months) due to the lower initial capital investment with respect to the running cost reductions. Despite these benefits, excluding the heat exchanger increases the system's reliance on LPG, exposing it to potential price fluctuations and supply risks. Therefore, heat recovery offers a promising solution to explore, as it could potentially enable the system to operate primarily on solar energy. While increasing the number of solar collectors could achieve similar results, this approach would substantially expand the system's spatial footprint—a critical limitation in humanitarian settings where space is constrained. A more comprehensive market study is required to assess the feasibility and cost of heat exchangers, as uncertainties still exist regarding their practical deployment in the context of our technology.

## 4.3. Replicability analysis

This section evaluates the replicability of solar pasteurization technology in other humanitarian emergency contexts. Three sites were selected for analysis: Bentiu (South Sudan), Pemba (Mozambique), and Maiduguri (Nigeria). The evaluation was conducted through a solar assessment followed by a techno-economic analysis, using the optimal system configuration identified in the previous section. Due to significant uncertainties regarding the heat recovery unit, it was excluded from this study.

The replicability analysis can be found in Supporting Document K, L and M for Bentiu, Maiduguri and Pemba, respectively.

### *4.3.1. Solar assessment*

Table 11 presents the results of the solar assessment for Bentiu, Pemba, and Maiduguri. Among the three locations, Maiduguri shows the highest solar irradiance, closely followed by Pemba and Bentiu. All three locations exhibit higher irradiance levels (approximately 10% more) compared to Cox's Bazar. A trend emerges, indicating lower irradiance in regions with higher rainfall. In terms of ambient temperature, Bentiu records the highest average at approximately 29°C, followed by Maiduguri at 28°C, Pemba at 26°C, and Cox's Bazar at 25°C.

The optimal tilt angles for the three new locations are around 15°, slightly lower than the 20° optimal tilt in Cox's Bazar. These locations experience approximately six hours of peak solar radiation, one hour more than Cox's Bazar. Daily operation times are similar for Cox's Bazar, Maiduguri, and Bentiu, averaging around 9 hours, while Pemba offers an additional hour of operation. The most suitable start time for operations is 6 AM in Pemba and 7 AM in the other locations, with all sites concluding operations by 4 PM.

Regarding treatment capacity using only solar energy, Maiduguri and Bentiu achieve nearly 2000 L/day, treating approximately 500 L/day more sludge compared to Cox's Bazar. Pemba's

capacity falls between these two cases, reflecting the differences in solar irradiance at each site.

*Table 11. Solar assessment for Bentiu (South Soudan), Pemba (Mozambique) and Maiduguri (Nigeria), and comparison to the case from this project at the Rohingya refugee camp in Cox's Bazar (Bangladesh)*

| | Cox's Bazar | Bentiu | Pemba | Maiduguri |
|---|---|---|---|---|
| **Average ambient temperature (°C)** | 25.3 | 28.8 | 25.8 | 27.9 |
| **Cumulative rainfall (mm)** | 2643.2 | 869.0 | 1118.8 | 451.2 |
| **Solar irradiance at optimal angle (kWh/m$^2$/year)** | 1950.6 | 2172.1 | 2173.1 | 2218.4 |
| **Optimal tilting angle** | 25° | 14° | 15° | 16° |
| **Peak solar hours** | 5 | 6 | 6 | 6 |
| **Possible operation length (h)** | 9 | 9 | 10 | 9 |
| **Possible time beginning of operation** | 7 AM | 7 AM | 6 AM | 7 AM |
| **Possible time end of operation** | 4 PM | 4 PM | 4 PM | 4 PM |
| **Treatment capacity with only solar (L/day)** | 1566 | 1935 | 1770 | 1918 |

### *4.3.2. Techno-economic analysis*

The techno-economic analysis for the four regions is summarized in Table 12. While capital costs and surface footprints remain consistent across all sites, operating costs vary due to differences in treatment capacity. The higher treatment capacities observed in Maiduguri and Bentiu lead to the lowest operating costs and SEC, followed by Pemba, with Cox's Bazar ranking last.

*Table 12. Tecno-economic analysis for the installation and operation of a solar pasteuriser in Bentiu (South Soudan), Pemba (Mozambique) and Maiduguri (Nigeria), and comparison to the case from this project at the Rohingya refugee camp in Cox's Bazar (Bangladesh)*

| | Cox's Bazar | Bentiu | Pemba | Maiduguri |
|---|---|---|---|---|
| **Treatment capacity with only solar (L/day)** | 1745 | 2157 | 1973 | 2138 |
| **Total treatment capacity (L/day)** | 3000 | 3000 | 3000 | 3000 |
| **Capital cost (€)** | 38100 | 38100 | 38100 | 38100 |
| **Specific capital cost (€/m$^3$·day)** | 12700 | 12700 | 12700 | 12700 |
| **Operating cost (€/day)** | 7.82 | 6.14 | 6.96 | 6.22 |
| **Specific operating cost (€/m$^3$)** | 2.61 | 2.05 | 2.32 | 2.07 |
| **Energy consumption (kWh)** | 0.95 | 0.64 | 0.64 | 0.64 |
| **Specific energy consumption (kWh/m$^3$·day)** | 0.32 | 0.21 | 0.21 | 0.21 |
| **Surface area (m$^2$)** | 155 | 155 | 155 | 155 |
| **Specific surface area (m$^2$/m$^3$·day)** | 52 | 52 | 52 | 52 |

Operational costs for solar pasteurization plants are approximately 20% lower in Maiduguri and Bentiu compared to Cox's Bazar. In Pemba, operating costs are reduced by around 10%. This demonstrates the economic advantage of deploying solar pasteurization technology in regions with higher solar irradiance, enhancing the cost-effectiveness of the system.

#### *4.3.3. Summary*

The installation of solar pasteurizers is most advantageous in the sites in Bentiu and Maiduguri due to their higher treatment capacity using solar energy and lower associated costs. Pemba presents a similar case, albeit to a lesser extent. These advantages are directly linked to the higher solar irradiance received in these regions.

Although all four locations are in tropical areas, Bangladesh is farther from the equator, which affects solar intensity. Additionally, Bangladesh faces the challenge of the Indian monsoon, the strongest in the world, occurring from July to September. During this period, heavy rainfall and extensive cloud cover significantly reduce solar radiation, hindering solar energy collection. In contrast, rainy seasons in the other studied countries are less intense, minimizing this issue.

If an effective heat recovery system is implemented, there is potential for the pasteurization plants in Bentiu and Maiduguri to operate entirely on solar energy without the need for backup energy sources.

# 5. Conclusion

The project aimed to test and evaluate the implementation of a solar pasteurizer at the Rohingya refugee camp in Cox's Bazar, Bangladesh. This innovative approach leverages solar energy to pasteurise faecal sludge effluent that was treated in a decentralized wastewater treatment system (DEWATS) in order to reduce pathogen levels prior to discharge. Experimental data gathered from the pasteurizer informed the development of a model, and allowed for a comprehensive solar assessment and techno-economic analysis. The study's goal was to assess the feasibility of scaling this solution within the camp and replicating it in other humanitarian settings.

## 5.1. Pasteurization Temperature

Pasteurization tests were conducted across a temperature range of 50°C to 70°C, with the most practical operational range found between 55°C and 65°C. Below 55°C, pathogen inactivation is unsatisfactory, while temperatures above 65°C are challenging to sustain. A target temperature of 65°C was identified as the ideal balance, ensuring sufficient deactivation of key pathogens such as Escherichia coli, Vibrio cholerae (main focus pathogen in this project), Salmonella, Ascaris, Taenia, and Shigella. However, enteric viruses, including norovirus and rotavirus, exhibit higher heat resistance and may require higher temperatures or additional treatment beyond the solar pasteurization process.

## 5.2. Treatment Capacity

A clear inverse relationship between pasteurization temperature and treatment capacity was observed—higher temperatures led to reduced treatment volumes. While pasteurization at 55°C allows for greater throughput, achieving higher levels of pathogen reduction requires operation at 65°C. Given the current state of the technology, selecting the appropriate pasteurization temperature involves balancing treatment capacity with pathogen reduction goals, considering contextual constraints. However, even with system optimization and supplementary energy from a diesel generator, the treatment target could not be fully met. Although the generator helped increase throughput, it did so at the expense of significantly higher operational costs. Additionally, the monsoon season in Bangladesh presents further challenges, as reduced solar irradiance and heavy cloud cover limit the availability of solar energy, further constraining system performance.

To address these challenges, system improvements were proposed, including increasing the number of solar collectors, using vacuum tube collectors instead flat plate collectors, recovering heat from the pasteuriser hot effluent, and integrating an liquified petroleum gas (LPG) boiler for backup energy. These modifications substantially enhance treatment capacity, potentially increasing throughput by two to three times. Although capital costs rise, operational savings enable a return of investment (ROI) in under one year compared to the current system configuration. Pre-heating the sludge before pasteurization, through a heat recovery unit utilizing hot effluent, has been identified as the only viable approach to enable

full system operation primarily on solar energy, while minimizing reliance on backup energy sources.

For optimal operation, the pasteurizer should be heated directly by solar collectors during peak solar hours, which typically occur from 9 AM to 2 PM. Outside of these hours, the pasteurizer must rely on heat stored in buffer tanks. This approach is also essential on days with low solar irradiance, such as overcast or rainy conditions. The temperature of the buffer tanks will be replenished using either the LPG boiler or surplus solar energy, assuming that the solar energy collection would be enhanced by utilizing a greater number of solar collectors and employing vacuum tube collectors.

### 5.3. Replicability

The replicability of the solar pasteurizer was assessed in humanitarian settingsin Bentiu (South Sudan), Maiduguri (Nigeria), and Pemba (Mozambique). These locations exhibit higher solar irradiance, longer sunshine hours, and lower rainfall compared to Cox's Bazar, resulting in greater system efficiency and lower operating costs. In Bentiu and Maiduguri, optimized systems could potentially almost operate solely on solar energy without the need for an energy backup, unlike in Bangladesh. This highlights the suitability of solar pasteurization technology for semi-arid and tropical regions with minimal cloud cover and high solar potential.

### 5.4. Compliance with Regulations

While effective in pathogen reduction, the solar pasteurizer does not significantly alter the physicochemical properties of the effluent, such as chemical oxygen demand (COD), biological oxygen demand (BOD), or nutrient levels. Consequently, pasteurized effluent may not meet discharge regulations without additional downstream treatment. The pasteurizer must be integrated into broader treatment chains, contributing to microbial compliance while combined with complementary processes, such as DEWATS, to address organic and nutrient pollution.

### 5.5. Final Remarks

The solar pasteurizer can prevent cholera outbreaks at the Rohingya camp, which is the primary objective of this project. Beyond this, the technology has demonstrated significant potential as a scalable and modular sanitation solution for humanitarian settings. Its reliance on solar energy aligns with sustainable development goals, offering a low-operational-cost alternative that reduces greenhouse gas emissions. The system's modular design facilitates scalability, with the capacity to expand through the addition of solar collectors.

While initial capital costs are high, sourcing materials from local markets (Bangladesh, India, or China) could mitigate expenses. The system's low electricity demand enables off-grid operation through photovoltaic panels, enhancing resilience and energy independence.

Additionally, the pasteurizer has demonstrated its adaptability to climate change by withstanding extreme weather conditions during testing, making it suitable for deployment in challenging environments. It also helps mitigate the likelihood of cholera outbreaks due to increasing floods and provides a source of reused water addressing water scarcity issues (as it could be the case of South Soudan).

By primarily relying on solar energy, the system contributes to lower greenhouse gas emissions.

In conclusion, the solar pasteuriser project successfully demonstrated the feasibility of using solar energy to enhance sanitation, and reduce cholera outbreaks and other pathogen disease transmission in densely populated humanitarian settings . Solar pasteurization represents a promising innovation for improving sanitation in humanitarian contexts, addressing urgent health needs while contributing to climate resilience and sustainable development.

### 5.6. Way forward

Looking to the future, a new phase of the project is set to commence in 2025, supported by new funding. This phase will focus on several key initiatives:

- Continuation of the solar pasteuriser testing at the Rohingya camp (Cox's Bazar, Bangladesh): Ongoing testing of the current solar pasteurizer will be conducted to optimize the pasteurization process, drawing on the outcomes and insights gained from this project. This continuous evaluation aims to refine operational parameters and improve system performance. Notably, it will be valuable to assess the process's operation during the peak irradiance season from March to May.
- Model Development: The project will continue to the existing model, improving its correlation with new data. This will include incorporating deactivation kinetics of additional pathogens to broaden the understanding of the pasteurization process**.**
- Refinement of Techno-Economic Analysis: A more thorough market research effort will be undertaken to refine the techno-economic analysis, particularly focusing on vacuum tube collectors and sludge heat exchangers. This research will help identify cost-effective solutions and improve system efficiency.
- Replication in South Sudan: Building on the insights and learnings from this project, we aim to replicate the solar pasteurization initiative in South Sudan. An improved version of the pasteurizer will be deployed, tailored to the specific conditions and needs of the region.

By pursuing these initiatives, we aim to enhance the effectiveness and scalability of solar pasteurization technology, further contributing to improved sanitation in humanitarian contexts.

# References


Alam, M., Ahsan, S., Pazhani, G. P., Tamura, K., Ramamurthy, T., Gomes, D. J., Rahman, S. R., Islam, A., Akhtar, F., & Shinoda, S. (2006). Phenotypic and molecular characteristics of Escherichia coli isolated from aquatic environment of Bangladesh. *Microbiology and Immunology*, *50*(5), 359–370.

Atenodoro-Alonso, J., Ruíz-Espinoza, J. E., Alvarado-Lassman, A., Martínez-Sibaja, A., Martínez-Delgadillo, S. A., & Méndez-Contreras, J. M. (2015). The enhanced anaerobic degradability and kinetic parameters of pathogenic inactivation of wastewater sludge using pre-and post-thermal treatments Part 2. *Revista Mexicana de Ingeniería Química*, *14*(2), 311–319.

Bohnert, K. (2017). *A Comparison of the Microbiological Effectiveness of Treatment Systems*.

Dey, D., Ridwanul Haque, A. T. M., Kabir, B., & Ubaid, S. F. (2016). Fecal indicator and Ascaris removal from double pit latrine content. *Journal of Water and Health*, *14*(6), 972–979.

Espinosa, M. F., Sancho, A. N., Mendoza, L. M., Mota, C. R., & Verbyla, M. E. (2020). Systematic review and meta-analysis of time-temperature pathogen inactivation. *International Journal of Hygiene and Environmental Health*, *230*, 113595.

Feachem, R. G., Feachem, R. G. A., Bradley, D. J., Garelick, H., & Mara, D. D. (1983). *Sanitation and disease: health aspects of excreta and wastewater management* (Vol. 1). Wiley New York.

Foster, T., Falletta, J., Amin, N., Rahman, M., Liu, P., Raj, S., Mills, F., Petterson, S., Norman, G., & Moe, C. (2021). Modelling faecal pathogen flows and health risks in urban Bangladesh: implications for sanitation decision making. *International Journal of Hygiene and Environmental Health*, *233*, 113669.

Huq, A., Sack, R. B., Nizam, A., Longini, I. M., Nair, G. B., Ali, A., Morris Jr, J. G., Khan, M. N. H., Siddique, A. K., & Yunus, M. (2005). Critical factors influencing the occurrence of Vibrio cholerae in the environment of Bangladesh. *Applied and Environmental Microbiology*, *71*(8), 4645–4654.

JRB. (2020). *2019 for Rohingya Humanitarian Crisis, January–December*.

Koottatep, T., Phuphisith, S., Pussayanavin, T., Panuvatvanich, A., & Polprasert, C. (2014). Modeling of pathogen inactivation in thermal septic tanks. *Journal of Water, Sanitation and Hygiene for Development*, *4*(1), 81–88.

Lang, N. L., & Smith, S. R. (2008). Time and temperature inactivation kinetics of enteric bacteria relevant to sewage sludge treatment processes for agricultural use. *Water Research*, *42*(8–9), 2229–2241.

Longini Jr, I. M., Yunus, M., Zaman, K., Siddique, A. K., Sack, R. B., & Nizam, A. (2002). Epidemic and endemic cholera trends over a 33-year period in Bangladesh. *The Journal of Infectious Diseases*, *186*(2), 246–251.

Lopez, A. L., DeRoeck, D., Maskery, B., Levin, A., Bultman, J., Kim, Y. E., & Mogasale, V. (2012). Country Investment Case Study on Cholera Vaccination: Bangladesh. *Seoul, South Korea: International Vaccine Institute*.

SaniHUB. (2024). *IOM Decentralized Wastewater Treatment System (DEWATS) in the Rohingya refugee camps in Cox's Bazar, Bangladesh*. Https://Sanihub.Info/Topic/Iom-Decentralized-Wastewater-Treatment-System-Dewats-in-the-Rohingya-Refugee-Camps-in-Coxs-Bazar-Bangladesh/.

Spinks, A. T., Dunstan, R. H., Harrison, T., Coombes, P., & Kuczera, G. (2006). Thermal inactivation of water-borne pathogenic and indicator bacteria at sub-boiling temperatures. *Water Research*, *40*(6), 1326–1332.

UNHCR. (2020). *Figures at a Glance*. Https://Www.Unhcr.Org/Figures-at-a-Glance.Html.

UNHCR. (2022). *Rohingya Population by Location*. Https://Data.Unhcr.Org/En/Documents/Download/94163.

Walker Process Equipement. (2018). *Digester Heating Systems: Heat Exchangers*. Https://Www.Walker-Process.Com/Prod_digestion_heatexchangers.Htm.

Wazed, M. A., Nukman, Y. bin, & Islam, M. T. (2010). Design and fabrication of a cost effective solar air heater for Bangladesh. *Applied Energy*, *87*(10), 3030–3036.

Ziemba, C., & Peccia, J. (2011). Net energy production associated with pathogen inactivation during mesophilic and thermophilic anaerobic digestion of sewage sludge. *Water Research*, *45*(16), 4758–4768.

# Appendix A: Log of modifications of the installation

## General setup

- End of August
  - Installation of a ceiling fan

- 02 September 2024
  - Moving the expansion tank from the primary circuit at a higher height and placing the expansion tank below it
  - Installation of a shade tarp to make shadow in the front area of the testing shed

- 03 September 2024
  - Labelling the pipes (red tape: "hot" stream)
  - Labelling the valves (white tap: heating of the pasteuriser from the solar collectors; yellow tape: heating of the tanks; black tape: heating of the pasteuriser from the tanks)

- 04 September 2024
  - Continuation of labelling of the pipes (blue tape: "cold stream")

- 10 September 2024
  - Continuation of the labelling of the pipes (writing number in pipes and pumps corresponding to Mode 1, 2 or 3)
  - Labelling of the pumps and corresponding electric sockets involved in Mode 1, 2 or 3

- 15 September 2024
  - Posting poster indicating the weather conditions to consider in the datasheet
  - Labelling the valves and pumps from 2° circuit with green tape (+electric connections from the pump)

- 17 September 2024
  - Changes of labelling from the pipes, and pumps with electric connections (change of color of tape from black to green)

- 21 September 2024
  - Addition of blankets in gaps of the pasteuriser cover (which deformed after high temperature tests)

- 29 September 2024
  - Setup of the high pressure water jet pump for cleaning of the pasteuriser

- 01 October 2024
  - Change in the labeling in the primary circuit after adding the gate valve after one of the pumps (now, each pump  line corresponding to Mode 1 or 2)

- 03 October 2024
    - Setup of two light bulbs at the roof of the testing shed to bring light when the sky is too dark
    - Straightening of temperature gauge at the inlet of the pasteuriser double jacket

- 05 October 2024
    - Adding labelling to the added valves and electric connection of the pump from the secondary circuit (missing)
    - Modification of labelling in the pumps from the primary circuit (only the pump from the line with a temperature gauge to be used for Mode 1 and 2)

- 10 October 2024
    - Addition of labelling in the electric connection from the pump corresponding to Mode 3

## Civil work

- End of August
    - Closure of the pasteurization room by adding a wall, including a door with a lock and a window (leading to the change of the access to the room from the left inside the right side)

- 02 September 2024
    - Breaking a small section of the wall to place the pipe connecting the pressure booster with its water reservoir

- 15 September 2024
    - Structure of a pipe chamber outside the shed to house the inlet, outlet and overflow pipes from the pasteuriser (outlet pipe connected to drain and infiltration bed; inlet pipe for connection to the buffer tank at the outlet of the DEWATS; overflow pipe connected to outdoors drain), including a drain connected to FS tank inlet to the DEWATS

- 17 September 2024
    - Thermocouple to measure temperature in pasteuriser tied to sling holding the pasteuriser
    - Addition of a cover to the pipe chamber

- December 2024
    - Construction of a permanent structure to hold the solar collectors

## Electrical modifications

- 05 June
  Addition of PV system (panel + inverter + battery) to power the interface box and the pumps

- 13 June
  PV panels (x4) placed to power the stirrer in the pasteurizer, but not possible to finish installation due to problems with inverter, so PV panels removed

- 16 June
  Addition of solar charge controller for battery

- 03 July
  Setup of an electrical junction breaker to have a second electric connection for the Diesel generator circuit (in order to be able to operate with the stirrer and electric heater at the same time)

- End of August
  - Installation of PV system (installation of more panels, inverter and 2 batteries) for the electric supply of the pumps, solar station, stirrer of the pasteuriser and ceiling fan
  - Installation of electric switched sockets and circuit breaker
  - Installation of a wood electric backing board to place all new electric components and wiring

- 02 September 2024
  - Making more neat the electrical connection on the electric backing board
  - Installation of electric connection to the inverter for the pressure booster

- 03 September 2024
  - Setup of an electric switched socket connected to a breaker directly connected to the inverter, for the electric supply of the pumps from the primary circuit without passing through the solar station box (which only supplies electricity if the temperature of the collectors is higher than that from the tanks)

- 21 September 2024
  - Tying the cable from the diesel generator for a more neat setup

- 03 October 2024
  - Setup of an electric switch connected to the roof fan and the two newly added light bulbs
  - Addition of electric resistance to the first buffer tank

- 05 October 2024
  - Addition of a switched electric socket for the electric resistance from the first tanks

## Hydraulic modifications

- 11 June
  Setup of the piping at the outlet of the pasteurizer tank

- End of August
  - Adding pipes, T-junctions and ball valves to connect the solar collectors to the pasteuriser and tanks
  - Connecting the outlet of the pasteuriser jacket to the first tank by one of the bottom ports (at the level of the heating coil) and addition of a ball valve
  - Closure of one of the ports from the second tank (the one that was connected to the first tank at the bottom)
  - Addition of a short length of linear pipe for the second and third solar collectors row, after the flow divider, to allow for a more even distribution of flow between the solar collectors

- 02 September 2024
  - Installation of the pressure booster inside the pasteurization chamber and a water reservoir tank at the other side of the wall (outdoors)

- 03 September 2024
  - Installation of a non-return valve at the inlet of the pipe of the pressure booster (placed in water reservoir)
  - Disconnection of some of the pipes connecting the solar panels to the pasteurization tank to put the proper fittings
  - Shortening of some of the pipes that were too long
  - Teeing the pipes for a more neat setup

- 04 September 2024
  - Re-adjustment of the opening of the valves in the lines from each solar collector row for even distribution of the flow
  - Addition of transparent pipes in air purge valves

- 05 September 2024
  - Pipes from collectors shorten and tied for more neat setup
  - Fixing a few leaks located at the T-junction at the outlet of the tank and pasteuriser to the solar collectors ("cold" stream) but persistence of one leak

- 08 September 2024
  - Fixing leak

- 09 September 2024
  - Readjustment valve position of the collectors rows since most of the flow for the middle row
    Final adjustment: 1st row between B and C position; 2nd row at D position; 3rd row between C and D position (all positions leadings to around +5 in the reader with flow)

- 10 September 2024
  - Thermal insulation added to the pipes from the panels, pipes from the hydraulic panel, connections and T-junctions from the tanks and pasteuriser, and pipes from the 2°circuit
  - Pipe from the purge from the tied to pipe connecting second buffer tank to the pasteuriser to make a more neat setup
  - Valve for the second solar collector row readjusted to position C because of too much flow

- 15 September 2024
  - Installation of thermal insulation in the missing exposed pipes in the collectors side (outlet pipe from the middle row; flow divider at the inlet of the collectors)
  - Addition of plastic bottle at the end of the tubes from the pressure relief valve in the pasteuriser and air purge from the secondary circuit

- 25 September 2024
  - Added extension to the tube from the air purge valve from the secondary circuit to the pipe chamber for drainage

- 01 October 2024
  - Installation of a gate valve in the pipe line of Pump 1 in order to replaced the damaged tap valve, in order to switch between Mode 1 and 2 without the need of change of pumps

- 03 October 2024
  - Addition of gate valves in the connection between tanks in order to heat one of the tanks without the need to heat the other
  - Addition of a by-pass line through a T-junction in order to connect the first buffer tank to the secondary circuit for the pasteuriser heating, including two gate valves to allow to use the first or both tanks for the pasteuriser heating

- 05 October 2024
  - Change of pipe diameter and fittings (from 1.5'' to 1") in the connection of the first tank with second tank and secondary circuit (through T-junction)
  - Fixing leaks
  - Thermal insulation added to the new pipe sections

- 10 October 2024
  - Fixing a few leaks in the connections from the line connecting the first buffer tank to the secondary circuit
  - Change of the opening position of the valves controlling the water flow in the solar collector rows (because no flow in the middle row)
    Final adjustment: 1st row between B and C position; 2nd row at D position; 3rd row between C and D position (all positions leadings to around +5 in the reader with flow)

## Thermal insulation

- 06 June
  Installation of thermal insulation in the pipes

- 09 June
  Installation of thermal insulation in the pipes and expansion tank from the secondary circuit

- 10 June
  Thermal insulation of the expansion tank from the 2°circuit and the sensor caps

- 11 June
  Thermal insulation of pipes

- 13 June
  Thermal insulation placed in inlet and outlet pipes from pasteurizer

- 03 July
  Thermal insulation of the outlet pipes from the pasteuriser

- 10 September 2024
  - Thermal insulation added to the pipes from the panels, pipes from the hydraulic panel, connections and T-junctions from the tanks and pasteuriser, and pipes from the 2°circuit

- 15 September 2024
  - Installation of thermal insulation in the missing exposed pipes in the collectors side (outlet pipe from the middle row; flow divider at the inlet of the collectors)

- 05 October 2024
  - Thermal insulation added to the new pipe sections

- 10 October 2024
  - Thermal insulation of the piping sections that were exposed for the leak reparation

# Appendix B: photographs from the solar pasteurisation installation




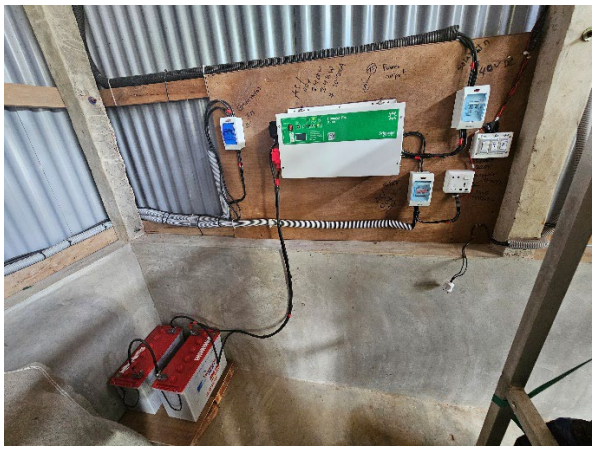

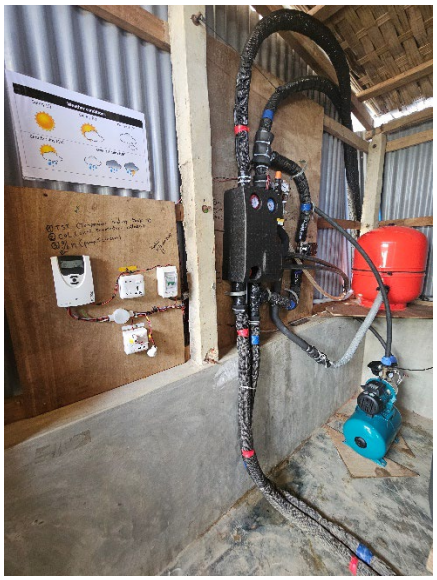


Fondation
VEOLIA


VEOLIA

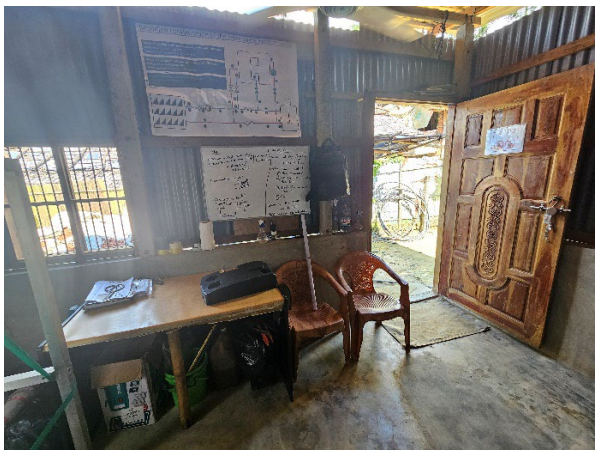


MRF Site 02

## Appendix C: log tests in the solar pasteuriser

| Date | Average weather | Feedstock | Test |
|---|---|---|---|
| 09/06 | Sunny | - | Mode 2b |
| 10/06 | Sunny | - | One batch in Mode 3b without pasteurisation |
| 11/06 | Cloudy | Water | One batch in Mode 3b without pasteurisation |
| 12/06 | Overcast | Water | Pasteurization at 67°C |
| 13/06 | Overcast | Water | Pasteurization at 67°C |
| 16/06 | Cloudy | Water | Pasteurization at 50°C |
| 18/06 | Sunny | Water | One batch in Mode 3b with pasteurisation at 50°C |
| 19/06 | Cloudy | Water | One batch in Mode 3b with pasteurisation at 50°C |
| 20/06 | Sunny | Water | One batch in Mode 3b without pasteurisation |
| 23/06 | Cloudy | - | Mode 2b |
| 24/06 | Cloudy | Water | One batch in Mode 3b with pasteurisation at 55°C |
| 25/06 | Cloudy | - | Mode 2b |
| 26/06 | Cloudy | - | Mode 2b |
| 27/06 | Cloudy | Sludge | One batch in Mode 3b with pasteurisation at 60°C |
| 29/06 | Cloudy | - | Mode 2b |
| 30/06 | Overcast | - | Mode 2b |
| 01/07 | Overcast Rainy | - | Mode 2b |
| 02/07 | Overcast Rainy | - | Mode 2b |
| 03/07 | Overcast Rainy | Sludge | One batch in Mode 3b with pasteurisation at 55°C |
| 04/07 | Cloudy | - | Mode 2b |
| 06/07 | Cloudy | - | Mode 2b |
| 07/07 | Cloudy | - | Mode 2b |
| 08/07 | Cloudy | Sludge | One batch in Mode 3b with pasteurisation at 65°C |
| 09/07 | Cloudy | - | Mode 2b |
| 10/07 | Cloudy | Sludge | One batch in Mode 3b with pasteurisation at 55°C |
| 09/09 | Sunny | - | Mode 2b |
| 10/09 | Cloudy | Water | One batch in Mode 1 without pasteurisation and Mode 2 |
| 11/09 | Cloudy | Water | One batch in Mode 1 without pasteurisation |
| 12/09 | Cloudy | Water | One batch in Mode 1 without pasteurisation |
| 15/09 | Overcast | Water | One batch in Mode 1 without pasteurisation |
| 16/09 | Cloudy | - | Mode 2b |
| 17/09 | Sunny | Water | One batch in Mode 1 without pasteurisation and Mode 2b |
| 18/09 | Cloudy | Sludge | One batch in Mode 1 combined with Mode 3b without pasteurisation, and Mode 2b |
| 19/09 | Cloudy | Water | One batch in Mode 3b |

| | | | |
|---|---|---|---|
| 21/09 | Cloudy | Water | Two batches in Mode 1 with pasteurisation at 60°C, and Mode 2b |
| 22/09 | Cloudy | Water | One batch in Mode 3b and two batches Mode 1 with pasteurisation at 55°C, and Mode 2b |
| 23/09 | Cloudy | Sludge | Two batches in Mode 1 with pasteurisation at 60°C and 55°C, and Mode 2b |
| 24/09 | Cloudy | Water | One batch in Mode 1 without pasteurisation and Mode 2b |
| 25/09 | Overcast | Sludge | One batch in Mode 3b with pasteurisation at 55°C |
| 26/09 | Cloudy | - | Mode 2b |
| 28/09 | Sunny | - | Mode 2b |
| 29/09 | Cloudy | Sludge | One batch in Mode 1 with pasteurisation at 70°C and Mode 2b |
| 30/09 | Rainy cloudy | Water | Two batches in Mode 1 with pasteurisation at 40°C and without pasteurisation, and Mode 2b |
| 01/10 | Cloudy | Sludge | One batch in Mode 1 with pasteurisation at 50°C and Mode 2b |
| 02/10 | Overcast | Water | Four batches in Mode 3b without pasteurisation |
| 06/10 | Cloudy | - | Mode 2a |
| 07/10 | Cloudy | - | Mode 2a |
| 08/10 | Sunny | - | Mode 2b |
| 09/10 | Sunny | - | Mode 2b |
| 10/10 | Cloudy | Sludge | Mode 3b |
| 14/10 | Sunny | Sludge | One batch in Mode 1 and one batch in Mode 3a without pasteurisation, and Mode 2a |
| 15/10 | Cloudy | Sludge | One batch in Mode 1 and two batches in Mode 3b without pasteurisation, and Mode 2a |
| 16/10 | Sunny | Sludge | Four batches in Mode 1 without pasteurisation |
| 27/10 | Cloudy | - | Mode 2a |
| 28/10 | Sunny | - | Mode 2a |
| 29/10 | Sunny | - | Mode 2a |
| 30/10 | Sunny | Sludge | One batch in Mode 3a without pasteurisation |

## Appendix D: Heat balance calculations

(i) Total solar thermal energy available

$$P_{solar} = G \cdot A_{collector} \cdot N_{collectors}$$

(ii) Heat received by the solar collectors from the solar radiation

$$P_{collectors} = Q_{primary\ circuit} \cdot \rho_{water} \cdot Cp_{water} \cdot \Delta T_{collectors}$$

(iii) Heat received by the pasteuriser from the solar collectors (Mode 1) or the buffer tanks (Mode 3)

$$P_{pasteuriser} = V_{pasteuriser} \cdot \rho_{water} \cdot Cp_{water} \cdot \left(\frac{\Delta T}{\Delta t}\right)_{pasteuriser}$$

(iv) Heat received by the buffer tanks from the solar collectors (Mode 2) and/or transferred to the pasteuriser

$$P_{tanks} = V_{tanks} \cdot \rho_{water} \cdot Cp_{water} \cdot \left(\frac{\Delta T}{\Delta t}\right)_{tanks}$$

(v) Heat transferred to the heating jacket of the pasteuriser

$$P_{jacket} = Q_{secondaruy\ circuit} \cdot \rho_{water} \cdot Cp_{water} \cdot \Delta T_{jacket}$$

(vi) Efficiency of the solar collectors heating

$$\eta_{collectors} = \frac{P_{collectors}}{P_{solar}}$$

(vii) Efficiency of the pasteuriser heating

$$\eta_{pasteuriser} = \frac{P_{pasteuriser}}{P_{jacket}}$$

(viii) Efficiency of the tanks

$$\eta_{tanks} = \frac{P_{tanks} + P_{jacket}}{P_{solar} + P_{electric}}$$

(ix) Efficiency Mode 1

$$\eta_{Mode\ 1} = \frac{P_{pasteuriser}}{P_{solar}}$$

(x) Efficiency Mode 2

$$\eta_{Mode\ 2} = \frac{P_{tanks}}{P_{solar} + P_{electric}}$$

(xi) Efficiency Mode 3

$$\eta_{Mode\ 3} = \frac{P_{pasteuriser}}{P_{solar} + P_{electric}}$$

(xii) Efficiency of the system

$$\eta_{system} = \frac{P_{tanks} + P_{pasteuriser}}{P_{solar} + P_{electric}}$$

Variable:

$A_{collector}$: surface area of the collector ($m^2$)

$Cp_{water}$: heat capacity of water (kJ/kg/°C)

$G$: irradiance (W/m2)

$N_{collectors}$: number of collectors

$P_{collectors}$: heat transferred to the collectors (kW)

$P_{jacket}$: heat transferred to the heating jacket of the pasteuriser (kW)

$P_{pasteuriser}$: heat transferred to the pasteurizer (kW)

$P_{solar}$: total solar power available (kW)

$P_{tanks}$: heat transferred to the buffer tanks (kW)

$Q_{primary\ circuit}$: flowrate of the heat carrier in the primary circuit (L/s)

$Q_{secondaruy\ circuit}$: flowrate of the heat carrier in the secondary circuit (L/s)

$V_{pasteuriser}$: volume of the pasteuriser (L)

$V_{tanks}$: volume of the tanks (L)

$\eta_{collectors}$ : efficiency of the solar collection of solar thermal energy by the collectors

$\eta_{Mode\ 1}$ : efficiency of Mode 1

$\eta_{Mode\ 2}$ : efficiency of Mode 1

$\eta_{Mode\ 3}$ : efficiency of Mode 1

$\eta_{pasteuriser}$ : efficiency of the heat transfer to the pasteuriser

$\eta_{tanks}$ : efficiency of the heat transfer to the pasteuriser

$\eta_{system}$ : efficiency of the system

$\rho_{water}$: water density (L/kg)

$\Delta T_{collectors}$: difference of temperature between the solar collectors inlet and outlet (°C)

$\left({}^{\Delta T}/_{\Delta t}\right)_{pasteuriser}$ : temperature variation in the pasteuriser during a given time (°C/s)

$\left({}^{\Delta T}/_{\Delta t}\right)_{tanks}$ : temperature variation in the tanks during a given time (°C/s)

# Appendix E: Development of the solar pasteuriser model

**Concept of the model**

The developed model is designed to predict the thermal behavior of the system over the course of a 24-hour operational period. It operates by integrating several key factors and processes, including solar irradiance, temperature dynamics within the system, and the energy consumption of various components. Below is a breakdown of the model's functionalities:

- Temperature Prediction: The model begins by using solar irradiance data to predict the temperature of the solar collectors. The solar irradiance is the primary input driving the heating process in the system. Based on the temperature of the solar collectors, the model computes the temperatures of the buffer tanks and the pasteurizer.
- Escherichia coli Inactivation: The model further evaluates the pasteurization process by calculating the removal of Escherichia coli (E. coli), a key factor in ensuring the safety and quality of the product being treated. The model assesses the thermal conditions required to achieve a certain level of microbial reduction.
- Heat Loss Considerations: The model accounts for the heat loss in the system, including losses in the buffer tanks and pasteurizer. This is essential for improving the accuracy of temperature predictions and ensuring realistic energy use calculations.
- Mode of Operation (Mode 1, 2, and 3): The model includes considerations for different modes of operation—Mode 1, Mode 2, and Mode 3. Each mode represents distinct operational scenarios, affecting the system's behavior and performance. The model dynamically adjusts to these modes, ensuring accurate predictions under varying conditions.
- Electric Consumption: The model also incorporates the electric consumption of various electrical components within the system. This includes pumps, sensors, and other control systems. By factoring in electricity usage, the model allows for the calculation of the specific energy consumption (SEC) of the system.

This comprehensive model offers an integrated approach for predicting thermal performance, ensuring optimal operation, and evaluating energy efficiency during daily operation.

**Inputs of the model**

- Volume of the buffer tanks (800 L for Mode 2a and 3a; 1600 L for Mode 2b and 3b)
- Initial temperature of the pasteuriser
- Initial temperature of the tanks
- Start and end times for Mode 1 and 3

- Start and end times for pasteurisation
- Start and end times for the use of the electric heater
- Hourly average irradiance
- Initial concentration of E. coli

**Equations of the model**

Heating of the collectors

The temperature of the solar collectors is directly correlated to the total solar energy absorbed by the system. This relationship has been determined experimentally and is modelled through an equation derived from experimental data (Figure 27).

$$T_{collectors} = 1.2296 \cdot P_{solar} + 44.812$$

$$T_{collectors} = 1.2296 \cdot (N_{collectors} \cdot A_{collectors} \cdot G) + 44.812$$

With:

$A_{collectors}$: surface area per solar collector ($m^2$)

$G$: solar irradiance ($W/m^2$)

$P_{solar}$: total solar power available (kW)

$N_{collectors}$: number of solar collectors

$T_{collectors}$: temperature at the outlet of the solar collectors (°C)

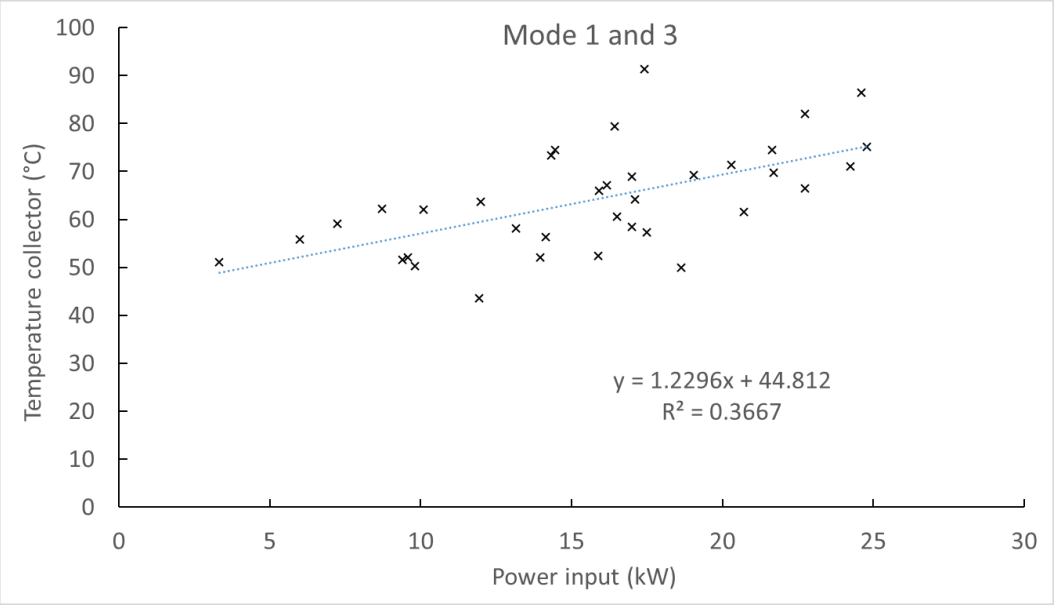


*Figure 27. Experimental correlation of the temperature in the collectors with the solar power input*

Heating of the pasteuriser

The pasteuriser heating was determined based on the heat transfer equation:

$$P_{pasteuriser} = h_{pasteuriser} \cdot A_{pasteuriser} \cdot (T_{inlet\ jacket} - T_{pasteuriser})$$

$$P_{pasteuriser} = V_{pasteuriser} \cdot \rho_{water} \cdot Cp_{water} \cdot \left(\frac{dT}{dt}\right)_{pasteuriser}$$

With:

$A_{pasteuriser}$: surface area of the pasteuriser for heat transfer ($m^2$)

$Cp_{water}$: heat capacity of water (J/kg/°C)

$\left({}^{dT}/_{dt}\right)_{pasteuriser}$: differential of temperature with time for the pasteuriser (°C/s)

$h_{pasteuriser}$: heat transfer coefficient for pasteurisation heating ($W/m^2/°C$)

$P_{pasteuriser}$: heat transferred to the pasteuriser (kW)

$T_{inlet\ jacket}$: temperature at the inlet of the heating jacket of the pasteuriser (°C)

$T_{pasteuriser}$: temperature of the pasteuriser (°C)

$V_{pasteuriser}$: volume of the pasteuriser (L)

$\rho_{water}$: water density (kg/L)

The parameter "$h_{pasteuriser} \cdot A_{pasteuriser}$" was determined experimentally based on Figure 28.

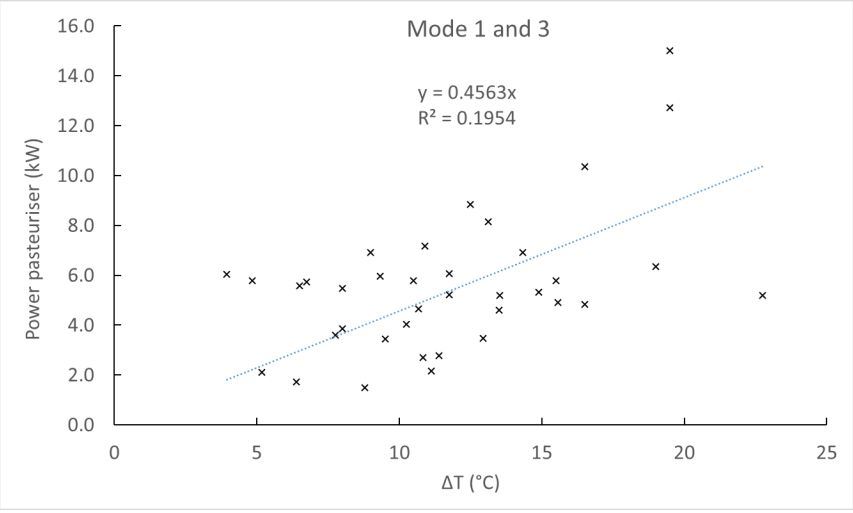


*Figure 28. Experimental correlation of the power of the pasteuriser with respect to the driven temperature gradient (i.e. difference between the temperature of the heating jacket inlet and the temperature of the pasteuriser)*

The temperature at the inlet of the heating jacket depends if the system is operated in Mode 1 (Figure 29) or Mode 3 (Figure 30).

Mode 1: $T_{inlet\ jacket} = 0.9142 \cdot T_{collector}$

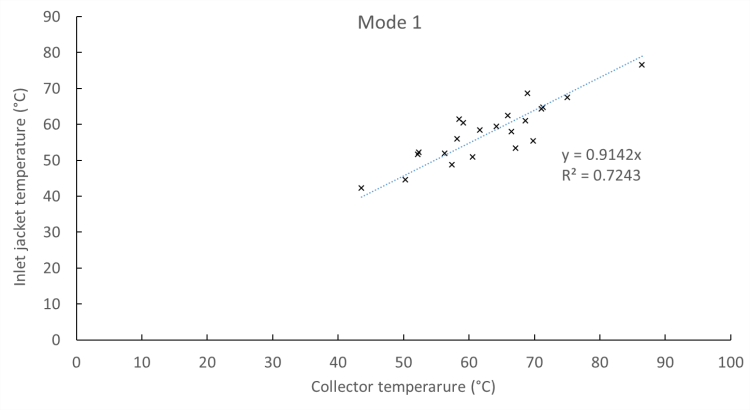


*Figure 29. Experimental correlation of the inlet temperature at the heating jacket of the pasteuriser with the collectors temperature (Mode 1)*

Mode 3: $T_{inlet\ jacket} = 1.0623 \cdot T_{tanks}$

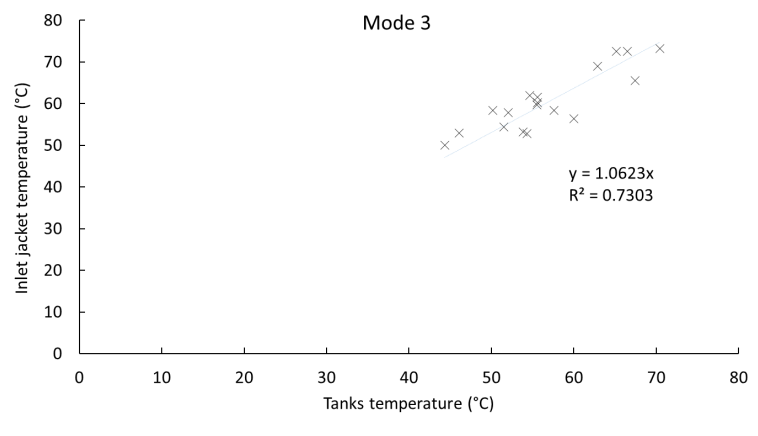


*Figure 30. Experimental correlation of the inlet temperature at the heating jacket of the pasteuriser with the tanks temperature (Mode 3)*

The heat loss in the pasteuriser can be expressed as following:

$$\dot{\Delta q}_{pasteuriser} = V_{pasteuriser} \cdot \rho_{water} \cdot Cp_{water} \cdot \left(\frac{\Delta T}{\Delta t}\right)_{heat\ loss\ pasteuriser}$$

With:

$\dot{\Delta q}_{pasteuriser}$: heat loss in the pasteuriser (kW)

$\left({}^{\Delta T}/_{\Delta t}\right)_{heat\ loss\ pasteuriser}$: heat loss rate in the pasteuriser (°C/s)

According to the experimental results: $\left({}^{\Delta T}/_{\Delta t}\right)_{heat\ loss\ pasteuriser}$ = 0.3°C/h.

Heating of the buffer tanks

The equation of the heating of the buffer tanks (Mode 2) can be expressed as follow:

$$P_{tanks} = h_{tanks} \cdot A_{tanks} \cdot (T_{collector} - T_{tanks}) + P_{electric}$$

$$P_{tanks} = V_{tanks} \cdot \rho_{water} \cdot Cp_{water} \cdot \left(\frac{dT}{dt}\right)_{tanks}$$

With:

$A_{tanks}$: surface area of the heating coils (m²)

$\left({}^{dT}/_{dt}\right)_{tanks}$: differential of temperature with time for the tanks (°C/s)

$h_{tanks}$: heat transfer coefficient for tanks heating (W/m²/°C)

$P_{electric}$: electric heating power (kW)

$P_{tanks}$: heat transferred to the tanks (kW)

$T_{tanks}$: temperature of the tanks (°C)

$V_{tanks}$: volume of the tanks

The parameter "$h_{tanks} \cdot A_{tanks}$" was determined through the experimental correlation shown in Figure 28.

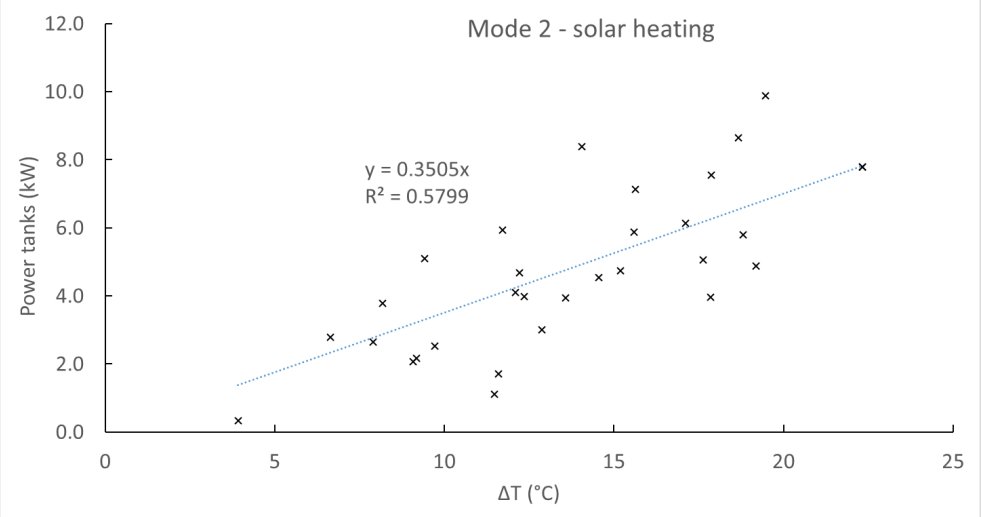


*Figure 31. Experimental correlation of the power of the tanks with respect to the driven temperature gradient (i.e. difference between the temperature of the collectors oulet and the temperature of the pasteuriser)*

The heat loss in the buffer tanks can be calculated as:

$$\dot{\Delta q}_{tanks} = V_{tanks} \cdot \rho_{water} \cdot Cp_{water} \cdot \left(\frac{\Delta T}{\Delta t}\right)_{loss\ tanks}$$

With:

$\dot{\Delta q}_{tanks}$: heat loss in the tanks (kW)

$\left({}^{\Delta T}/_{\Delta t}\right)_{loss\ pasteuriser}$: heat loss rate in the buffer tanks (°C/s)

According to an experimental correlation, the heat loss rate can be correlated to the buffer tanks temperature (Figure 32):

$$\left(\frac{\Delta T}{\Delta t}\right)_{loss\ tanks} = 0.0091 \cdot T_{tanks} - 0.3814$$

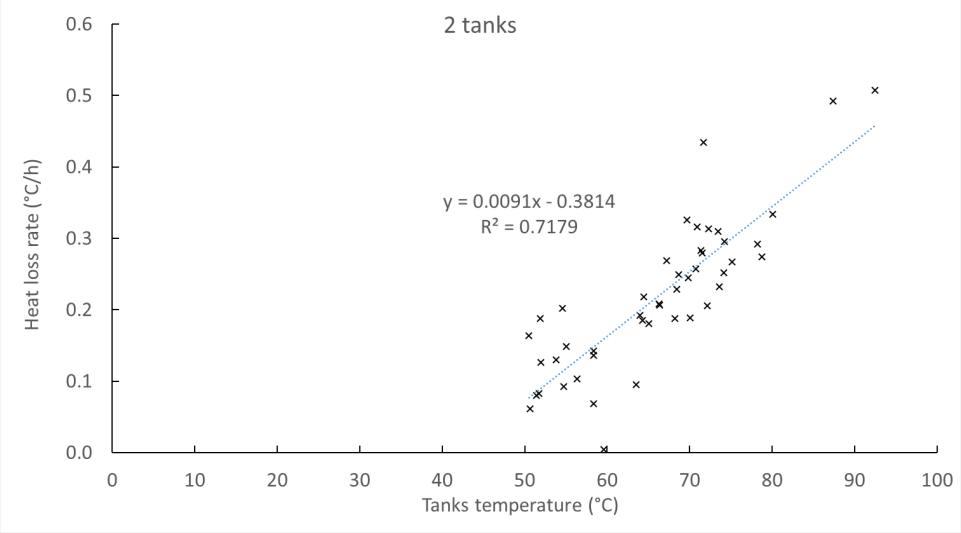


*Figure 32. Experimental correlation of the heat loss rate with the buffer tanks temperature*

In the case of operation in Mode 3, the next equation must be considered for the heat transfer in the tanks:

$$P_{tanks} = h_{tanks} \cdot A_{tanks} \cdot (T_{collector} - T_{tanks}) + P_{electric} - P_{pasteuriser}$$

<u>Deactivation of E. Coli:</u>

The Chick-Watson model was used to compute the concentration of E.coli at a given instant:

$$N_{E.coli}(t) = N_{0\ E.coli}(t) \cdot e^{-k \cdot t}$$

With:

$k$: deactivation constant rate (min)

$N_{E.coli}$: initial concentration of E. coli (cfu/mL)

$N_{0\ E.coli}(t)$: concentration of E. coli at any instant (cfu/mL)

$t$: deactivation time (min)

The deactivation constant rate can be expressed by an Arrhenius law:

$$k = k_0 \cdot e^{Ea/R \cdot T}$$

With:

$Ea$: activation energy (kJ/mol)

$k_0$: pre-exponential constant ($min^{-1}$)

$R$: constant of the perfect gas (kJ/mol/°K)

T: deactivation temperature (°K)

The parameters from this model were calculated from linear regressions using the experimental data obtained from the laboratory pasteurisation tests using wastewater from Delft.

The deactivation constant rate $k$ was determined for each pasteurisation temperature after linearizing the deactivation rate equation (Figure 33). For each temperature, this parameter corresponds to the gradient of the line.

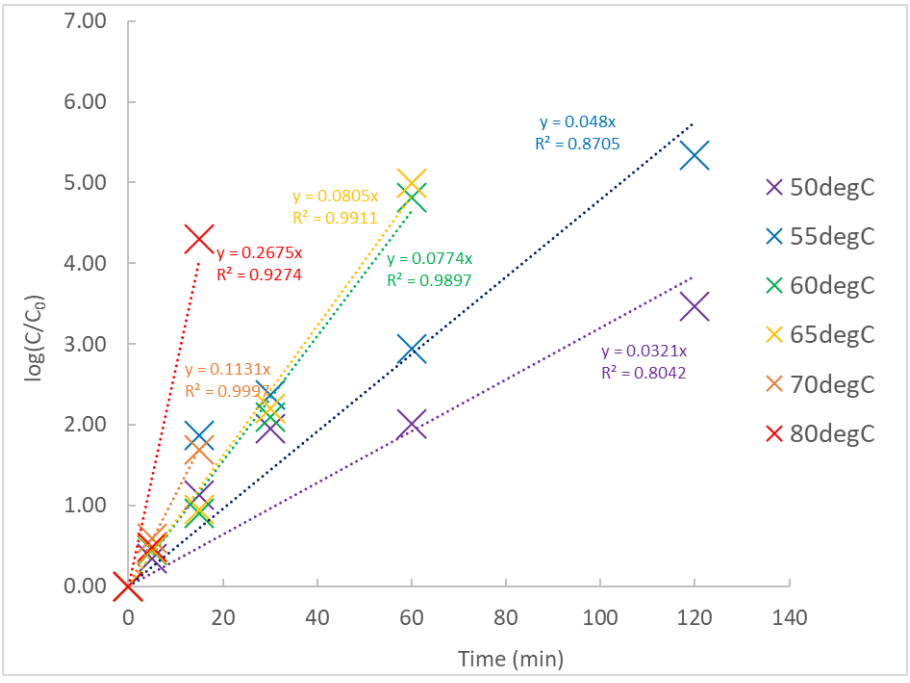


*Figure 33. Log (C/C0) as a function of time for different pasteurisation temperatures*

The parameters $Ea$ and $k_0$ were then calculated by linearizing the Arrhenius law (Figure 34). The activation energy $Ea$ can be deduced from the gradient of the line (equal to $^{Ea}/_{R}$) and the pre-exponential factor $k_0$ from the y-intercept (equal to $ln(k_0)$): $Ea$=63.4 kJ/mol; $k_0$=5.68·108 min$^{-1}$.

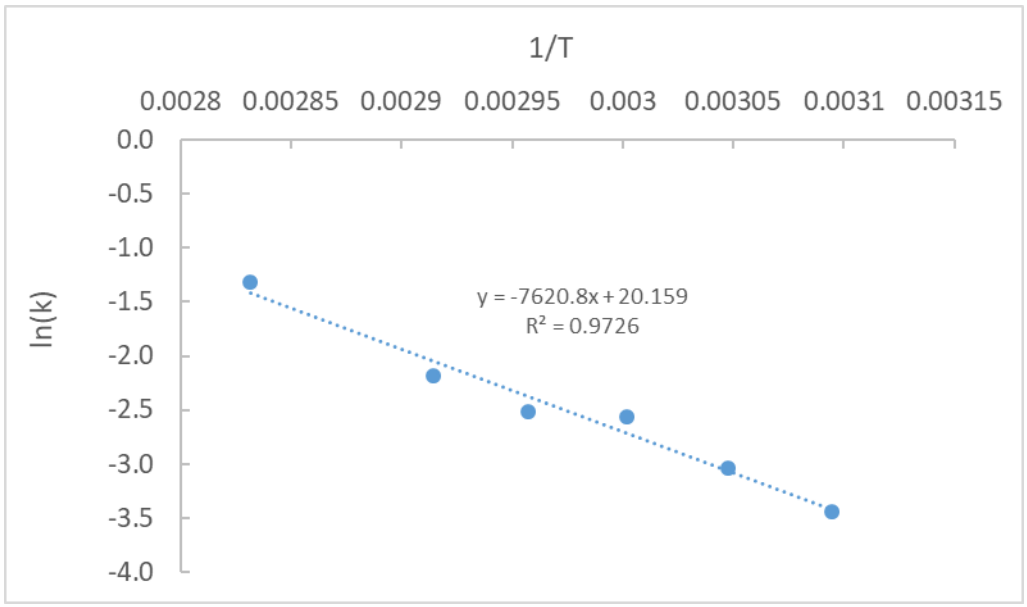


*Figure 34. (1/T) versus ln(k)*

Specific energy consumption:

The SEC can be calculated using the following equation:

$$SEC = \frac{P_{pumps} \cdot \Delta t_{pumps} + P_{stirrer} \cdot \Delta t_{stirrer} + P_{heater} \cdot \Delta t_{heater} + P_{other} \cdot \Delta t_{other}}{V_{treated\ sludge}}$$

With:

$P_{heater}$: power of the electric heater (kW)

$P_{other}$: power of the minor electric items other than the pumps, stirrer and electric heater (kW)

$P_{pumps}$: power of the pumps from the primary and secondary circuit (kW)

$P_{stirrer}$: power of the stirrer (kW)

$SEC$: specific energy consumption (kWh/m$^3$)

$V_{treated\ sludge}$: volume of the treated sludge after one day of operation (m$^3$)

$\Delta t_{heater}$: duration of the operation of the electric heater (h)

$\Delta t_{other}$: duration of the operation other than the pumps, stirrer and electric heater (h)

$\Delta t_{pumps}$: duration of the operation of the pumps from the primary and secondary circuit (h)

$\Delta t_{stirrer}$: duration of the operation of the stirrer (h)

The pump from the 1°circuit was assumed to work during Mode 1 and 3, and during pasteurisation (during which Mode 2 is run). The pump from the 2°circuit was assumed to operate during Mode 3 only. The electric heater and stirrer were operated during the time indicated by the user of the model. The minor electric equipment ran during the whole operation time

**Resolution of the equations**

The model employs a numerical approach to solve the differential equations and compute the required parameters. A time step $dt_i$ of 1 minute is selected for the calculations.

The final equations from the model are:

- Collectors

$$T_{collectors,i} = 1.2296 \cdot (N_{collectors} \cdot A_{collectors} \cdot G) + 44.812$$

- Pasteuriser

$$T_{pasteuriser,i+1} = \frac{0.4563 \cdot (0.9142 \cdot T_{collector,i} - T_{pasteuriser,i})}{V_{pasteuriser} \cdot \rho_{water} \cdot Cp_{water}} \cdot \frac{dt_i}{60} + T_{pasteuriser,i}$$

(Mode 1)

$$T_{pasteuriser,i+1} = \frac{0.4563 \cdot (1.0623 \cdot T_{tanks,i} - T_{pasteuriser,i})}{V_{pasteuriser} \cdot \rho_{water} \cdot Cp_{water}} \cdot \frac{dt_i}{60} + T_{pasteuriser,i}$$

(Mode 3)

$$T_{pasteuriser,i+1} = T_{pasteuriser,i} - 0.3 \cdot \frac{dt_i}{60}$$

(Pasteurisation)

- Buffer tanks

$$T_{tanks,i+1} = \frac{0.3505 \cdot \left(T_{collector,i} - T_{tanks,i}\right) + P_{electric}}{V_{tanks} \cdot \rho_{water} \cdot Cp_{water}} \cdot \frac{dt_i}{60} + T_{tanks,i}$$

(Mode 2)

$$T_{tanks,i+1} = \frac{0.3505 \cdot \left(T_{collector,i} - T_{tanks,i}\right) + P_{electric} - 0.4563 \cdot\cdot (1.0623 \cdot T_{tanks,i} - T_{pasteuriser,i})}{V_{tanks} \cdot \rho_{water} \cdot Cp_{water}} \cdot \frac{dt_i}{60} + T_{tanks,i}$$

(Mode 3)

$$T_{tanks,i+1} = T_{pasteuriser,i} - (0.0091 \cdot T_{pasteuriser,i} - 0.3814) \cdot \frac{dt_i}{60}$$

(Mode 1 and resting time)

- E. coli concentration reduction

$$N_{E.coli,i+1} = N_{E.coli,i} \cdot e^{-5.69 \cdot 10^8 \cdot e^{\left(\frac{63.4}{R \cdot (273 + T_{pasteuriser,i})}\right)} \cdot \frac{dt_i}{60}}$$

$$\log\left(\frac{N_{E.coli,i+1}}{N_{E.coli,i}}\right) = -5.69 \cdot 10^8 \cdot e^{\left(\frac{63.4}{R \cdot (273 + T_{pasteuriser,i})}\right)} \cdot \frac{dt_i}{60}$$

- Volume of treated sludge

$$V_{treated\ sludge} = number\ of\ batches\ treated\ \cdot V_{pasteuriser}$$

- Specific energy consumption

$$SEC = \frac{P_{pumps} \cdot \Delta t_{pumps} + P_{stirrer} \cdot \Delta t_{stirrer} + P_{heater} \cdot \Delta t_{heater} + P_{other} \cdot \Delta t_{other}}{V_{treated\ sludge}}$$

# Appendix F: Methodology for the solar assessment and techno-economic analysis methodology

**Concept of the analysis**

The analysis combines solar assessment with techno-economic analysis, applied to the locations of the Rohingya Camp, as well as the camps at Bentiu (South Soudan), Pemba (Mozambique), and Maiduguri (Nigeria). Based on solar irradiance data, the model determines the maximum volume of material that can be treated by the system. By selecting a given configuration mode, the associated capital and operational costs are calculated, followed by the determination of return on investment (ROI), specific energy consumption, and surface footprint.

**Treatment capacity**

The first step in the analysis involves determining the typical meteorological year (TMY) data for each location using Solargis software, after entering the coordinates for each site. This step includes:

- Calculation of the average monthly radiation at various tilting angles.
- Determination of the typical hourly global horizontal irradiance (GHI) for each month.
- Collection of other key weather parameters, including monthly average ambient temperature and rainfall.

Using the monthly average irradiance at the optimum angle, the model calculates the volume of sludge that can be heated to the required pasteurization temperature using the available solar energy. This is done through an energy balance approach:

$$Sensible\ heat\ for\ sludge\ temperature\ increase = available\ solar\ energy$$

$$\dot{V}_{treated\ sludge} \cdot \rho_{water} \cdot Cp_{water} \cdot \left(T_{final,pasteuriser} - T_{initial,pasteuriser}\right) = N_{collector} \cdot A_{collector} \cdot 3600 \cdot G_{optimal} \cdot \eta_{system}$$

$$\dot{V}_{treated\ sludge} = \frac{N_{collector} \cdot A_{collector} \cdot 3600 \cdot G_{optimal} \cdot \eta_{system}}{\rho_{water} \cdot Cp_{water} \cdot \left(T_{final,pasteuriser} - T_{initial,pasteuriser}\right)}$$

With:

$A_{collector}$: surface area of collector ($m^2$)

$Cp_{water}$: heat capacity of water (kJ/kg/°C)

$G_{optimal}$: irradiance at the optimum angle ($kWh/m^2/day$)

$N_{collector}$: number of collectors

$T_{initial,pasteuriser}$: temperature initial of the sludge in the pasteuriser (°C)

$T_{final,pasteuriser}$: temperature final of the sludge in the pasteuriser (°C)

$\dot{V}_{treated\ sludge}$: volume of sludge treated (L/day)

$\eta_{system}$: efficiency of the system

$\rho_{water}$: density of water (L/kg)

The temperature of the sludge is assumed to increase of a few degrees due to the thermal inertia of the pasteuriser walls that were heated from the previous batch, following the equation below:

$$V_{pasteuriser} \cdot \rho_{water} \cdot Cp_{water} \cdot \left(T_{initial,pasteuriser} - T_{inlet\ sludge}\right) = m_{pasteuriser} \cdot \rho_{stainless\ steel} \cdot Cp_{stainless\ steel} \cdot \left(T_{final,pasteuriser} - T_{inlet\ sludge}\right)$$

$$T_{initial,pasteuriser} = \frac{m_{pasteuriser} \cdot T_{pasteurisation} + \rho_{water} \cdot V_{pasteuriser} \cdot T_{pasteurisation}}{m_{pasteuriser} \cdot Cp_{stainless\ steel} + \rho_{water} \cdot V_{pasteuriser} \cdot Cp_{water}}$$

With:

$Cp_{stainless\ steel}$: heat capacity of stainless steel (kJ/kg/°C)

$m_{pasteuriser}$: thermal inertia mass of the pasteuriser (kg)

$T_{inlet\ sludge}$: temperature of the sludge introduced in the pasteuriser (°C)

$V_{pasteuriser}$: volume of the pasteuriser (L)

The thermal inertia mass of the pasteurizer is determined based on its dimensions, considering the portion involved in heat transfer, and the density of stainless steel.

In the scenario of heat recovery to pre-heat the inlet sludge using outlet sludge, the following equation applies:

$$\eta_{heat\ exchanger} = \frac{V_{pasteuriser} \cdot \rho_{water} \cdot Cp_{water} \cdot \left(T_{sludge} - T_{ambient}\right)}{V_{pasteuriser} \cdot \rho_{water} \cdot Cp_{water} \cdot \left(T_{final.\ pasteuriser} - T_{ambient}\right)}$$

$$T_{sludge} = \eta_{heat\ exchanger} \cdot \left(T_{pasteurisation} - T_{ambient}\right) + T_{ambient}$$

With:

$T_{ambient}$: ambient temperature (°C)

$\eta_{heat\ exchanger}$: heat exchanger efficiency

The efficiency of the system was determined from the experimental efficiencies of the solar collectors, buffer tanks, pasteuriser and fraction of usable energy, through the following formula:

$\eta_{system} = \eta_{collectors} \cdot \eta_{tanks} \cdot \eta_{pasteuriser} \cdot Y_{usable\ solar\ energy}$

With:

$Y_{usable\ solar\ energy}$: fraction of usable solar energy

$\eta_{collectors}$: efficiency of the solar collectors

$\eta_{pasteuriser}$: efficiency of the pasteuriser

$\eta_{tanks}$: efficiency of the buffer tanks

**CAPEX and OPEX**

Capital Costs (CAPEX) are the sum of the costs for the main equipment: solar collectors, buffer tanks, pasteurizer, photovoltaic (PV) system, diesel generator, and liquefied petroleum gas (LPG) boiler.

Operating Costs (OPEX) include basic consumables and fuel (LPG and/or diesel).

The fuel cost is determined based on the amount needed to supplement the system in order to achieve the treatment objective by the following equation:

$OPEX_{fuel} = m_{fuel} \cdot C_{fuel}$

With:

$C_{fuel}$: cost of the fuel (€/kg)

$m_{fuel}$: mass of the fuel (kg)

$OPEX_{fuel}$: operating costs related to the fuel consumption (€)

The mass of fuel can be calculated considering the volume of sludge that must be heated to the pasteurisation temperature using this backup energy source.

$$\left(V_{treatment\ target} - V_{treated\ sludge}\right) \cdot \rho_{water} \cdot Cp_{water} \cdot \left(T_{final,pasteuriser} - T_{initial,pasteuriser}\right) = m_{LPG} \cdot H_{LCV,LPG} \cdot \eta_{boiler}$$

For LPG:

$$m_{LPG} = \frac{\left(V_{treatment\ target} - V_{treated\ sludge}\right) \cdot \rho_{water} \cdot Cp_{water} \cdot \left(T_{final,pasteuriser} - T_{initial,pasteuriser}\right)}{H_{LCV,fuel} \cdot \eta_{boiler/engine}}$$

With:

$H_{LCV,lpg}$: lower calorific value of the fuel (kJ/kg)

$m_{LPG}$: mass of LPG (kg)

$V_{treatment\ target}$: target treatment volume (L)

$\eta_{boiler}$: efficiency of the LPG boiler

For diesel:

$$m_{diesel} = (V_{treatment\ target} - V_{treated\ sludge}) \cdot \rho_{water} \cdot Cp_{water} \cdot (T_{final,pasteuriser} - T_{initial,pasteuriser}) \cdot \rho_{diesel} \cdot X_{diesel\ to\ electricity}$$

With:

$X_{diesel\ to\ electricity}$: conversion rate of diesel engine to electricity (L/kWh)

$\rho_{diesel}$: density of diesel (kg/L)

The specific capital cost and specific operating costs can be calculated by dividing these metrics by the target treatment volume. The return of investment can be estimated by the following formula:

$$ROI = \frac{\Delta CAPEX}{\Delta\ OPEX}$$

With:

$ROI$: return of investment for a modification of the system configuration (days)

$\Delta CAPEX$: difference of CAPEX between the original and modified system configuration (€)

$\Delta OPEX$: difference of OPEX between the original and modified system configuration (€/day)

**Specific energy consumption**

The specific energy consumption is calculated by considering the electrical consumption of the pumps, stirrer, electric heater, and minor items (such as sensors, displays, lights, fans, etc.), and dividing this by the total volume treated.

**Specific surface area**

The specific surface area is determined by dividing the surface area by the target treatment volume.

**Parameters used**

- Characteristics of pasteuriser

Cost: €17,232.00

Volume: 500 L

Efficiency: 98%

Thermal inertia mass: 155 kg

Stirrer power: 300 W

- Characteristics of buffer tanks and related equipment

Cost: €10,868.00

Volume per tank: 800 L

Efficiency: 78%

Pumps power: 60 W

- Characteristics of the solar collectors

| COLLECTORS | Option 1 | Option 2 | Option 3 |
|---|---|---|---|
| **Type** | Flat solar collector | Flat solar collector | Evacuated tubes |
| **Country** | France | India | India |
| **Cost per unit** | € 520.00 | € 150.00 | € 200.00 |
| **Aperture surface ($m^2$/collector)** | 2.28 | 2.28 | 1.40 |
| **Raw surface ($m^2$/collector)** | 2.53 | 2.53 | 2.53 |
| **Efficiency** | 35% | 35% | 62% |

- Characteristics Diesel generator

| Diesel generator | Option 1 | Option 2 |
|---|---|---|
| **Capacity** | 5 kW | 10 kW |
| **Use** | Electric appliances | Electric appliances and heating |
| **Cost** | € 800.00 | € 1,600.00 |

Conversion rate: 0.35 L/kWh

Cost of diesel per kg: € 0.84

- Characteristics of LPG boiler

LPG boiler cost: €2,000.00

Efficiency LPG boiler: 90%

Cost LPG per kg: €0.97

- Characteristics of PV system

Capacity: 3 kW

PV system cost: €2,000.00

- Characteristics of the heat recovery unit

| Heat recovery unit | Option 1 | Option 2 |
|---|---|---|
| **Cost** | € 3000 | € 8000 |
| **Effeciency** | 35% | 70% |

- Other

Cost of minor items (Pressure booster, piping, electric material, instrumentation, furniture.): €1,000.00

Cost of consumables (cleanining material, PPE, prints, paper, pens...): €100.00 / month

Fraction of usable solar energy: 80%

Power of minor electric items (lights, fans, displayers…): 50 W

Surface of installation: 130 $m^2$

- Weather data

Ukhia, Bangladesh (coordinates: 21°10'43", 092°09'14")

Optimum titling angle:~ 20°

| Month | G (kWh/m²/day) | $T_{ambient}$ (°C) |
|---|---|---|
| January | 6.0 | 20.6 |
| February | 5.9 | 22.6 |
| March | 6.5 | 25.9 |
| April | 6.0 | 27.9 |
| May | 5.1 | 28.0 |
| June | 3.8 | 26.7 |
| July | 3.9 | 26.2 |
| August | 4.2 | 26.2 |
| September | 4.7 | 26.5 |
| October | 5.2 | 26.4 |
| November | 5.8 | 24.6 |
| December | 5.7 | 21.8 |
| YEAR | 5.2 | 25.3 |

Bentiu, South Soudan (coordinates: 09°15'36", 029°48'00")

Optimum angle: ~15°

| Month | G (kWh/m²/day) | $T_{ambient}$ (°C) |
|---|---|---|
| | | |
| January | 6.9 | 29.1 |
| February | 6.3 | 31.0 |
| March | 6.8 | 32.6 |
| April | 6.0 | 32.6 |
| May | 5.4 | 30.3 |
| June | 4.6 | 27.9 |
| July | 4.6 | 26.0 |
| August | 4.9 | 25.5 |
| September | 5.3 | 26.0 |
| October | 5.9 | 26.8 |
| November | 6.5 | 28.5 |
| December | 6.9 | 29.1 |
| YEAR | 5.8 | 28.8 |

Maiduguri, Nigeria (coordinates: 11°50'22", 013°09'13")

Optimum angel: ~15°C

| Month | G (kWh/m²/day) | $T_{ambient}$ (°C) |
|---|---|---|
| January | 6.6 | 23.0 |
| February | 6.0 | 25.8 |
| March | 6.5 | 29.9 |
| April | 5.9 | 32.7 |
| May | 5.7 | 32.5 |
| June | 5.1 | 30.6 |
| July | 5.1 | 28.0 |
| August | 5.1 | 26.2 |
| September | 5.7 | 27.3 |
| October | 6.5 | 28.7 |
| November | 6.6 | 26.9 |
| December | 6.7 | 23.7 |
| YEAR | 6.0 | 27.9 |

Pemba, Mozambique (coordinates: -12°57'52", 040°31'01")

Optimum angel: ~15°C

| Month | G (kWh/m²/day) | $T_{ambient}$ (°C) |
|---|---|---|
| January | 5.1 | 27.1 |
| February | 4.8 | 27.0 |
| March | 5.7 | 26.9 |
| April | 5.7 | 26.3 |
| May | 6.0 | 25.4 |
| June | 5.3 | 24.2 |
| July | 5.5 | 23.5 |
| August | 6.3 | 23.8 |
| September | 6.7 | 24.8 |
| October | 7.0 | 26.1 |
| November | 6.4 | 27.2 |
| December | 5.7 | 27.5 |
| YEAR | 5.8 | 25.8 |

# Supporting documents

Supporting Document A: Literature review report

Supporting Document B: Research framework report

Supporting Document C: Process flow diagram of the solar pasteuriser

Supporting Document D: Standard operating procedure of the solar pasteuriser

Supporting Document E: ICDDR'B laboratory analysis report

Supporting Document F: IHE-Delft internship report

Supporting Document G: Compiled data from the physiochemical and microbial analysis

Supporting Document H: Data from the first experimental campaign

Supporting Document I: Data from the second experimental campaign

Supporting Document J: Compiled data from the experimental campaigns

Supporting Document K: Solar pasteuriser model

Supporting Document L: Solar assessment coupled with the techno-economic analysis

Supporting Document M: Replicability analysis for Bentiu, South Soudan

Supporting Document N: Replicability analysis for Maiduguri, Nigeria

Supporting Document O: Replicability analysis for Pemba, Mozambique